1-1-2012

Database Development For Ontario's Local Calibration Of Mechanistic – Empirical Pavement Design Guide (MEPDG) Distress Models

Gulfam E. Jannat
Ryerson University

DATABASE DEVELOPMENT FOR ONTARIO'S LOCAL CALIBRATION OF MECHANISTIC – EMPIRICAL PAVEMENT DESIGN GUIDE (MEPDG) DISTRESS MODELS

by

Gulfam-E-Jannat

A thesis

presented to Ryerson University

in partial fulfillment of the

requirements for the degree of

Master of Applied Science

in the Program of

Civil Engineering

Toronto, Ontario, Canada

Author's Declaration

I hereby declare that I am the sole author of this thesis. This is a true copy of the thesis, including any required final revisions, as accepted by my examiners.

I authorize Ryerson University to lend this thesis to other institutions or individuals for the purpose of scholarly research

I further authorize Ryerson University to reproduce this thesis by photocopying or by other means, in total or in part, at the request of other institutions or individuals for the purpose of scholarly research.

I understand that my thesis may be made electronically available to the public.

Signature _____

Gulfam-E-Jannat

Department of Civil Engineering

Ryerson University

Title: Database Development for Ontario's Local Calibration of Mechanistic-Empirical Pavement Design Guide (MEPDG) Distress Models

Written by: Gulfam-E-Jannat

Master of Applied Science in Civil Engineering, 2012

Ryerson University

Abstract

The AASHTO Mechanistic-Empirical Pavement Design Guide (MEPDG) includes empirical distress models that need both global and local calibrations. The local calibration requires developing a database that would reflect local environments, design and maintenance practices in a particular jurisdictional region. The objective of the thesis is to develop a pavement database for local calibration before the MEPDG is to be implemented in Ontario. The database involves a hierarchical framework of the input parameters required for DARWin-ME, and the measured performance data are based on the MTO's PMS-2. To demonstrate the validity of the developed database a preliminary local calibration including clustering analysis is carried out for the IRI and total rutting. The calibration-validation analysis suggests that the IRI model can be best clustered based on the geographical zone whereas the highway functional class is the best clustering parameter for rutting during the local calibration.

Acknowledgements

At first, the author would like to express her wholehearted gratefulness to the Almighty Allah for each and every achievement of her life.

The author becomes delighted to state that this study was supervised by Dr. Arnold Yuan and Dr. Medhat Shehata, Department of Civil Engineering, Ryerson University. The author wishes to express her sincerest gratitude to Dr. Arnold Yuan and Dr. Medhat Shehata for their continued guidance and enthusiastic encouragement. Throughout the whole study they have timely extended their experienced views and understanding of the problem for the successful completion of the research.

The author would like to express her heartfelt thanks officials (Dr. Joseph Ponniah, and Mr. Warren Lee, Pavement and Foundation Section) of the Ministry of Transportation Ontario (MTO) for their help during the course of the research work. Lastly, the author would also like to admit the inspiration and unconditional support by her family members.

TABLE OF CONTENTS

LIST OF TABLES

LIST OF FIGURES

LIST OF APPENDICES

Chapter 1

INTRODUCTION

1.1 Background

Most of the previous and recent pavement design methods including American Association of State Highway and Transportation Officials (AASHTO) 1993 pavement design are empirical in nature. These were developed based on road tests in late 1950's (Schwartz and Carvalho 2007). Although these pavement design methods are still being widely used in majority of highway agencies in North America, they do not incorporate all possible local factors for pavement materials and environmental conditions. They also fail to capture the realistic local characteristics of the existing and future traffic volume and types.

A Mechanistic-Empirical Pavement Design Guide (MEPDG) was developed in the USA under NCHRP 1-37A in 2004 to address the shortcomings of empirical pavement design methods (Hall et al. 2010). MEPDG and related software have capabilities to analyze and predict performance of different types of pavements. Many highway agencies have plans to implement the MEPDG as their pavement design method. Implementation of MEPDG, however, requires data collection, training and local calibration/ validation of performance models in MEPDG.

The MEPDG uses mechanistic-empirical models to analyze input data for traffic, climate, materials and proposed structure. The models estimate damage accumulation over service life.

The MEPDG is applicable for designs of both flexible and rigid pavements. In addition, MEPDG also incorporates pavement performance (both structural and functional performance) in the design process. These performance predictions consist of pavement distresses and ride quality. The MEPDG for flexible pavements includes the following performance prediction modes (Velasquez et al. 2009):

- Alligator cracking
- Transverse cracking
- Longitudinal cracking
- Rutting
- International Roughness Index (IRI)

The important aspect of MEPDG method is to evaluate and recalibrate the models of the above performance predictions for the local characteristics. To calibrate these models, a number of investigations are conducted (Velasquez et al. 2009; Hall et al. 2010; Hoegh et al. 2010; Darter et al. 2005 etc.) by different agencies (the Minnesota Department of Transportation (MnDOT) and the Local Road Research Board (LRRB)) for specific local conditions.

The MEPDG incorporates a lot of improvement in pavement design, which brings more accuracy to the existing AASHTO Design Guide. Among the improvements this guide is likely to improve the implementation of performance prediction of transverse cracking, faulting, smoothness, the addition of climate inputs, better characterization of traffic loading inputs, more sophisticated structural modeling capabilities, and the ability to model real-world changes in material properties. It is found that the data base, material properties, traffic characteristics, and climatic conditions used in the global calibration are not enough to carry out day-to-day

pavement design activities for specific local conditions, and so their effect and adequacy needs to be determined in addition to other factors that will facilitate the efficient implementation of the MEPDG.

The performance models in the MEPDG were calibrated and validated by using the Long Term Pavement Performance (LTPP) program data, which includes pavement sections from many states in the USA and Canada as well. Such calibrations are normally referred as global calibration. Data sets from the LTPP database used in the global calibrations not only spanned the climatic conditions of several states, including some Canadian provinces, but also encompassed wide ranges of traffic, materials, and surface layer thicknesses. The purpose of the calibration is to establish transfer functions relating pavement responses (stresses, strains, and deflections) to specific forms of physical distresses, which mainly includes permanent deformation, cracking, and roughness. Although the national calibration-validation process has been very comprehensive, it is obvious that there is significant potential difference between 'national' and 'local' conditions including climate, material properties, traffic patterns, construction and maintenance activities. For these reasons, the pavement performance models in the MEPDG should be compared to and verified against local conditions.

One of the challenging issues in the local calibration exercise is to develop a suitable pavement distress database that can be used to calibrate the pavement distress models. A major source of the distress data are from the Pavement Management System (PMS), which is placed in many transportation agencies, including the Ministry of Transportation, Ontario (MTO). The MTO has been using the PMS since the 1980s, and now has evolved into its second generation, referred to as MTO PMS-2. Each year, MTO collects data regarding in-service field evaluation

of pavement performance, such as roughness, surface distress, ride quality and overall pavement condition from more than 1,700 sections across Ontario. These data are stored and managed in the PMS. However, the pavement distress data from the PMS cannot be directly used for local calibration of the MEPDG models because the PMS is for existing pavements, with the ultimate goal being network-level budget analysis and project prioritization. Therefore, there is a gap to convert the PMS condition data to a database that can be used for the MEPDG local calibration.

1.2 Objective and Significance

The main objectives of this study are: (1) to develop a pavement database for MEPDG calibration to local practices in Ontario; and (2) to develop a framework for local calibration. This project is funded by the MTO's Highway Infrastructure Innovation Funding Program (HIIFP).

The database developed in this study will allow a comprehensive local calibration and validation process in the future. The study will facilitate to assess the efficiency of local calibration of MEPDG distress models, and hence ensure better prediction of pavement distress, leading to an economic pavement maintenance program.

1.3 Methodology and Scope of the Study

In this thesis, the investigations focus on the review of existing distress database, formulation of damage indices from severity and density of cracking, characterization and clustering of pavement sections, development of calibration database and finally calibration of distress

models based on local conditions. Ontario Highway Systems are used for the empirical investigations. The major steps are:

- Review the existing pavement distress database (PMS-2) of MTO;
- Identify and partition pavement sections based on their material properties, layer thickness, traffic, climatic conditions, and construction and rehabilitation history;
- Develop the calibration database including all input data of traffic pattern, vehicle classifications, traffic growth factor, climate data for proximate weather stations, material properties, and layer information;
- Perform pavement analysis for the selected sections in the calibration database;
- Calibrate the distress models.

The calibration of database is developed in the Microsoft Access environment. Pavement analysis is conducted by using the latest MEPDG package DARWin-ME that has only become recently available for public use.

There are plenty of issues regarding local calibration of the MEPDG models requiring special attentions. However, this study mainly focuses on two major aspects: the database development, and local calibration. Due to data limitation, only flexible pavement is considered in the database development. In this study of the local calibration, only certain distress models (International Roughness Index (IRI), Rutting and Alligator cracking) are analyzed.

1.4 Organization of the Thesis

A detailed flow chart of the thesis structure is presented in Figure 1.1. The thesis is organized in five chapters with background and introduction in this first chapter. Chapter 2 presents a comprehensive review of relevant literature. Items covered in this chapter include: basic concepts of MEPDG, design process of MEPDG DARWin-ME software, calibration of MEPDG distress models, current practices of local calibration, and different types of distress models.

Chapter 3 discusses the input data design, study design and analytical framework of the analysis. Chapter 4 analyses the pavement and calibrates the pavement sections. Chapter 5 contains the concluding remarks on the findings of the study. It also discusses the implication of the results of the study. Future research topics are also recommended in the chapter 5.

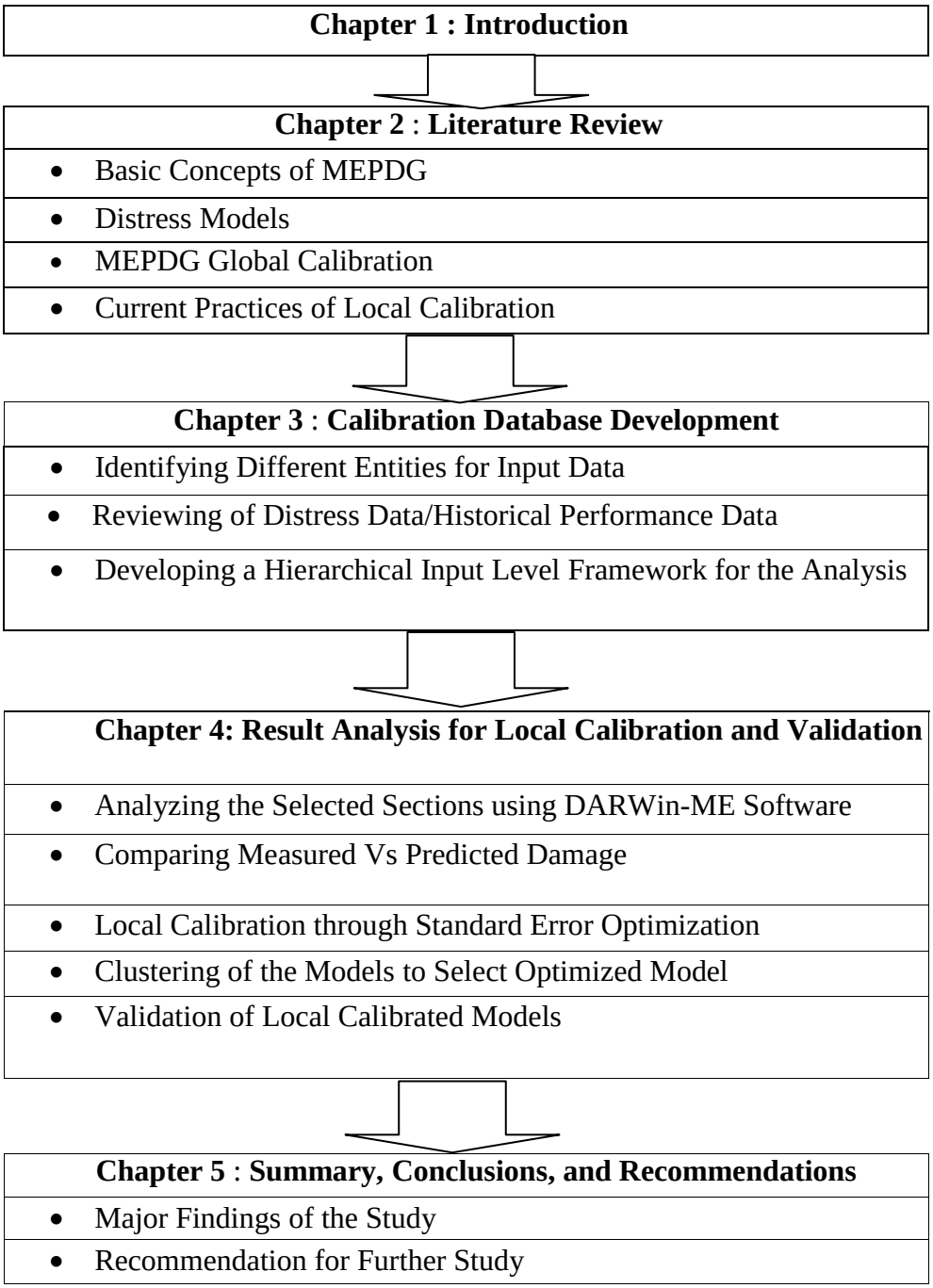

Figure 1 1: Organization of the Thesis

Chapter 2

LITERATURE REVIEW

This chapter presents a comprehensive review of relevant literature. Items covered include the basic concepts of MEPDG, design process of MEPDG, general and local calibration of MEPDG, and different types of distress models.

2.1 Historical Development of Pavement Design Methods

At the very starting stage of pavement design and analysis, the design was based on empirical design approach generated from the results of experiments or experience. The first empirical methods for flexible pavement design were found during mid-1920s when the first soil classifications were developed (Schwartz and Carvalho 2007).

One of the first published article was the Public Roads (PR) soil classification system (Hogentogler and Terzaghi 1929, after Huang 2004). In 1929, the California Highway Department developed a method using the California Bearing Ratio (CBR) strength test (Porter 1950; after Huang 2004). The CBR method related the material's CBR value to the required thickness to provide protection against subgrade shear failure. The thickness computed was defined for the standard crushed stone used in the definition of the CBR test. The CBR method was improved by U.S. Corps of Engineers (USCE) during the World War II and later became the most popular design method. In 1945 the Highway Research Board (HRB) modified the PR classification. Soils were grouped in 7 categories (A-1 to A-7) with indexes to differentiate soils

within each group. The classification was applied to estimate the sub-base quality and total pavement thicknesses.

In 1950s, pavement design methods were based on a limited amount of performance data acquired through road tests sponsored by the American Association of State Highway Officials (AASHO). Based on the result of the road tests, the empirical design equations were developed and the AASHTO Interim Guide for the Design of Pavement Structures was published in 1972 (Dzotepe and Ksaibati 2011).

These equations are developed using regression analysis from test results of pavement serviceability, supporting value of the sub-grade, quantity of the predicted traffic, quality of the construction materials, and climate. The Interim Guide is developed mainly based on the AASHO road tests with limited range of design parameters. They include only one climate, one sub-grade, two years duration, limited cross sections and 1950s materials, traffic volumes, specifications, and construction methods (AASHTO 2008). Consequently, covering some improvements within the material input parameters and design reliability, this guide is updated in 1986 and 1993.

However, the materials, climate and traffic of highways are different for different locations. Therefore, the empirical design equations in those design guides are inevitably used in an extrapolative manner, resulting in less accurate and also less precise prediction of pavement performance. To address this limitation and also to utilize mechanistic-based models and databases relevant to the current state of knowledge of highway performance, AASHTO initiated in the mid 1990s further investigation and research, aiming to develop a new pavement

design guide. Finally, AASHTO and the National Cooperative Highway Research Program (NCHRP) developed the MEPDG under NCHRP Project 1-37A in 2004 (Timm et al. 2010; Hall et al. 2010).

The mechanistic-empirical method represents one step forward from the previous empirical methods. In this mechanistic approach, a mathematical model is used to define the relationship between different structural response (stresses, strains and deflection) and the physical consequences. According to Flintsch and McGhee, the "mechanistic–empirical (M-E) procedures use pavement models based on the mechanics of materials to predict pavement responses (deflections, strains, and stresses) and empirically based transfer functions to estimate distress initiation and development based on these responses" (Flintsch and McGhee 2009). Figure 2.1 presents the basic flow chart of the M-E design process. The design procedures of the MEPDG are shown in Figure 2.2.

The MEPDG manual and associated software provide a design and analysis procedure based on engineering mechanics. More importantly, the design equations are also validated with wide-ranged performance data of both test roads and in-service roads, providing with distress models for predicting the structural and functional performance of various types of flexible and rigid pavements. Using input of traffic, climate and materials data, these models can be used to more accurately analyze and predict the damage of the pavement sections. As a result, more reliable and economic design can be achieved.

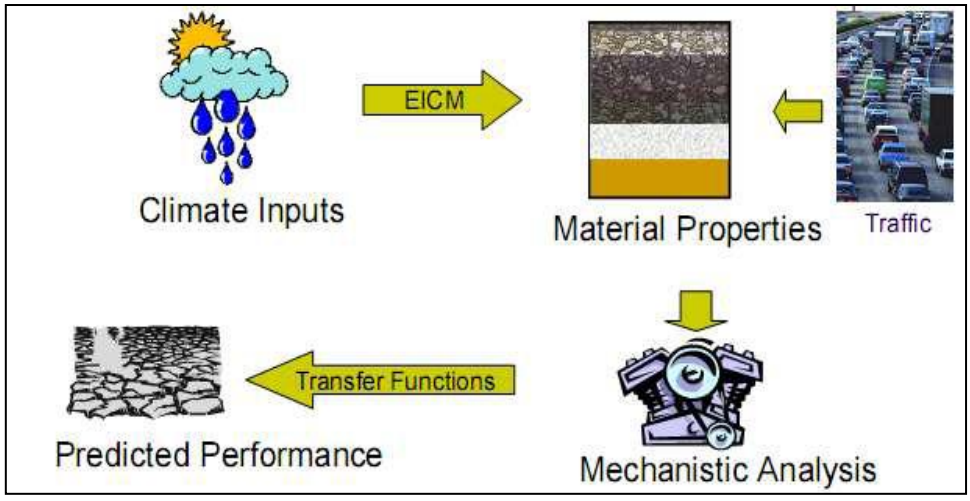

Figure 2.1: M-E Design Process

(Yu 2010)

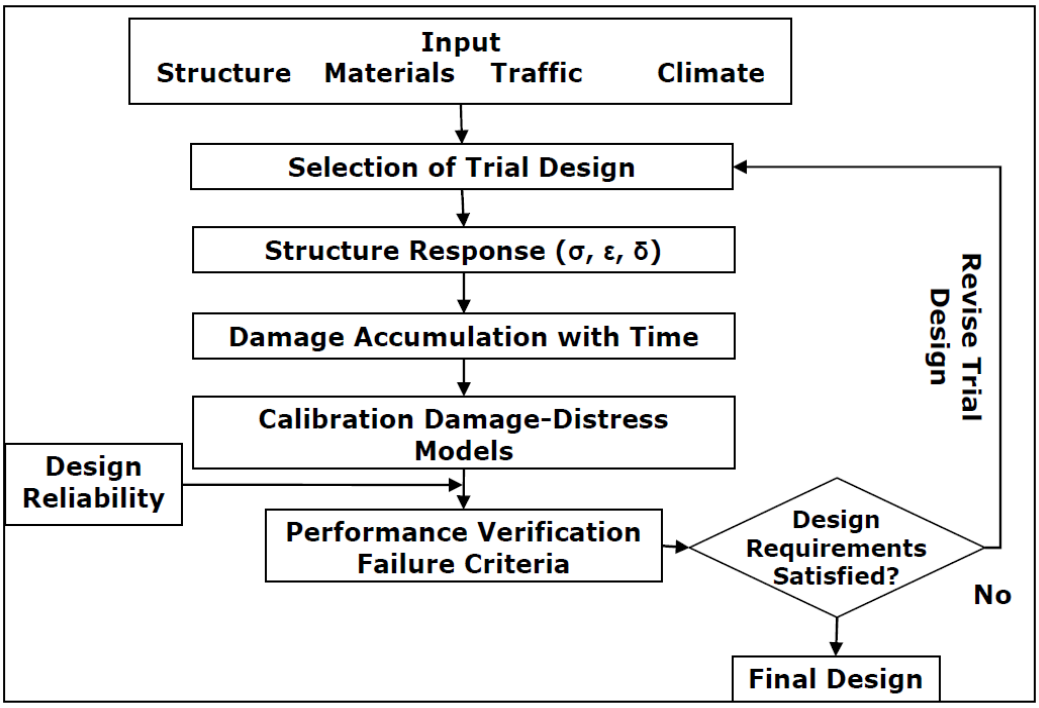

Figure 2.2: MEPDG Procedure

(NCHRP 2004**)**

Moreover, an implementation of the mechanistic–empirical pavement analysis and design methodology is expected to affect pavement management practices and, in particular, pavement condition data collection.

2.2 MEPDG Software

The MEPDG Software is developed as a part of NCHRP project by AASHTO with NCHRP and MEPDG Version 1.1 is available. It mechanistically calculates pavement responses (stresses, strains, and deflections) and empirically correlates damage over time to the pavement distresses. At design stage, the software use an iterative process with inputs in trial design, estimating damage and key distress over design life and then design is verified against the performance criteria with a desired level of reliability. To meet the specified performance and reliability requirements, the initial design may have to be modified as per requirement. For this reason, in this approach, a selected trail design is performed first to determine whether it meets the criteria of specified performance. The generalized basic steps for the MEPDG are shown in Table 2.1.

DARWin-ME1.0 is the next generation of AASHTOWare pavement design software which builds upon the research grade MEPDG software. It is intended to support AASHTO's interim MEPDG manual of practice. The development of this software product was undertaken by AASHTO. This software greatly simplifies the pavement design and analysis methodology described in the AASHTO MEPDG Manual of Practice. DARWin-ME also has additional interface features for importing data from third party software. Key components of the software can be identified in Figure 2.3

Table 2.1**:** Generalized Basic Steps for the MEPDG Software

1. Performing a trial design for the specified location (based on traffic, climate, and material conditions)
2. Defining the pavement layer arrangement for Hot Mix Asphalt (HMA) and other underlying material properties
3. Setting the criteria of the different distress models for performance at acceptable level at the end of the design period
4. Setting the desired level of reliability for the above performance criteria
5. Selecting hierarchical input of traffic data, material properties, climatic data and pavement layer structural properties for desired level of accuracy
6. Computing the structural responses (stress, strain, deformation) for each damage calculation throughout the design period.
7. Estimating the accumulated damages for the entire design life
8. Predicting distresses (cracking, rutting) for a certain period using the calibrated mechanistic-empirical performance models
9. Predicting the smoothness as a function of the initial IRI, distresses over time, and site factors at the end of each month.
10. Evaluating the expected performance of the trial design at the given reliability level for adequacy.
11. Modifying the design repeating the process, if the performance criteria are not met.

Following the basic steps of MEPDG, each DARWin-ME pavement design project, whether new construction, an overlay, restoration, uses an iterative process. Three major basic steps are:

a. Create a trial design for project.

b. Run DARWin-ME to predict the key distresses and smoothness for trial design.

c. Review the predicted performance of trial design against the performance criteria and modify trial design as needed until a feasible design is produced that satisfies the performance criteria. This step may require several runs of DARWin-ME.

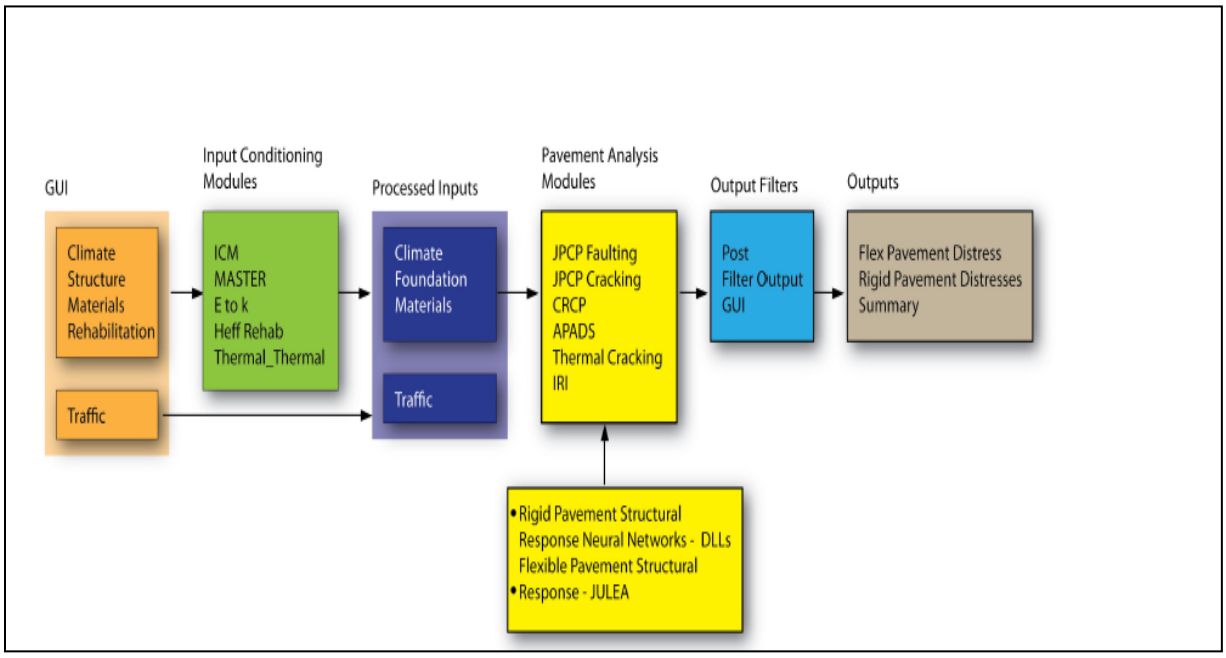

Figure 2.3: DARWin-ME Software Components

(TAC 2011)

Pavement design and analysis using DARWin-ME requires the inputs of general project information, performance criteria, pavement layers and materials, traffic, climate, pavement design features/properties, rehabilitation information (if applicable), analysis calibration factors, Sensitivity inputs and Optimization inputs.

DARWin-ME includes a database option that enables enterprise operation. It can

- Archive projects: Any valid DARWin-ME project can be stored in its entirety in the database
- Create data libraries: Individual material or other analysis objects, such as traffic and climate, can be stored and retrieved by users
- Search archived projects: Any archived DARWin-ME project can be searched in the database
- Compare project inputs: Project inputs can be compared with data libraries.

DARWin-ME uses a three-level hierarchical input scheme for most of the input parameters related to traffic, material, and pavement condition. The following defines each hierarchical input level:

- Input Level 1 – Input parameter is measured directly; it is site or project specific value. This level represents the greatest knowledge about the input parameter for a specific project but has the highest testing and data collection costs to determine the input value.
- Input Level 2 – Input parameter is estimated from correlations or regression equations. In other words, the input value is calculated from other site specific data

or parameters that are less costly to measure. Input level 2 may also represent measured regional values that are not project-specific.

- Input Level 3 – Input parameter is based on "best-estimated" or default values. Level 3 inputs are based on national or regional default values – the median value from a group of data with similar characteristics.

The DARWin-ME design process contains more than 85 total inputs with 13 or more general information, 30 or more traffic information, 16 or more layer properties , 16 structural properties (per layer), and more than 1000 weather station.. This can be compared with the 1993 AASHTO Guide, which contains 5 inputs for flexible pavement and 10 inputs for rigid pavements (AASHTO 2008). The software currently uses 1000 or more weather stations.

DARWin-ME outputs reports in two formats: PDF and Excel. The data contained in these reports include input summary, climate summary, design pass/fail checks, material properties summary, distress and smoothness prediction summary and charts. The output of the analysis software is a prediction of the distresses and smoothness against set reliability targets and so it is anticipated that a more reliable design will be created and there will no longer be a dependence on extrapolation of empirical relationships. It will also allow for calibration nationally, regionally, or to local performance data for materials, climate, and traffic.

2.3 MEPDG Performance Indicators

One of the important improvements of the MEPDG in comparison with the empirical design approaches is that the MEPDG estimates damage accumulation and hence predicts pavement performance over the whole service life of the pavement section. These performance predictions consist of pavement distresses and ride quality. For flexible pavement the following performance prediction indicators are considered in the MEPDG (Velasquez et al. 2009):

- Alligator cracking
- Transverse cracking
- Longitudinal cracking
- Rutting
- IRI

Alligator Fatigue (bottom up) cracking

This is commonly referred to as "bottom-up" or "classical" fatigue cracking. This cracking is one of the major distress types occurring in flexible pavement systems. Tensile and shear stresses developed at the bottom of the HMA layer due to repeated traffic loads and structural stability of the pavement layer becomes unsteady. Fatigue cracks starts at points where the critical tensile strains and stresses occur. Stiffer mixtures or thin layers are more likely to exhibit bottom-up fatigue cracking problems, which makes it a problem often aggravated by cold weather. Soft layers placed immediately below the asphalt concrete layer increase the tensile strain magnitude at the bottom of the asphalt concrete and consequently increase the possibility of fatigue crack development. After the damage is initiated at the critical location, these cracks propagate along with accumulative traffic loading.

A number of reasons are associated with an increase in alligator cracking. Mostly, higher wheel loads and tire pressures, inadequate HMA layers for the magnitude and repetitions of the loading, and weakness in base layers resulting from high moisture contents, soft spots, or poor compaction are the common reasons.

The cracks which form a network of multisided (polygon) blocks resemble the skin of an alligator. The block size can range from a few millimeters to about a meter. The block size is indicative of the level (depth) at which failure is taking place.

Longitudinal (top down) cracking

In thick pavements, cracks are most likely to initiate from the top in localized areas of high tensile stresses resulting from a tire-pavement interaction and asphalt binder aging (Myersr et al. 2001). This type of surface-initiated longitudinal wheel-path cracking is known as top-down or surface down cracking. The initiation of longitudinal surface cracks is advanced by the presence of high vertical and lateral stresses induced under radial truck tires at the pavement's surface. In most instances, the aging of the HMA layer tends to create stiffness in the layer, which worsens the effect. A shearing effect is induced in the layer from the tire contact pressure which combines with the tension from the loading resulting in cracking. This distress is calculated as feet of cracking per mile or m/km.

Rutting

Generally, permanent deformation results in any of a pavement's layers or subgrade due to consolidation or lateral movement of the materials under traffic and environmental loadings. Rutting refers to vertical surface depression in the wheel-path. Pavement uplift (shearing) may occur along the sides of the rut.

There are two basic types of rutting: mix rutting and subgrade rutting. Mix rutting occurs when the subgrade does not rut yet the pavement surface exhibits wheel-path depressions as a result of compaction or mix design problems. Subgrade rutting occurs when the subgrade exhibits wheel-path depressions due to loading. In the latter case, the pavement settles into the subgrade ruts causing surface depressions in the wheel path. Rutting damage due to different axle configurations is approximately proportional to the number of axles within an axle group. In other words, rutting damage is proportional to the gross weight of the axle group or truck, with multiple axles causing slightly less damage than a combination of smaller axle groups, for the same load carried (Chatti 2009).

Rutting is computed in the MEPDG in inches or millimeters and appears as a permanent deformation occurring along the wheel paths. This depression could be as a result of traffic loading, poor compaction of any of the layers during construction stage, or the shearing of the pavement caused by the traffic wheel loading (AASHTO 2008).

Thermal cracking

Cracks that are perpendicular to the pavement's centreline or lay down direction are normally known as thermal cracks, or transverse cracks. They tend to appear on the surface. Mainly, the

shrinkage of the HMA surface due to low temperatures or seasonal/daily temperature differences, asphalt binder hardening is considered as major reason for this type of cracking. Transverse cracking is computed as feet of cracking per mile or meter/ kilometer.

Smoothness/IRI

Pavement roughness is generally defined as an expression of irregularities in the pavement surface that adversely affect the ride quality of a vehicle. Developed by the World Bank in the 1980s (WSDOT 2005), the IRI is used to define a characteristic of the longitudinal profile of a travelled wheel-track and constitutes a standardized roughness measurement. It is used to determine the functional serviceability of the pavement design. The commonly recommended units are meters per kilometer (m/km) or millimeters per meter (mm/m). The IRI is based on the average rectified slope (ARS), which is a filtered ratio of a standard vehicle's accumulated suspension motion (in mm, inches, etc.) divided by the distance travelled by the vehicle during the measurement (km, mi, etc.). IRI is then equal to ARS multiplied by 1,000 (WSDOT 2005). The MEPDG predicts the IRI by means of an empirical function combining the other performance indicators.

The results obtained for the MEPDG analysis for the performance indicators is generally verified against the user-specified design criteria or threshold limits. These threshold limits can be nationally or locally established by the agencies. . The comparison is to help determine how well the particular pavement will perform throughout its design life. The general criteria set is that interstate projects require more stringent design or thresholds values when compared with secondary and primary roads. Evaluating the specified threshold limits against the performance prediction outputs from the design helps establish the acceptability or adjustment of the trial

design. During the design analysis of the pavement, the point where the performance indicators exceed the specified ranges during the design life, the pavement would need reconstruction or rehabilitation. Table 2.2 shows the recommended design criteria limits provided by the MEPDG. However, these values are adjusted based on different local conditions.

Table 2.2 Recommended Threshold Design Values for Flexible Pavements (AASHTO 2008)

Performance Criteria	**Recommended Maximum Value**
Alligator Cracking (HMA)	Interstate: 10% lane area Secondary: 35% lane area Primary: 20% lane area
Transverse Cracking (HMA)	Interstate: 500 ft/mi Secondary: 700 ft/mile Primary: 700 ft/mile
Rutting (HMA)	Interstate: 0.40 in Others: (<45mph): 0.65 in Primary: 0.50 in
IRI (All Pavements)	Interstate: 160 in/mi Secondary: 200 in/mi Primary: 200 in/mi

In MEPDG, the critical stress or strain values obtained from the structural response model are converted to incremental distresses, either in absolute terms, such as in rut depth calculation, or in terms of a damage index in fatigue cracking. The cumulative damage is converted to physical cracking using calibrated distress prediction models.

Although, different researches are carried out to predict the pavement life by predicting the above mentioned distresses, it still is not possible to make accurate and precise prediction of pavement life. This becomes very difficult due to the complexity in predicting many of the factors that influence the pavement performance. It is challenging to predict infrequent hot summers, cold winters, wet springs etc. Furthermore, traffic forecasts are also unreliable for different road zone or area and there is a large disparity in the local characteristics of pavement materials and structures. Figure 2.4 illustrates the complexity of the performance prediction problem. For these reasons, an important aspect is to evaluate the performance prediction models, re-calibration of the performance prediction models for the local characteristics. To calibrate these models a number of researches are conducted (Velasquez et al. 2009; Hall et al. 2010; Hoegh et al. 2010; and Darter et al. 2005) for different locations by different agencies.

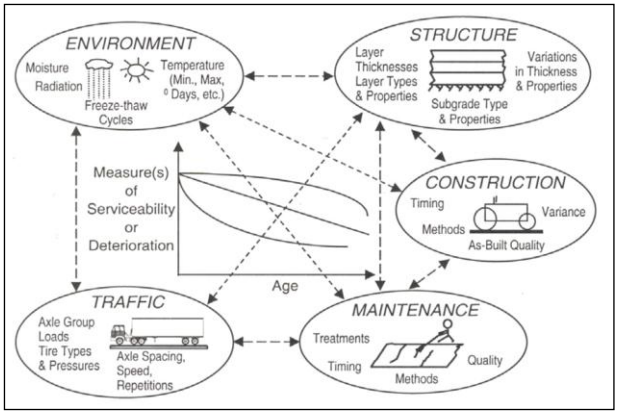

Figure 2.4: Factors affecting Pavement Performance (NCP 2010)

2.4 MEPDG Distress Models for Flexible Pavements

Pavement distress or above mentioned performance indicators are expected to be affected by several parameters. The equations used to predict the performance indicators are known as

distress models. Different models are used for different types of distresses by different agencies which are discussed below.

Fatigue Cracking (Top down and Bottom Up) Models

Fatigue damage of pavements is a very complex process affected by pavement structural capacity, vehicle characteristics, mix properties, climatic effects, and time. Pavement structural capacity and the vehicle's characteristics affect the stress level at the bottom of the HMA layer and accordingly affect the fatigue life of the pavement (Pell and Copper 1975; Chatti et al. 1995; Simmons and Seaman 2000).

Fatigue cracking is directly related to the strain development in the HMA layer and it starts when the tensile strains exceed a threshold value of the HMA. Numbers of models are developed to characterize the fatigue of flexible pavements. Some of these models are developed to best suit specific characteristics of a particular institute, and some are just the output of an extensive laboratory testing. The number of repetitions to fatigue cracking is expressed by the following equation:

$$N_f = f_1(\varepsilon_t)^{-f_2}(E_1)^{-f_3} \quad (1)$$

Where:

N_f = *Number of repetitions to fatigue cracking;*

E_1 = *Modulus of HMA*

ε_t = *tensile strain at critical locations*

f_1, f_2, f_3 = *Laboratory regression coefficient*

Or, Similarly the above equation (1) can also be expressed as follows:

$$N_f = C\, k_1 \left(\frac{1}{\varepsilon_t}\right)^{k_1} \left(\frac{1}{E_1}\right)^{k_3} \quad (2)$$

Where,

k_1, k_2, k_3 = *Laboratory regression coefficients*

C = Laboratory to field adjustment factor

The most commonly used model form to predict the number of load repetitions to fatigue cracking is a function of the tensile strain and mix stiffness (modulus). The critical locations of the tensile strains may either be at the surface (result in top-down cracking) or at the bottom of the asphaltic layer (result in bottom-up cracking).

Some of these models were developed to best suit specific characteristics of a particular institute, and some were just the output of an extensive laboratory testing. Many other fatigue cracking models available in literature are listed in Table 2.3.

Table 2.3: Different Types of Fatigue Cracking Models of Different Agencies

Sl No.	Equation	Agency/Equation Name	Source/ Reference
1	$N_f = 0.0796\ (\varepsilon_t)^{-3.2914}\ (E_1)^{-0.854}$	Asphalt Institute Method by AI (1981)	Yang 1993
	$N_f = 0.00432\ C\ (1/\varepsilon_t)^{3.291}(1/E_1)^{0.854}$		NCHRP 2004 ; Walid 2001
2	$Nf = 0.0685\ (\varepsilon_t)^{-5.671}\ (E_1)^{-2.363}$	Shell Design Method by Shell Oil, Shook (1982)	Yang 1993
	For Constant Strain: $N_{f\varepsilon} = 13909 A_f K_{1\alpha}(\varepsilon_t)^5 (E^{-1.8})$ *For Constant Stress:* $N_{f\sigma} = A_f K_{1\alpha}(\varepsilon_t)^5 (E^{-1.4})$		NCHRP 2004
3	$N_f = 5(10^{-6})(\varepsilon_t)^{-3}$	Illinois Department of Transportation by Thompson (1987)	Yang 1993
4	$N_f = 1.66(10^{-10})*(\varepsilon_t)^{-4.32}$	Transport and Road Research Laboratory by Powell (1984)	Yang 1993; Walid 2001
5	$N_f = 4.92(10^{-14})(\varepsilon_t)^{-4.76}$	Belgian Road Research Center (BRRC) by Verstraeten (1984)	Walid 2001
6	$N_f = 9.33\ 10^{-7}\ \varepsilon_t^{-3.84}$	Arizona Dot Model developed by Arizona Department of Transportation	Walid 2001
7	$N_f = 9.73\ 10^{-15}\ \varepsilon_t^{-5.16}$	Federal Highway Administration Model	Salem 2008; Walid 2001
8	$N_f = 497.156\ (\varepsilon_t)^{-5}\ (E_1)^{-2.665}$	U.S. Army Corps of Engineering by Department of Defense (1988)	Salem 2008; Walid 2001

Sl No.	Equation	Agency/Equation Name	Source/ Reference
9	$Log\ N_f = 15.947\text{-}3.291\ log\ (\varepsilon t\ /10^{-6})\text{-}0.854\ log\ (E/10^3)$	Washington Department of Transportation	Walid 2001
10	$N_f = 7.56E^{-12}\ (\varepsilon_t)^{-4.68}$	Austin Research Engineers (ARE)	Walid 2001
11	$N_f = 0.0636\ (\varepsilon_t)^{-3.291} (E_1)^{-0.854}$	UC-Berkeley by Craus (1984)	Hsiang et al 2007
12	$N_f = 0.1001\ (\varepsilon_t)^{-3.565} (E_1)^{-1.474}$	Indian by Das, Pandey (1999)	Hsiang et al 2007
13	$N_f = 2.83\ 10^{-7}\ (\varepsilon_t)^{-3.21}$	Mn/ROAD by Timm (2003)	Hsiang et al 2007

The rutting model used in the DARWin-ME which is considered for local calibration is shown in Table 2.6.

Table 2.4: Fatigue Cracking Model used in the DARWin-ME

AC Fatigue Equation	Coefficients
$N_f = 0.00432\ C\ Bf_1\ k_1(1/\varepsilon_t)^{k_2 Bf_2}(E_1)^{k_3 Bf_3}$	k_1= 0.007566
	k_2= 0.39492
$C = 10^M$	k_3= 1.281
$M = 4.84\ (V_b\ /(V_a+V_b)) - 0.69$	Bf_1=1
	Bf_2=1
	Bf_3=1
	Va= air voids (%), which is material input variable
	V_b= effective binder content (%),which is material input variable

Rutting Models:

Vertical compressive strains on the top of subgrade of asphalt pavement are important pavement response to predict the potential subgrade rutting in HMA pavements. Several rutting models are developed to relate the asphalt modulus and/or the measured strains to the number of load repetitions to pavement failure. Most of the rutting failure models take the following form:

$$N_d = = f_4 (\varepsilon c)\text{-}^{f_5} \quad (3)$$

Where,

N_d = *number of load repetitions;*

ε_c = *Vertical compressive strains on the top of subgrade*

Different rutting models are found from literatures and listed in Table 2.5.

Table 2.5: Different Rutting Models of Different Agencies

Sl No.	**Equation**	**Agency/Equation Name**	**Source/ Reference**
1	$N_d = 1.365\ 10^{-9} (\varepsilon_c)^{-4.477}$	AI Method	Yang 1993
2	*For 50% Reliability,* $N_d = 6.1510^{-7} (\varepsilon_c)^{-4}$	Shell Design Method by Shell Oil	Yang 1993
3	*For 85% Reliability,* $N_d = 1.94\ 10^{-7} (\varepsilon_c)^{-4}$		Yang 1993
4	*For 95% Reliability,* $N_d = 1.0510^{-7} (\varepsilon_c)^{-4}$		Yang 1993
5	$N_d = 6.18\ 10^{-8} (\varepsilon_c)^{-3.95}$	U.K. Transport and Road Research Laboratory	Yang 1993
6	$N_d = 3.0510^{-9} (\varepsilon_c)^{-4.35}$	BRRC	Yang 1993
7	$N_d = 1.807\ E_1^{-15} \times (\varepsilon_c)^{-6.527}$	U.S. Army Corps of Engineering by Department of Defense (1988)	Salem 2008
8	$N_d = 1.13\ 10^{-6} (\varepsilon_c)^{-3.570}$	Transport and Road Research Laboratory	Salem 2008
9	$N_d = 1.337\ 10^{-09} (\varepsilon_c)^{-4.484}$	CHEVRON	Salem 2008

Sl No.	Equation	Agency/Equation Name	Source/ Reference
10	$N_d = (0.008511/\varepsilon_c)^{7.14}$	Austroads	Wardle 1998
11	$N_d = 1.07710^{18} (10^6/\varepsilon_c)^{4.4843}$	Other Method	Jackson and Mahoney 2007
12	$N_d = 4.1656\ 10^{-8} (1/\varepsilon_c)^{4.5337}$	Other Method	Mathew and Rao 2007

The rutting model used in the DARWin-ME which is considered for local calibration is shown in Table 2.6.

Table 2.6: Rutting Model Used in the DARWin-ME

Rutting Equation	Coefficients
$\varepsilon_p/\varepsilon_r = k_z B_{r1} (10)^{k_1} (T)^{k_2 B_{r2}} (N)^{k_3 B r_3}$	$k_1 = -3.35412$
$k_z = (C_1 + C_2\ (Depth))\ 3.28196^{Depth}$	$k_2 = 1.5606$
$C_1 = -0.1039\ H_{ac}{}^2 + 2.4868\ H_{ac} - 17.342$	$k_3 = 0.4791$
$C_2 = 0.0172\ H_{ac}{}^2 - 1.7331\ H_{ac} + 27.428$	$B_{r1} = 1$
Where,	$B_{r2} = 1$
H_{ac}= Total AC Thickness in inch	$B_{r3} = 1$
ε_p= Plastic Strain (in/in)	
ε_r= Resilient Strain (in/in)	
T= Layer Temperature (^{0}F)	
N= Number of Load Repetitions	
And, $RD = \sum_{i=1}^{n} \varepsilon p_i\ h_i$	
Where,	
RD = pavement permanent deformation	
n = number of sublayers	
εp_i = total plastic strain in sublayer i	
h_i = thickness of sublayer i	

Thermal Cracking Models

The procedure requires the characterization of the HMA mix in an indirect tensile mode to measure the creep compliance at one or three temperatures depending on the level of analysis. Thermal fracture analysis in the MEPDG is based on the visco-elastic properties of the asphalt mixture.

The thermal cracking model is an enhanced version of the approach originally developed under the Strategic Highway Research Program (SHRP) A-005 research contract. The amount of crack propagation induced by a given thermal cooling cycle is predicted using the Paris law of crack propagation.

$$\triangle C = A(\triangle K)^n \quad (4)$$

Where,

ΔC = Change in the crack depth due to a cooling cycle,

ΔK = Change in the stress intensity factor due to a cooling cycle, i.e., the difference between the stress intensity factor at maximum and minimum loading and

A, n = Fracture parameters for the HMA mixture.

The degree of cracking is predicted by the MEPDG using an assumed relationship between the probability distribution of the log of the crack depth to HMA-layer thickness ratio and the percent of cracking. The following equation shows the expression used to determine the extent of thermal cracking (AASHTO. 2008).

$$TC = \beta\, t_1\, N[1/\sigma_d \operatorname{Log}(C_d/H_{HMA})] \quad (5)$$

Where,

TC = Observed amount of thermal cracking, ft/mi,

β_{t1} = Regression coefficient determined through global calibration

Nz = Standard normal distribution evaluated at [z],

σ_d = Standard deviation of the log of the depth of cracks in the pavement

C_d = Crack depth, in., and

H_{HMA} = Thickness of HMA layers, in

The thermal cracking model used in the DARWin-ME which is considered for local calibration is shown in Table 2.7.

Table 2.7: Thermal Cracking Model Used in the DARWin-ME

Thermal Cracking Equation	**Coefficients**
$C_f = 400\ N(\frac{\log C/\ \ H_{ac}}{6})$ $\triangle C = (k\beta_t)^{n+1}\ A\ \triangle K^n$ $A = 10^{(4.389-2.52\log(E6m\ n)}$ Where, C_f = Observed amount of Thermal Cracking in ft/500ft k= Regression coefficient determined through field calibration N()= Standard Normal Distribution evaluated at () б= Standard deviation of the log of the depth of cracks H_{ac}= Total AC Thickness in inch △C= Change in crack depth due to a cooling cycle △K= Change in the stress intensity due to a cooling cycle A, n= Fracture parameter for the asphalt mixture E=Mixture stiffness $б_m$ = Undamaged mixture tensile strength β_t = Calibration Parameter	*k= 1.50 for level 1* *k= 0.50 for level 2* *k= 1.50 for level 3*

IRI Models

Distresses predicted by the mechanistic-empirical models, such as fatigue cracking, permanent deformation and thermal cracking are correlated to smoothness. In addition the smoothness model optionally considers other distresses, such as potholes, longitudinal cracking outside the wheel path, and block cracking if there is potential of occurrence.

The design premise included in the MEPDG for predicting smoothness degradation is that the occurrence of surface distress will result in increased roughness (increasing IRI value), or in other words, a reduction in smoothness. (AASHTO 2008).

$$IRI = IRI_0 + 0.150(SF) + 0.400(FC\ Total) + 0.0080(TC) + 40.0(RD) \quad (6)$$

Where,

IRIo = Initial IRI after construction in in/mi,

SF = Site factor,

FC Total = Area of fatigue cracking (combined alligator, longitudinal, and reflection cracking in the wheel path), percent of total lane area. All load related cracks are combined on an area basis-length of cracks is multiplied by 1 ft to convert length into an area basis,

TC = Length of transverse cracking (including the reflection of transverse cracks in existing HMA pavements), ft/mi, and

RD = Average rut depth in in.

The site factor (SF) is calculated in accordance with the following equation.

$$SF=Age[0.2003(PI+1)+0.007947(Precip+1)+0.000636(FI+1) \quad (7)$$

Where,

Age = Pavement age, yr,

PI = Percent plasticity index of the soil,

FI = Average annual freezing index, ^{O}F days, and

Precip = Average annual precipitation or rainfall, in.

2.5 Calibration of MEPDG Distress Models: Global Calibration

Calibration is a systematic process to eliminate any bias and minimize the residual errors between observed or measured results from the real world (e.g., the measured mean rut depth in a pavement section) and predicted results from the model (e.g., predicted mean rut depth from a permanent deformation model). This is accomplished by modifying empirical calibration parameters or transfer functions in the model to minimize the differences between the predicted and observed results.

These calibration parameters are necessary to compensate for model simplification and limitations in simulating actual pavement and material behavior.

The primary objective of model calibration is to reduce bias. A biased model will consistently produce either over-designed or under-designed pavements, both of which have important cost consequences. The secondary objective of calibration is to increase precision of the model predictions.

A model that lacks precision is undesirable because it leads to inconsistency in design effectiveness including some premature failures. As part of the calibration process, predicted distress is compared against measured distress and appropriate calibration adjustment factors are applied to eliminate significant bias and maximize precision in the model predictions.The MEPDG combines empirical procedures with mechanistic procedures. In MEPDG, calibration is defined to reduce the the total error between the measured and predicted distresses by varying the appropriate model coefficients. In global calibration process, generally three important steps are followed (Dzotepe and Ksaibati 2010):

Step One: perform verification runs on pavement sections using the calibration factors from the national calibration effort.

Step Two: This involves calibrating the model coefficients to eliminate bias and reduce standard error between the predicted and measured distresses. Once this is accomplished and the standard error is within the acceptable level set by the user, the validation process is advanced.

Step Three: Validation, the third step, is used to check if the models are reasonable for performance predictions. The validation process determines if the factors are adequate and appropriate for the construction, materials, climate, traffic and other conditions that may be encountered within the system. This is done by selecting a number of independent pavement sections that were not used in the local calibration effort and testing those. Figure 2.5 shows the framework of the global calibration of distress models.

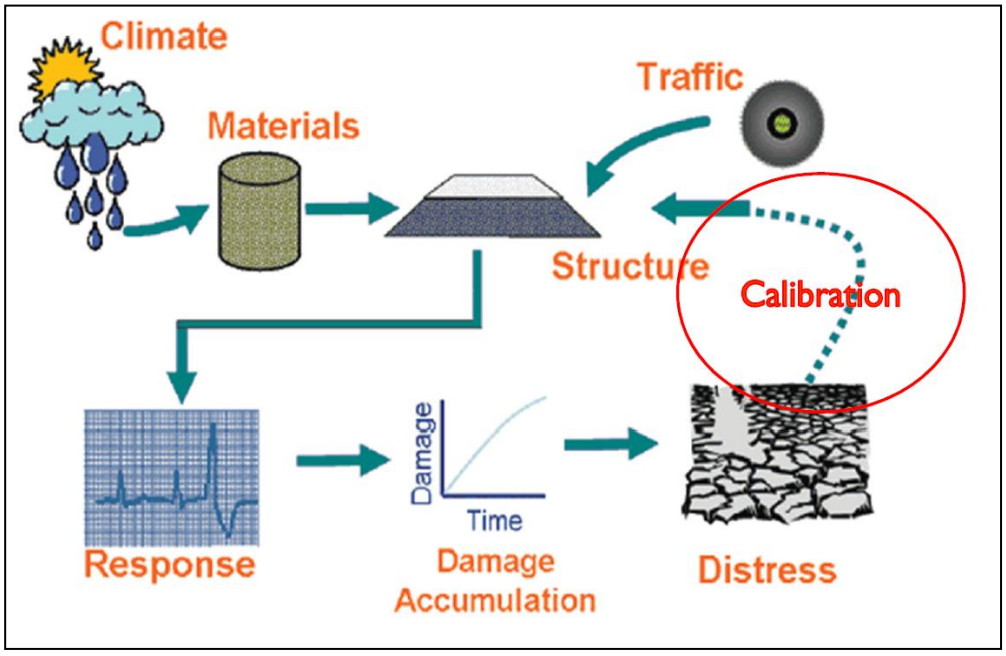

Figure 2.5: Framework for Global Calibration of MEPDG Distress models

(Xiao et al. 2010)

In the M-E design procedures for flexible pavements, the primary transfer functions are those that relate (a) maximum tensile strain in the HMA surface layer to fatigue cracking and (b) compressive strain at the top of the subgrade layer to rutting at the surface. These functions, called fatigue and rutting equations, are derived from statistically based correlations of pavement condition with observed different laboratory specimen performance, full-scale road test experiments or by both methods.

Fatigue Cracking Models:

Appendix II-1 of Guide for Mechanistic-Empirical Design of New and Rehabilitated Pavement Structures (NCHRP 2004) analysed the calibration of these fatigue cracking models for flexible pavements. That study focused on the selection, development, of calibration and validation

aspects of the fatigue cracking models selected for the design guide. Both types of fatigue cracking (bottom up and top down) are discussed separately. This study mainly discussed about two widely used fatigue models (AI and Shell method) and evaluated for inclusion in the design guide. For calibration, each model is evaluated based on the data collected from the LTPP database.

Fatigue cracking prediction is normally based on the classic Miner's rule for cumulative damage for metallic materials (Yang 1993). The damage is generally calculated as the ratio of the predicted number of traffic repetitions to the allowable number of load repetitions (to some failure level) as shown in equation 8. Theoretically, fatigue cracking should occur at an accumulated damage value of 1. If a normal distribution is assumed for the damage ratio calculated, the percentage of area cracked can be computed and checked with field performance (NCHRP 2004).

Thus,

$$D = \sum_{i=1}^{T} \frac{ni}{Ni} \qquad (8)$$

where,

D = damage.

T = total number of periods.

n_i *= actual traffic for period i.*

N_i *= allowable failure repetitions under conditions prevailing in period i.*

The fatigue-cracking model, which calculates the number of cycles to failure is only expressing the stage of fatigue cracking described as the crack initiation stage. The second stage, or vertical crack propagation stage, is accounted for in these models by using the field adjustment factor. Other models in the literature use two different equations to express each stage of the fatigue cracking.

In calibration of the models (NCHRP 2004), two types of controlled loading are generally applied for fatigue characterization: constant stress and constant strain in the laboratory. In constant stress (load) testing, the applied stress during the fatigue testing remains constant. As the repetitive load causes damage in the test specimen, the stiffness of the mix is decreased due to the micro cracking observed. This, in turn, leads to an increase in tensile strain with load repetitions. In the constant strain test, the strain remains constant with the number of repetitions. Because of specimen damage due to the repetitive loading; the stress must be reduced to obtain the same strain. This leads to a reduced stiffness as a function of repetitions. The constant stress type of loading is generally considered applicable to thick asphalt pavement layers usually more than 8 inches. The constant strain type of loading is considered more applicable to thin asphalt pavement layers usually less than 2 inches. However, for intermediate thicknesses, fatigue life is generally governed by a situation that is a combination of constant stress and constant strain.

The Shell Oil Co. has developed fatigue damage prediction equations for the two major forms of laboratory fatigue testing: for constant stress and constant strain, since the known impact between stress states and damage mechanism for different thicknesses of asphalt layers. In this model, K_1 value in the equations is replaced by the $K_{1\alpha}$ value which represents the K_1 value for the constant stress situation.

For Constant Strain: $N_{f\varepsilon} = 13909 A_f K_{1\alpha} (\varepsilon_t)^5 (E^{-1.8})$ *(9)*

For Constant Stress: $N_{f\sigma} = A_f K_{1\alpha} (\varepsilon_t)^5 (E^{-1.4})$ *(10)*

Taking the ratio of the two above equations results in the following relationship (NCHRP, 2004):

$$N_{f\varepsilon} = F * N_{f\sigma} \quad (11)$$

where,

F = the ratio between the constant strain and constant stress and is a function of the modulus (E) of asphalt layer

The F values are determined for the two extreme conditions: constant strain (thickness <= 2 inch) and constant stress situation (thickness => 8 inch). In order to have a continuous function between constant strain and stress conditions, it is assumed that a sigmoidal relationship, between the two F conditions and all intermediate thickness (2 inches to 8 inches), would be applicable.

On the other hand, the AI's fatigue equation is based upon modifications to constant stress laboratory fatigue criteria. The number of load repetitions to failure is expressed in the same mathematical form as the Shell Oil model and can be expressed as (NCHRP 2004):

$$N_f = .00432\, C\, (1/\varepsilon_t)^{3.291} (1/E_1)^{0.854} \quad (12)$$

where, $C = 10^M$; and

$$M = 4.84[\{V_b/(V_a + V_b)\} - 0.69] \quad (13)$$

where,

V_b = *effective binder content (%).*

V_a = *air voids (%)*

Comparing the Shell Oil model to the MS-1 (AI) model, it is found that both models are exactly the same form. However, the coefficients are less for the MS-1 model compared to the Shell Oil. This would be reasonable to accept because the Shell Oil relationships are based upon laboratory testing while the MS-1 equation (derived from NCHRP 1-10) was heavily based upon actual field calibration studies.

In Appendix II-1 (NCHRP 2004), the asphalt concrete mix fatigue-cracking models (both bottom-up cracking and top-down cracking) were calibrated following the process noted below:

a) Calibration (performance) data is collected from the LTPP database for each field section.
b) Simulation (predictive) runs are done using the 2002 design guide software and using a different set of calibration coefficients in the number of load repetition model.
c) The predicted damage from each calibration coefficient combination is compared to the measured cracking observed in the field. The coefficient combination with the least scatter of the data and the correct trends is selected.
d) The predicted damage is correlated to the measured cracking in the field by minimizing the square of the errors.

The calibration data collection is done at the same time for both types of fatigue cracking as the same sections were used for both bottom-up and top-down cracking calibration.

2.6 Current Practice of Local Calibration

Pavement performance prediction models contained in the current MEPDG were calibrated primarily using data from the LTPP. Due to the possible differences between 'national' and 'local' conditions – including climate, material properties, traffic patterns, construction and maintenance activities – pavement performance predicted by the MEPDG should be compared to and verified against local experience. Now-a-days, different states are reporting either a partial or full calibration of the MEPDG on a local level. All performance indicator prediction models in the MEPDG were calibrated to observed field performance from a representative sample of pavement test sites located throughout North America. These models are defined as being globally calibrated. Data from the LTPP test sections were used extensively in the global calibration process, because of their consistency in the monitored data over time and the diversity of test sections spread throughout North America. Other experimental test sections, such as Minnesota Road (MnRoad) and Vandalia, were also included in the global calibration process.

Ali and Tayabji (1998) evaluated and calibrated MEPDG performance models using the LTPP data for specific loading and environmental conditions of the selected pavements. The predicted performances are compared with actual fatigue cracking and rutting observed in these pavements. Although more data are required to arrive at a more conclusive evaluation, fatigue

cracking models appeared to be consistent with observations, whereas rutting models showed poor agreement with the observed rutting.

Schram and Abdelrahman (2006) used Roads Pavement Management System data of Nebraska to calibrate two smoothness models in the Design Guide at the local project level. The data set is categorized by annual daily truck traffic and surface layer thickness. From the study results, it is revealed that that project-level calibrations reduced default model prediction error by nearly twice that of network-level calibration. This study offers a window into the accuracy that can be achieved with local focus calibrations of design guide prediction models.

Moulthrop and Quintus (2007) calibrated MEPDG distress transfer functions for flexible and semi-rigid pavements HMA overlays constructed in Montana. Global calibration coefficients included in Version 0.9 of the MEPDG were used initially to predict the distresses and smoothness of the Montana calibration refinement test sections to determine any prediction model bias. Material test data together with historical traffic and climatic data are used to predict rutting and fatigue cracking in the HMA layer and rutting in the unbound layers. The results show that fatigue cracking (bottom up) model is reasonable, a local calibration factor for predicting thermal cracking is developed, but for top-down fatigue cracking model no consistent trend in the predictions is not identified to reduce bias and standard error.

Kang and Adams (2007) calibrated two important calibration factors (longitudinal and alligator fatigue cracking models). Pavement performance data are collected to manage the calibration data from state transportation agencies in Michigan, Ohio, and Wisconsin. Calibration factors are then derived by minimizing the differences between observed and predicted pavement

performance. The pavement performance field data in Wisconsin are collected for calibration initially, and the distresses predicted with these calibration factors are compared to pavement field performance in the other states. These calibrated models in the MEPDG assure the reliable prediction of pavement distress, such as longitudinal and alligator cracks. The results of this study are shown in Table 2.8.

Table 2.8: Local Calibration Factors for Prediction Models in the MEPDG

(Ref Table 4, Kang and Adams 2007)

Type	**Parameter**	**Formula**	**Calibration Factor**	**Default Value**	**Recommended Calibrated Values**
Flexible	Fatigue	$N_f = \beta_{f1} k_1 (\varepsilon_t)^{-\beta_{f2}k2} (E_1)^{-B_{f3}k3}$	β_{f1} $\mathcal{B}_{f2}$ $\mathcal{B}_{f3}$	1.0 1.0 1.0	1.0 1.2 1.5
	Longitudinal cracking	$F.C = \frac{1000}{1 + e^{c1 - c2 * LogD}} * (10.56)$	c_1 c_2	7.0 3.5	Default Default
	Alligator cracking	$F.C = \frac{6000}{1 + e^{c1 - c2 * LogD}} * (1/60)$	c_1 c_2	1.0 1.0	Default Default

Velasquez et al.(2009) analyzed the performance prediction and evaluated of different types of flexible and rigid pavements for local conditions. To achieve these objectives, the MnDOT and LRRB initiated a study “Implementation of the MEPDG for New and Rehabilitated Pavement Structures for Design of Concrete and Asphalt Pavements in Minnesota.” Performance prediction models of the latest version of the MEPDG are evaluated and modified or

recalibrated to reduce bias and error in performance prediction for Minnesota conditions. The performance models: rutting, alligator cracking, transverse cracking and IRI are investigated. The results show that local adaptation for Minnesota conditions require modification of the MEPDG rutting model for base and subgrade, as well as modification of the coefficients for the MEPDG fatigue cracking model and thermal cracking for flexible pavements. However, the use of the longitudinal cracking model is not recommended for adaptation, the IRI model could not be locally calibrated.

Siraj et al (2009) verified the accuracy of the predicted performance from the MEPDG software for the state of New Jersey for level 2 and level 3 inputs. In this study the MEPDG distress models for rutting, alligator cracking, longitudinal cracking, thermal cracking, and roughness (IRI) are verified. In this verification, nine LTPP and sixteen non-LTPP sections in the state of New Jersey are evaluated. The level 3 material input and level 2 traffic input are used during the analysis. The M-EPDG version 1.0 software is used for analysis. The input data and measured field performance data are collected from multiple sources. Form the analysis it is found that the average difference between measured rutting and the average predicted asphalt concrete layer rutting is statistically insignificant at 95% confidence level. The measured longitudinal cracking, thermal cracking and roughness (IRI) are found statistically similar to the predicted values. In addition the difference between measured and predicted alligator cracking is reasonable considering the error of field measured data, and prediction error due to level 3 material input.

Hoegh et al. (2010) conducted local calibration of rutting model using time history rutting performance data for pavement sections at the MnDOT full-scale pavement research facility. In this study, detailed comparison of the predicted total rutting, asphalt layer rutting, and measured

rutting is shown. Here, the MEPDG inputs that closely represent the asphalt MnRoad sections, are obtained as first step of methodology. Then the MEPDG software for flexible test sections are run to obtain predicted rutting. Predicted and measured rutting for asphalt test sections are compared to recalibrate rutting model of the MEPDG by adjusting the parameters by reducing error between predicted and measured performance. The paper also explains the reasons for not finding the conventional MEPDG model calibration as feasible and recommends a modification of the rutting model. Finally, the results show that the locally calibrated models are less biased than the predictions using the nationally calibrated rutting models.

Hall et al. (2010) summarized the initial local calibration of flexible pavement models in the MEPDG for Arkansas. Pavement performance prediction models are calibrated using data from the LTPP. In this study, the states are reporting either a partial or full calibration of the MEPDG on a local level because of the potential differences between 'national' and 'local' conditions. For the current MEPDG, predicted distresses did not accurately reflect measured distresses, particularly for longitudinal and transverse cracking. However, due to the lack of measured transverse cracking, the transverse cracking model is not calibrated. Calibration coefficients are optimized for the alligator cracking and longitudinal cracking models minimizing the sum of standard error. It is found that the alligator cracking and longitudinal cracking models are improved by calibration. Finally, the procedure for local calibration of the MEPDG using LTPP and PMS data in Arkansas is established.

2.7 Summary

In this chapter, the MEPDG, the basis of DARWin-ME software, distress models and requirement issue for local calibration are discussed. The materials, climate and traffic of highways are different for different locations. For these reasons, the previous empirical generalized methods are considered as less accurate and also less precise in predicting the performance of pavement. Now, the important aspect is to evaluate the performance prediction models, re-calibration of the performance prediction models for Ontario local conditions. Based on the described basic concepts, the analysis framework and input data requirements can be developed.

Chapter 3

CALIBRATION DATABASE DEVELOPMENT

This chapter discusses the requirement and development of the local calibration database. The detailed input requirements and their level of accuracy are discussed step by step. The method of selecting the road section cycles is also discussed. The condition rating process for distresses and IRI practiced in Ontario is shown accordingly. Finally a hierarchical framework of input data along with level of accuracy is developed for the analysis.

3.1 Data Requirement for Local Calibration

Local calibration is a process of fitting the observed pavement distress data against the predicted pavement damage from the MEPDG design software outputs. Therefore, data required for the local calibration basically are of two types: observed distress data (or field pavement condition data) and data of corresponding pavement distress predictions. For the latter, they are also the input data for pavement analysis and design.

As discussed in Chapter 1, the observed pavement distress data are retrieved from the MTO's PMS system. However, the pavement condition data cannot be used directly without any modification for the local calibration. Screening, selection and conversion are necessary steps before they can be integrated into the calibration database. These steps are explained in detail in Section 3.3 and 3.4.

The prototype computational software used to be available online and free for evaluation. However, this has been terminated since September 2011. Pavement engineers who would like to use MEPDG for pavement design are suggested to use DARWin-ME. DARWin-ME is the AASHTOWare pavement design software that builds upon the MEPDG, and expands and improves the features in the prototype software. DARWin-ME supports AASHTO's MEPDG, Interim Edition: A Manual of Practice (AASHTO 2011). In this study, DARWin-ME is used for pavement analysis, with the understanding that it will most likely be used for day-to-day pavement design in future. Therefore, the following discussions on the input requirement for pavement analysis and design are based on DARWIN-ME. The pavement distress models to be locally calibrated will then be those prescribed in the AASHTO Manual of Practice. In DARWinME, three major categories of the input variables for the evaluation of pavement distresses are required. These are

i) Traffic data

ii) Climate data

iii) Properties of Materials/ Structure

3.2 Accuracy Levels of Input Data

DARWin-ME allows input data at three levels depending on the importance of the project and the availability of resources (AASHTO 2011), as described below.

Level 1: inputs generally are the most accurate that a certain type of data can be. For example, site-specific and laboratory data or results of actual field testing are considered as Level 1 input. Generally, for material properties, laboratory test values are used for

this level (e.g., dynamic modulus master curve for asphalt concrete, nonlinear resilient modulus for unbound materials). For traffic, site specific traffic data (AADTT, lane number, growth factor, etc.) are required.

Level 2: input parameters are estimated from mathematical correlations or regression equations. In some cases, the input value is calculated or estimated from other site specific data (or taken from similar properties). Regional values are also used as level 2 input, whenever project or site specific values are not available. For material properties, inputs can be obtained through empirical correlations with other parameters (e.g., resilient modulus estimated from CBR values). For traffic, region specific data (axle configuration, truck vehicle classification, etc.) are used for analysis.

Level 3: input parameters are the least accurate. They are normally default values or based on best estimates. Generally, national level or regional level values are used.

In DARWin-ME, normally three levels of accuracy are incorporated in the input for traffic and materials. The climate data, however, is fixed and does not have a hierarchical input level. It is input from a climate database and installed in the software.

These three levels of accuracy provide design engineers with convenience and flexibility in practical pavement designs. Depending on the actual need and resources available, the design engineers shall decide how accurate the design input data should be. The recently published AASHTO guide for local calibration (AASHTO 2010) pointed out the importance of the selection of hierarchical input level for the inputs. Highest accuracy levels in the LTPP database

were used for the global calibration and recalibration under NCHRP 1-37A (completed in 2004) and 1-40D (completed in 2006), respectively. However, the local calibration guide (AASHTO 2010) seemed to suggest using the same accuracy levels for local calibration as the agency would use for future design. This may be inefficient because the benefits from extra effort for obtaining more accurate input data for local calibration could easily outweigh the efforts made for a single design. The main objective of local calibration is to reduce the bias and variability of the performance prediction models. For this purpose, the highest levels of input, which are not necessarily Level 1, should be used and are used in this study.

3.3 Selection of Pavement Sections

A guiding principle for the selection of pavement sections is efficiency of local calibration, which means a balance between the efforts of data collection and benefits from local calibration in terms of eliminating biases and maximizing precision. Two questions need to be answered: how many test pavement sections (i.e., sample size) should be used and which sections should be used? The AASHTO guide for local calibration (AASHTO 2010) recommends two statistical equations to determine the sample size. Based on the variability of the LTPP data, the guide provides minimum numbers of test sections for each distress, and they are no more than 30 section. The AASHTO guide also recommends the use of fractional factorial design to pick up test sections. This recommend is followed in this project.

As of the end of 2010, the historical pavement condition data stored in the MTO PMS2 database reached more than 30,000 section-years for the 1794 pavement sections. The pavement distress data cover the whole record period starting from 1985, when the PMS was first put in service in the MTO. During the period from 1985 to 2010, many pavement sections have undergone

several rehabilitation cycles. In this study, the sections with service life of more than 4 years are selected since the pavement performance curve with cycle length of less than 4 years will not capture the realistic trend of performance quality of that section.

Preliminarily, 5,555 pavement section cycles from PMS-2 are selected based on the quality of the performance curve of section cycle. The sections are selected considering all regions (east, west, south and north), highway types (King's highway or secondary), facility types (freeway, arterials, collectors), number of lanes (2,3, and 4 lanes), lengths of section and also quality of performance curves in terms of pavement condition index (PCI) and distress manifestation index (DMI). Based on the availability of rehabilitation history, detailed rehabilitation type, performance condition rating, and distress history the selection is further screened. Finally 101 section cycles from 66 road sections are selected for the empirical calibration. In addition, 46 road sections are selected for future validation of locally calibrated models. The purpose of the validation is to verify the calibrated predicted values and database. For these selected pavement sections, their design input data are then collected with assistance from MTO staff and verified to ensure the data is reliable. After all these data has been cross-verified, they are then combined to create a unified database for the use of local calibration.

3.4 Observed Distress and Smoothness Data

The MTO PMS2 follows a pavement performance condition rating standard (shown in Table 3.1) that is slightly different from the AASHTO condition evaluation manual. For each asphalt concrete pavement section, 14 types of surface distress ranging from raveling, flushing, to wheel-path rutting, distortion, and to various types of cracking are evaluated in terms of extent and severity at a scale from 0 to 5. Among the many cracking types, the wheel-path alligator

cracking is considered to the manifestation of fatigue cracking due to traffic loading (Bottom-up fatigue cracking), whereas the wheel-path longitudinal cracking corresponds to the top-down cracking predicted by the MEPDG model. The transverse cracking is considered to be mainly caused by thermal cracking.

In PMS-2 the IRI values are not recorded before 1997, the IRI values are estimated for the section cycles starting in 1997 or before 1997 using the following equation:

$$RCI = Max (0, Min (10, 8.5 – 3.02 \times \ln (IRI)))$$

The initial rutting depth was not recorded in the PMS-2 before 1997. For this reason, a minimum initial rut depth of 4.0 mm (which is average initial rut depth of the available rut depth record after 1997 to onwards) are considered for those section cycles starting before 1997. For bottom up (alligator) cracking, field observed values are converted to extent of occurrence following manual for condition rating of flexible pavements (Chong et al 1989) which are shown in Table 3.1. In this study, the field condition ratings from PMS-2 are converted to extent of occurrence in percentage. Midpoint values are used for the ranges.

Table 3.1: Condition Rating of Extent of Distress for Flexible Pavement

Condition Rating	**Extent of Occurrence**	**Density of Distress**
1	<10%	Few
2	10-20%	Intermittent
3	20-50%	Frequent
4	50-80%	Extensive
5	80-100%	Throughout

3.5 Major Inputs of DARWin-ME

The input data required for the DARWin-ME analysis are summarized and discussed step by step for traffic, climate and materials properties. The steps of input level are discussed below.

3.5.1 General Information

In DARWin-ME, some general information including design life, existing pavement constructions date, pavement overlay construction date, traffic open date, and new construction or rehabilitation history are required. Site specific level 1 data are required for this stage.

For analysis, site specific information is collected from Ontario PMS-2 database for each pavement section cycle. The design life is considered as the original cycle length of the pavement section for that certain cycle. All general information, traffic information, location information of all selected pavement section cycles are summarized in the database.

3.5.2 Traffic Data

The DARWin-ME traffic inputs include traffic volume adjustment factors, axle load distribution factors and general traffic inputs. It uses the concept of load spectra for characterizing traffic. Each axle type (e.g., single, tandem) is divided in a series of load ranges. Vehicle class distributions, daily traffic volume, and axle load distributions define the number of repetitions of each axle load group at each load level. This software does not incorporate equivalent single-axle loads (ESALs) as is the case in the current design guide, but instead were developed around axle load spectra. Full axle load spectra traffic inputs are used for estimating the magnitude, configuration, and frequency of traffic loads. The approach analyses the effects of actual traffic on pavement response and distress.

The site-specific traffic data are collected and if that is not possible, site-related, regional, or agency-wide traffic data (e.g. truck traffic classification) is substituted. The DARWin-ME software also includes default axle load spectra and other traffic parameters if no other sources of traffic data can be obtained. Throughout the analysis of traffic data in the DARWin-ME there are many elements used. Some of the major elements are as follows:

i. Truck Volume and Highway Parameters: Truck volume is calculated multiplying traffic (Average Annual Daily Traffic (AADT)) volume with the percentage of heavy trucks of FHWA class 4 or higher. The result is Average Annual Daily Truck Traffic (AADTT).
ii. Number of lanes in the design direction: This presents the number of lanes present in the design direction.
iii. Percent trucks in design lane: This defines the percentage of trucks in the design direction expected to use the design lane (typically the outer right lane).
iv. Operational speed (kph): This defines the expected speed of traffic traveling in the design lane.
v. Average axle width (m): This defines the distance in feet between two outside edges of an axle. DARWin-ME provides a default value of 2.59 meter.
vi. Dual tire spacing (mm): This defines the transverse distance in inches between the centers of a dual tire. This value is calculated from WIM data measured over time by averaging the distance measured between the dual tires of a tandem, tridem, or quad axle for each truck class. DARWin-ME provides a default value of 305 mm.
vii. Tire pressure (kPa): This defines the hot inflation pressure of tires in pounds per square inch. It is assumed that the hot inflation pressure equals the contact pressure and is 10% above cold inflation pressure. DARWin-ME provides a default value of 827.4 kPa.

viii. Tandem axle spacing (m): This defines the center-to-center longitudinal spacing in inches between two consecutive axles in a tandem configuration. This value is calculated using WIM data by averaging distance measured between the tandem axles for each truck class. DARWin-ME provides a default value of 1.31 meter.

ix. Tridem axle spacing (m): This defines the center-to-center longitudinal spacing in inches between two consecutive axles in a tridem configuration. This value is calculated using WIM data by averaging distance measured between the tridem axles for each truck class. DARWin-ME provides a default value of 1.25 meter.

x. Quad axle spacing (m): This defines the average distance in inches between two consecutive axles in a quad configuration. This value is calculated using WIM data by averaging distance measured between the quad axles for each truck class. DARWin-ME provides a default value of 1.25 meter.

xi. Mean wheel location (mm): This defines the distance in inches from the outer edge of the wheel to the pavement marking. DARWin-ME provides a default value of 460 mm.

xii. Traffic wander standard deviation (mm): This defines the divergence from average in inches of the lateral traffic wander. This standard deviation is used to estimate the number of axle load repetitions over a single point in a probabilistic manner for predicting distress and performance. DARWin-ME provides a default value of 254 mm.

xiii. Design lane width (m): This defines the distance in feet between the lane marking on either side of the design lane. DARWin-ME provides a default value of 3.7 meter.

xiv. Average spacing of short axles (m): This defines the average longitudinal spacing in feet of short axles. DARWin-ME provides a default value of 3.66 meter.

xv. Average spacing of medium axles (m): This defines the average longitudinal spacing in feet of medium axles. DARWin-ME provides a default value of 4.57 meter.

xvi. Average spacing of long axles (m): This defines the average longitudinal spacing in feet of long axles. DARWin-ME provides a default value of 5.49 meter.

xvii. Percent of trucks with short axles: This defines the percentage of trucks in design with short axles. DARWin-ME provides a default value of 33 percent.

xviii. Percent of trucks with medium axles: This defines the percentage of trucks in your design with medium axles. DARWin-ME provides a default value of 33 percent.

xix. Percent of trucks with long axles: This defines the percentage of trucks in your design with long axles. DARWin-ME provides a default value of 34 percent.

xx. Monthly Traffic Volume Adjustment Factors: These factors are used to distribute the AADTT volume a year's time. Once the monthly traffic volume adjustment factors have been created, they are assumed to be the same for the design life. Monthly traffic volume adjustment factors are used if there is significant monthly variation in truck volumes that affect pavement performance. This variation is most likely due to seasonal traffic, such as in summer or winter

xxi. Vehicle Classification Distribution: The software uses the FHWA scheme of classifying heavy vehicles. Ten different vehicle classes are used (classes 4 to 13). The subsequent three light vehicle classes (classes 1 to 3, motorcycle, passenger car, and pickup) are not used in the software.

xxii. Hourly Traffic Volume Adjustment Factors: Hourly traffic adjustment factors are expressed as a percentage of the AADT volumes during each hour of the day. These factors apply to all vehicle classes and are constant throughout the design life of the pavement system.

xxiii. Axle Load Distribution Factors: The distribution of the number of axles by load range is the definition of axle load spectra. An axle load spectrum distribution is referred to as

axle load distribution factors. The software allows different set of axle load distribution factors for each vehicle class and each month.

xxiv. Traffic Growth Factors: Anticipation of truck volume growth after a road has opened is expressed in traffic growth factors. These factors are applied to individual vehicle classes. Axle load distributions are assumed to be constant with time and no growth factors are applied to them. The software also has no provision for reduction in truck volume.

xxv. Number of Axles per Truck: For each class, the number of axles per truck by axle type is required. The axle type is single, tandem, tridem, and quad. The number of axles per truck has significant influence on the predicted pavement performance.

xxvi. Lateral Traffic Wander: Lateral traffic wander is defined as a lateral distribution of truck tire imprints across the pavement. Traffic wander plays an important role in the prediction of distresses associated with rutting. Default values for traffic wander are recommended unless quality data are available on a regional or local basis.

xxvii. Axle Configuration: The software allows two types of axle spacing. The first is axle spacing within the axle group, and it is defined as the average spacing between individual axles within the axle group (for example, the average spacing for all tandem axles for all vehicle types). Separate entries for tandem, tridem and quad axles are required. The second possibility is axle spacing between major axle groups. This is defined as the spacing between the steering axle and the first subsequent axle. Axle spacing between the major axle groups is required for short, medium, and long trucks. Axle configuration has a marginal effect on pavement performance predicted by the MEPDG, and is at the discretion of the user to pick default values or use measured values.

The specific traffic input that are required for analysis, are shown in Table 3.2.

Table 3.2: Specific Traffic Input Requirement for Analysis

Sl	Item Name	Input Requirement
1	General	i. Two-way AADT and percentage of heavy vehicle ii. Traffic Geometric Factors • Number of Lane in design direction • Percent of Truck in design Direction • Percent of Truck in design Lane • Directional Speed
2	Traffic Volume Adjustment	• Truck Traffic Classification • Traffic Growth Factor • Monthly adjustment factor • Hourly Distribution
3	Axle Load Distribution	• Single • Tandem • Tridem, and • Quad axles
4	Axle Configuration and Parameter	Number of Axles
		Lateral Traffic Wander • Mean Wheel Location (This is the distance from the outer edge of the wheel to the pavement marking) • Traffic Wander Standard Deviation • Design Lane Width (defined by the distance between the lane markings on either side of the design lane
		Axle Configuration • Average axle width • Dual tire spacing • Tire pressure • Axle Spacing
		Wheel Base • Average Axle Spacing • Percentage of Trucks (for specific axles)

Traffic input data are usually entered for the base year (starting year of the cycle length). The base year is the year the pavement is expected to open to traffic. Within the software, there is a provision for future growth in truck volumes after the base year. The summary of traffic input and their accuracy level that are used in the analysis are shown in Table 3.3.

Table 3.3: Summary of Traffic Input and Level used for Analysis

Sl	Input	Input value and Level
1	Two-way AADT and percentage of Truck	Level 1 Inputs (Site Specific Values are) are used.
2	Number of Lanes	Level 1 Inputs (Site Specific Values) are used.
3	Percent of Truck in design Direction	50% are considered for Ontario Highway Systems, which is of level 3 accuracy.
4	Percent of Truck in design Lane	Level 2 Input are used. Table 3.4 shows the Ontario AADT Standard Value for Percent of Truck in design Lane.
5	Directional Speed	Level 2 Input are used. Table 3.5 shows the Ontario standard speed for different highway class.
6	Average axle width	Ontario Standard value 2.6 m; which is of level 2 accuracy.
7	Dual tire spacing	Ontario Standard value 300 mm; which is of level 2 accuracy
8	Tire pressure	Ontario Standard value 830 kPa; which is of level 2 accuracy
9	Tandem Axle Spacing	Ontario Standard value 1.45m; which is of level 2 accuracy.
10	Tridem Axle Spacing	Ontario Standard value 1.68m; which is of level 2 accuracy.
11	Quad Axle Spacing	Ontario Standard value 1.32m; which is of level 2 accuracy.
12	Mean Wheel Location	Ontario Standard value 460 mm; which is of level 2 accuracy.
13	Traffic Wander Standard Deviation	Ontario Standard value 254 mm; which is of level 2 accuracy.
14	Design Lane Width	Level 1 Inputs (Site Specific Values) are used.
15	Average Spacing for short axles	Ontario Standard value is 5.1 m; which is of level 2 accuracy.
16	Average Spacing for medium axles	Ontario Standard value is 4.6 m; which is of level 2 accuracy.
17	Average Spacing for long axles	Ontario Standard value is 4.7 m; which is of level 2 accuracy.
18	Percent Truck with short axles	Ontario Standard value is 33; which is of level 2 accuracy.
19	Percent Truck with medium axles	Ontario Standard value is 33; which is of level 2 accuracy.
20	Percent Truck with long axles	Ontario Standard value is 34; which is of level 2 accuracy.
21	Traffic Growth Factor	Level 1 Inputs (Site Specific Values) are used.

Sl	Input	Input value and Level
22	Truck Traffic Classification	Ontario Truck Traffic Classification is used for specific region, which has accuracy of level 2. Table 3.6 shows the vehicle classification. The vehicle classification for road sections are identified and shown in Appendix A.
23	Monthly adjustment factor and Hourly Distribution	Software default value is used which is of level 3.
24	Axle per Truck	Level 2 Input are used. Table 3.7 shows the Ontario Axle per Truck Value.
25	Axle Distribution	Level 2 Input are used for Ontario Standard. Two different load spectra are used for Northern and Southern Ontario.

Table 3.4: Ontario's AADT Standard Value for Percent of Truck in Design Lane

Number of Lanes in One Direction	Average Annual Daily Traffic Volume (both Direction)	Lane Distribution Factors
1	All	1.0
2	<15,000	0.9
	> 15,000	0.8
3	<25,000	0.8
	25,000-40,000	0.7
	> 40,000	0.6
4	<40,000	0.7
	> 40,000	0.6
5	<50,000	0.6
	>50,000	0.6

Table 3.5 Ontario's Standard Speed for different Highway Class

Highway Type	Speed (Km/hr)
Freeway	100
Arterial	80
Collector	60
Local	50
ST Pavements	50

Table 3.6: FWHA System of Vehicle Classification (Source: www.fhwa.dot.gov)

Vehicle Class	Vehicle Type	Description
Class 4	Buses	All vehicles manufactured as traditional passenger-carrying buses with two axles and six tires or three or more axles. This category includes only traditional buses (including school buses) functioning as passenger-carrying vehicles. Modified buses should be considered to be a truck and should be appropriately classified.
Class 5	Two-Axle, Six-Tire, Single-Unit Trucks	All vehicles on a single frame including trucks, camping and recreational vehicles, motor homes, etc., with two axles and dual rear wheels.
Class 6	Three-Axle Single-Unit Trucks	All vehicles on a single frame including trucks, camping and recreational vehicles, motor homes, etc., with three axles.
Class 7	Four or More Axle Single-Unit Trucks	All trucks on a single frame with four or more axles.

Vehicle Class	Vehicle Type	Description
Class 8	Four or Fewer Axle Single-Trailer Trucks	All vehicles with four or fewer axles consisting of two units, one of which is a tractor or straight truck power unit.
Class 9	Five-Axle Single-Trailer Trucks	All five-axle vehicles consisting of two units, one of which is a tractor or straight truck power unit.
Class 10	Six or More Axle Single-Trailer Trucks	All vehicles with six or more axles consisting of two units, one of which is a tractor or straight truck power unit.
Class 11	Five or fewer Axle Multi-Trailer Trucks	All vehicles with five or fewer axles consisting of three or more units, one of which is a tractor or straight truck power unit.
Class 12	Six-Axle Multi-Trailer Trucks	All six-axle vehicles consisting of three or more units, one of which is a tractor or straight truck power unit.
Class 13	Seven or More Axle Multi-Trailer Trucks	All vehicles with seven or more axles consisting of three or more units, one of which is a tractor or straight truck power unit.

Table 3.7: Ontario Standard Value for Axle per Truck Vehicle

Class	Single	Tandem	Tridem	Quad
Class 4	1.62	0.39	0	0
Class 5	2	0	0	0
Class 6	1.001	1	0	0
Class 7	1.783	1.056	0.036	0
Class 8	2.171	0.842	0	0
Class 9	1.128	1.932	0.003	0
Class 10	2.087	1.459	0.465	0.032
Class 11	4.589	0.185	0	0
Class 12	3.336	1.332	0.06	0
Class 13	1.536	2.038	0.797	0.004

3.5.3 Climate data

Local climate play very significant role in pavement performance. Change in local temperature, precipitation, season, and frost depth can considerably affect pavement performance. The MEPDG requires these inputs to be locally calibrated. As a result, these climate conditions are needed to be observed and correlated to pavement performance. The climate parameters can be obtained from weather stations close to the project location. The DARWin-ME software includes a library of weather data for approximately 800 weather stations throughout the U.S. and Canada. The climate inputs are used to predict moisture and temperature distributions inside the pavement structure. Asphalt concrete stiffness is sensitive to temperature variations and unbound material stiffness is sensitive to moisture variations.

For a specific location, where there are no weather data available, the Integrated Climatic Model (ICM) is able to create a virtual weather station by interpolating the climatic data from neighboring weather stations. To generate a virtual climate file for a project location, the longitude, latitude and the elevation of the project are to be selected. The software will then automatically find weather stations closest to the location of the project. The number of weather stations selected is used to create a virtual weather station for the project location. Multiple weather stations are normally used due to the possibility of missing data and errors in the database for a single station, which may cause the software to hang or crash in the climatic module. It is also recommended that the weather stations selected to create the virtual station have similar elevations, if possible, although temperatures are adjusted for elevation differences (AASHTO 2008). In areas of wide-range climatic differences, AASHTO recommends that highway agencies divide such areas into similar climatic zones (approximately the same ambient temperature and moisture) and then identify representative weather stations for each of these zones (AASHTO 2008).

Therefore, DARWin-ME models daily and seasonal fluctuations in the moisture and temperature profiles in the pavement structure brought about by changes in ground water table, precipitation/infiltration, freeze-thaw cycles, and other external factors. The Canadian climate DARWin-ME has option for verifying weather that performs quality checks of climate data for the station selected.

"Verify Weather" allows DARWin-ME to check for the following:

a. If the data value of an hourly record is within an acceptable range;

b. If the difference between the data values of two consecutive hourly records are within an acceptable range;
c. If there are any missing or blank data in a record; and
d. If an hourly record does not meet all the criteria mentioned above, the program displays an error or a warning message listed in the Error List Pane area.

Ontario's available station in DARWin-ME are summarized in the Appendix B. Table 3.8 presents climate inputs requirement for DARWin-ME. Table 3.9 presents climate inputs data and level used for analysis.

Table 3.8: DARWin-ME Required Climate Inputs

Sl	**Item Name**	**Input**
1	Input	• Longitude • Latitude • Elevation • Depth of Water Table • Selecting climate Station /Creating virtual climate Station

Table 3.9: Climate Inputs Used for Analysis

Sl	Item Name	Input and Level of Accuracy
1	• Longitude • Latitude • Elevation	Level 1 Input (Site Specific Values are shown Appendix B) are used
2	Depth of Water Table	Level 2 Input (Ontario Standard 6.1 m) is used
3	Selecting climate Station /Creating Virtual Station	The climate station is selected from the list for distance is less than 10 km. But Virtual Station is created for site is more than 10 km distant from climate station.

3.5.4 Material Properties

The DARWin-ME requires the use of material properties of the pavement layers to create a mechanistic analysis of the pavement responses. With the implementation of the MEPDG underway, it is important to understand the performance of pavement materials under differing conditions.

In DARWin-ME, the material types that fall under the following general definitions can be defined as an asphalt layer:

- HMA
- Dense Graded
- Open Graded Asphalt

- Asphalt Stabilized Base Mixes
- Sand Asphalt Mixtures
- Stone Matrix Asphalt (SMA)
- Cold Mix Asphalt
- Central Plant Processed
- Cold In-Place Recycling

The key materials inputs required for asphalt concrete layers are:

- Dynamic modulus of asphalt mixtures
- Rheological properties of asphalt binder (e.g. viscosity, penetration, complex modulus and phase angles)
- Creep compliance and indirect tensile strength
- Mix related and other properties (e.g. effective binder content, air voids, heat capacity, thermal conductivity)

These inputs are required for predicting pavement responses, climatic analysis, asphalt aging as well as pavement performance. Table 3.10 presents material inputs requirement for asphalt concrete. Table 3.10 presents material inputs requirement for asphalt concrete. Table 3.11 presents material inputs used for asphalt concrete for the analysis.

Table 3.10: DARWin-ME Required Material Inputs for Asphalt Concrete

Sl	Item Name	Input
1.	Layer Information	• Number of Layers • Types • Materials • Thickness
2	HMA Design Properties	• Milled Thickness • Total Rutting • Existing Condition
3	Mixture Volumetric	• Unit Wt. • Effective Binder Content (%) • Air Voids • Poison's Ratio
4	Mechanical Properties	• Dynamic Modulus • Reference Temperature • Asphalt Binder (for Conventional: Penetration Grade) • Indirect Tensile Strength • Creep Compliance
5	Thermal Properties	• Thermal Conductivity • Heat Capacity • Thermal Contraction

Sl	Item Name	Input
6	Specific Layer Properties	• Asphalt Mix • Aggregate Gradation • Cumulative % Retained ¾ " sieve • Cumulative % Retained 3/8 " sieve • Cumulative % Retained #4 sieve • % Passing # 200 sieve • Asphalt Binder • For Super-pave binder grading ,high temp and low temp • For conventional viscosity grade, viscosity grade • For conventional penetration grade, pen grade • Asphalt General • Reference Temperature

Table 3.11 Material Input Used for Asphalt Concrete for the Analysis

Sl	Item Name	Input and Level
1	• Types • Materials • Thickness	Level 1 Input are used (Site Specific Layer information are shown Appendix E).

Sl	Item Name	Input and Level
2	• Unit Wt. • Effective Binder Content(%) • Air Voids • Poison's Ratio • Indirect Tensile Strength • Gradation	Level 1 Inputs are used. Specific Layer information are shown in Table 3.12
3	• Dynamic Modulus • Reference Temperature • Creep Compliance • Thermal Conductivity • Heat Capacity • Thermal Contraction	Level 3 Inputs are used.
4	• Asphalt Binder (for Conventional: Penetration Grade)	Level 2 input (Ontario Standard value for North East, North West, and Southern Region are used). Specific values are shown in Table 3.13.
5	• Milled Thickness • Total Rutting • Existing Condition	Level 1Input are used. Site specific Milled Thickness and Total Rutting are used. For identifying existing condition, PCI value is observed.

Table 3.12: Ontario Asphalt Concrete Properties Used for Analysis

Asphalt Layer	Unit Wt. (Kg/m^3)	Binder Content (%)	Air Void (%)	Effective Binder Content (%)	Poison's Ratio	Indirect Tensile Strength (MPa)	Thermal Conductivity (Watt/meter-Kelvin)	Heat Capacity (Joul/kg-Kelvin)	Sieve Passing %			
									19 mm	9.5 mm	4.75 mm	0.075 mm
HL-1	2520	5	4	12.4	0.35	2.51	1.16	963	100	82.5	55	2.5
HL-2	2410	6	5	14.2	0.35	2.51	1.16	963	100	100	92.5	5.5
HL-3	2520	5	4	12.4	0.35	2.51	1.16	963	100	82.5	55	2.5
HL-4B	2480	5	4	12.2	0.35	2.51	1.16	963	100	72	53.5	3
HL-4S	2480	5	4	12.2	0.35	2.51	1.16	963	100	72	53.5	3
HL-5	2520	4.5	4	10.9	0.35	2.51	1.16	963	97	72	53.5	3
HL-6	2460	4.5	4	10.9	0.35	2.51	1.16	963	97	72	53.5	3
HL-8	2460	4.5	4	10.9	0.35	2.51	1.16	963	97	63	42.5	3
DFC	2520	5	3.5	12.4	0.35	2.51	1.16	963	100	82.5	52.5	2.5
HDBC	2460	4.5	4	10.9	0.35	2.51	1.16	963	97	63	43.5	3
MDBC	2500	5	4	12.3	0.35	2.51	1.16	963	97	63	40	3

Table 3.13: Penetration Grade of Asphalt Binder for Ontario Zone (MTO's Design Standard Value)

Zone	Penetration Grade	Available Grade in DARWin-ME
Southern Ontario	85/100	85/100
North East Ontario	150/200	120/150
North West Ontario	300/400	200/300

Material inputs for base, sub-base and sub-grade are collected for all pavement sections. Table 3.14 presents material inputs requirement for base, sub-base and sub-grade and level of input data that are used in the analysis.

Table 3.14: Material Inputs and Level for Base, Sub-base and Sub-grade

Sl	Item Name	Input and Level
1	Types	Level 1 input are used (Site Specific Layer information are shown Appendix C).
2	Materials	Level 1 input are used (Site Specific Layer information are shown Appendix C).
3	Thickness	Level 1 input are used (Site Specific Layer information are shown Appendix C).
4	Poison's Ratio	Level 2 input are used.
5	Coefficient of Lateral Earth Pressure	
6	Resilient Modulus	Level 1 input are used (Site Specific Layer information are shown Appendix C).

Sl	Item Name	Input and Level
7	Gradation and other Properties	Level 2 input are used.

3.6 Integration of the Calibration Database

The input data are compiled for all section cycles. From historical pavement data, all the performance data including section name, rout name, Route direction, station beginning mile, station end mile, evaluation year, DMI, pavement condition rating (PCR), ride comfort rating (RCR), riding comfort index (RCI), PCI, IRI, facility type for all distress (both extent and severity), functional class, lanes, length, width, AADT, percent of truck, annual ESAL, cumulative ESA, construction year, subgrade modulus, are collected and compiled in Microsoft Access for the selected section cycles using their unique section code. Other traffic data (axle configuration, vehicle class etc.) are also collected from local traffic office and compiled into Microsoft Access for the unique section code. Materials properties are collected from the contract document of the road sections and complied accordingly. Latitude, longitude and elevation for specific section are collected from google map and complied in to the data file.

3.7 Summary

In this chapter, input data requirement for local calibration of pavement design models are discussed. The historical pavement performance data retrieved from the MTO PMS2 have been screened, selected and converted to the proper format for the use of local calibration. Based on the selected pavement sections, the input data required for pavement analysis and design in

DARWin-ME at different hierarchical level were also discussed. Depending upon the data availability, a proper input level of accuracy has been determined. Three major categories of input data (i.e., traffic, climate and materials) were described in detail. Finally, the pavement performance data and input data have been integrated to a Microsoft Access database.

Using the available input data, the pavement analysis is performed for the selected calibration sections. This will be discussed in the next chapter.

Chapter 4

RESULT ANALYSIS FOR LOCAL CALIBRATION AND VALIDATION

Based on available hierarchical input framework developed in chapter 3, the distresses of the selected sections are predicted using the DARWin-ME software. Finally using the software output and the observed distress, local calibration of distress models are carried out in this chapter. A validation is also carried out for the calibrated models using a separate validation data set.

4.1 DARWin-ME Output

At first all output of 101 section cycles are plotted and compared. A sample of the software output is shown in Appendix D.

The units used in the MEPDG for all predicted distresses are not the same for the measured distresses in the MTO PMS2 database. A comparison of the units is shown in Table 4.1. It is found that only the terminal IRI, permanent deformation (or rutting) and AC bottom-up fatigue cracking are measured with the similar units used in the MEPDG. For AC top-down fatigue cracking, the PMS2 measures it in absolute length rather than a linear percentage (m/km). In addition, PMS2 database does not specifically collect data for total cracking as predicted as the sum of reflective and alligator cracking; neither for the AC layer rutting. Therefore, only the terminal IRI, total rutting and AC bottom-up fatigue cracking are the candidate distresses whose transfer models can be locally calibrated in this study.

Table 4.1: Comparison of Units of Predicted and Measured distresses

Distress Type	Unit in MEPDG	Unit in MTO PMS2
Terminal IRI	m/km	m/km
Permanent deformation - total pavement	mm	mm
Total Cracking (Reflective + Alligator)	percent	Not recoded.
AC bottom-up fatigue cracking	percent	percent
AC top-down fatigue cracking	m/km	percent
Permanent deformation - AC only	mm	Not recorded

4.2 General Observations

Any calibration process involves comparison of predicted distress against measured or observed distress. The tabular comparison between observed values and predicted values of terminal IRI, permanent deformation and AC bottom-up fatigue cracking are shown in Appendix E. Figures 4.1-4.3 show the scatter plots of the predicted versus the observed values for IRI, alligator cracking, and total rutting and, respectively.

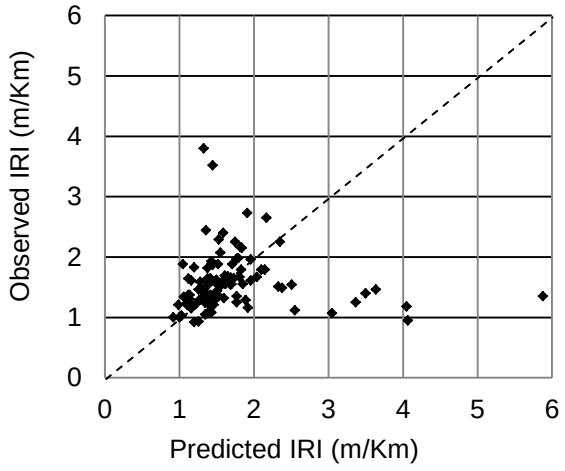

Figure 4.1: IRI Comparison between Predicted and Observed Values

From Figure 4.1, it is observed that, for some sections predicted values are very higher than the field observed values. From the historical data it is found that the observed values of some those sections are not recorded and estimated using RCI values. Finally, after dropping those section cycles, 79 sections are considered for further comparison of IRI.

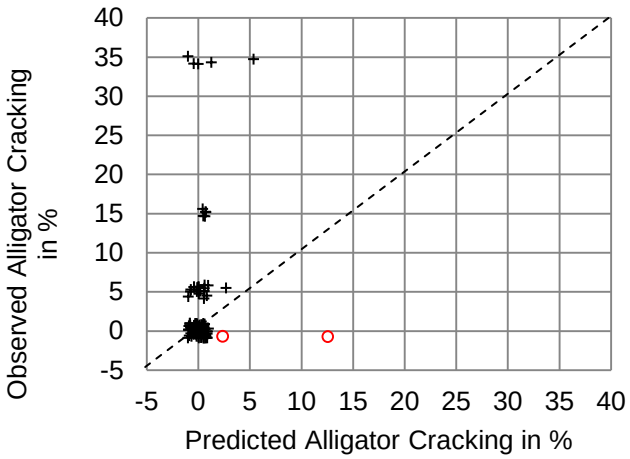

Figure 4.2: AC bottom-up fatigue Cracking (Alligator) comparison between Predicted and Observed Values

Figure 4.2 compares the predicted damage due to bottom-up fatigue cracking with the observed extent of wheel-path alligator cracking. To better visualize the repeated data points, small random perturbations are added in both observed and predicted values. Unlike the IRI discussed above, most of the predicted and observed fatigue crackings in the 101 sections are centered at zero. This makes further calibration impossible. However, this may be no concern if the fatigue cracking shall never be a life-limiting damage mode. Nevertheless, there are a few cases where the observed cracking is 35% whereas the predicted damage is still zero. This warrants a further investigation before a confirmative conclusion can be drawn for the AC bottom-up fatigue cracking. Of the 101 sections, only two sections (red circles) seem to be over-predicted by the MEPDG.

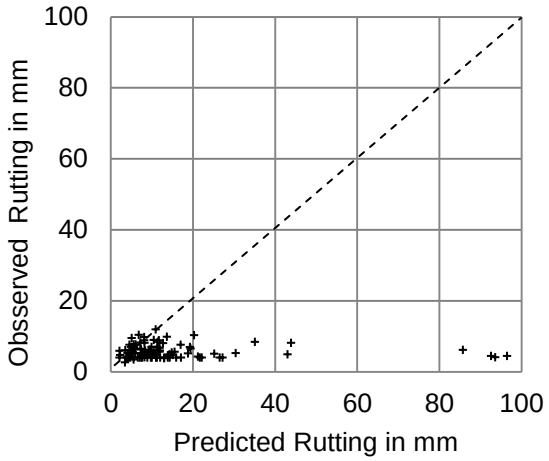

Figure 4.3: Rutting Comparison between Predicted and Observed Values

The comparison of the predicted and observed total pavement rutting is shown in Figure 4.3. It is observed that for a majority of the sections the predicted values are much higher than the field observed values. This big discrepancy may be attributed to the assumed 4mm for the initial rut depth for DARWin-ME input when it is unknown. Clearly a further investigation is important before meaningful local calibration is initiated. For these reasons, those inconsistent higher values are dropped for next step and finally 77 sections are considered for further comparison.

4.3 Sample Local Calibration

After those outliers have been removed, 79 sections remain for calibration of the IRI model. The scatter plot of the predicted vs. observed IRI is shown in Figure 4.4.

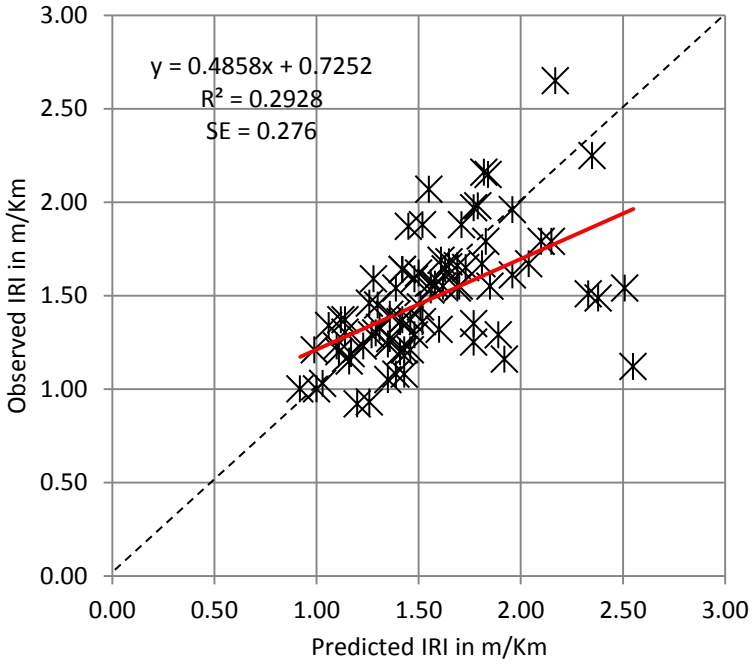

Figure 4.4: IRI comparison (after Removing Outliers)

In this Figure 4.4, it is observed that about 52% of the sections lie below the broken line, meaning they are over-predicted. The simple linear regression gives $y = 0.4858x + 0.7252$ with $R^2 = 0.2928$ and standard error = 0.276, where x and y are the predicted and observed IRI, respectively. To improve the goodness of fit, more sophisticated clustering regression analyses are carried out.

The location calibration of rutting is done in the same manner. After removing outliers with very higher predicted values, the rutting comparison is plotted in Figure 4.5.

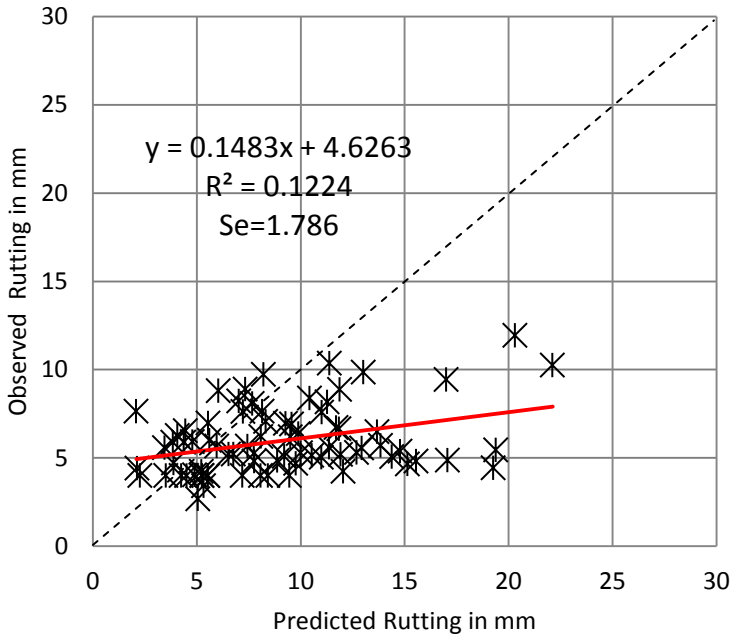

Figure 4.5: Rutting comparison (after Removing Outliers)

Form Figure 4.5, it is observed that about 74% of the sections lie below the broken line, meaning they are over-predicted. The simple linear regression gives $y = 0.1483\,x + 4.6263$ with $R^2 = 0.1224$ and standard error = 1.786. To improve the goodness of fit, more sophisticated clustering regression analyses are carried out.

These locally calibrated models are compared with globally calibrated models which are summarized in Table 4.2.

Table 4.2: Comparison of Global Calibration and Local Calibration

Distress	Global Calibration			Local Calibration	
	No of Observations	Standard Error	Reference	No of Observations	Standard Error
IRI	1926	0.298 m/km	AASHTO 2008	79	0.276 m/km
Rutting	334	2.71 mm	AASHTO 2008	77	1.79 mm

From Table 4.2, it is observed that, local calibration is giving lower standard error than that in global calibration. Although the number of observations in local calibration is less than the observations in global calibration, this lower standard error indicates the improvement in estimate of calibrated predicted values.

4.4 Clustering Analysis of the Local Calibration Models

To improve the goodness of fit for both the IRI and rutting models, more sophisticated clustering regression analyses are carried out. The models are sub-grouped based on the following criteria:

i. Road Section
ii. Highway Functional Class
iii. Ontario Zone
iv. Top Layer Material
v. Subgrade Modulus Strength (Only for Rutting)

Figure 4.6 presents the IRI clustering by road, Figure 4.7 by highway functional class, Figure 4.8 by zone, and Figure 4.9 by top layer material.

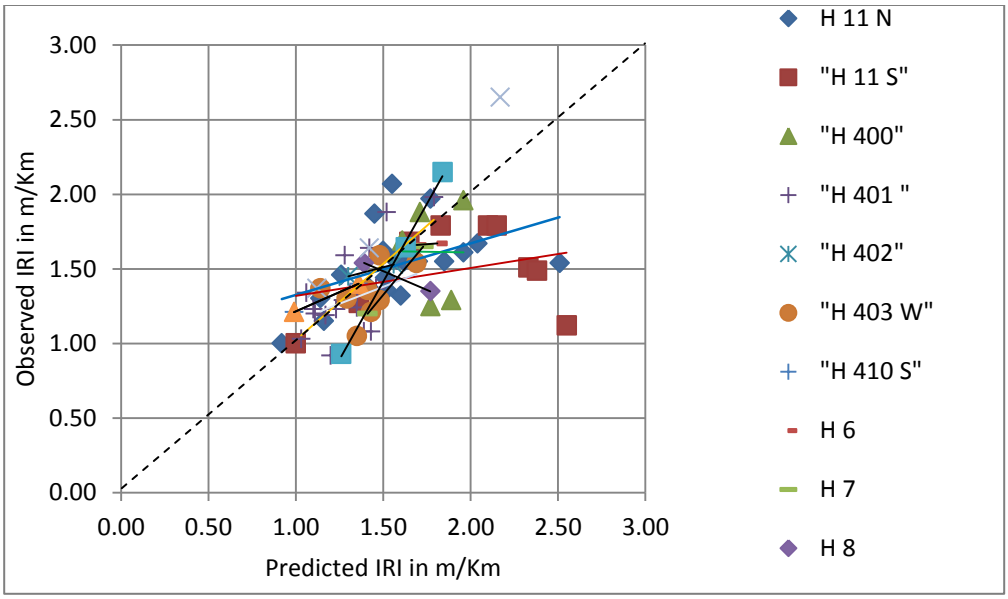

Figure 4.6 IRI Clustering by Road Section.

From Figure 4.6, it is found that based on the road section, IRI clustered model for highway 11, 17, 401, 403 and 417 improve the goodness of fit. For other road sections, the values cannot be compared since those samples have only two observations.

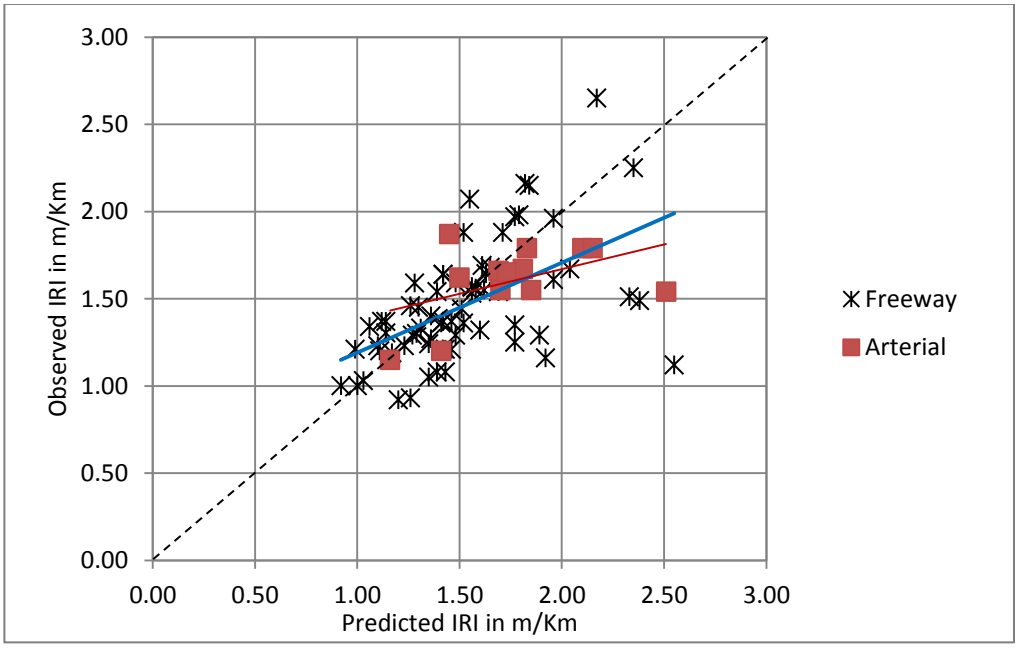

Figure 4.7: IRI Clustering by Highway Functional Class.

Similarly, from Figure 4.7, it is found that based on the road functional class, IRI clustering improves the goodness of fit for arterial road only. On the other hand it does not improve for Freeway.

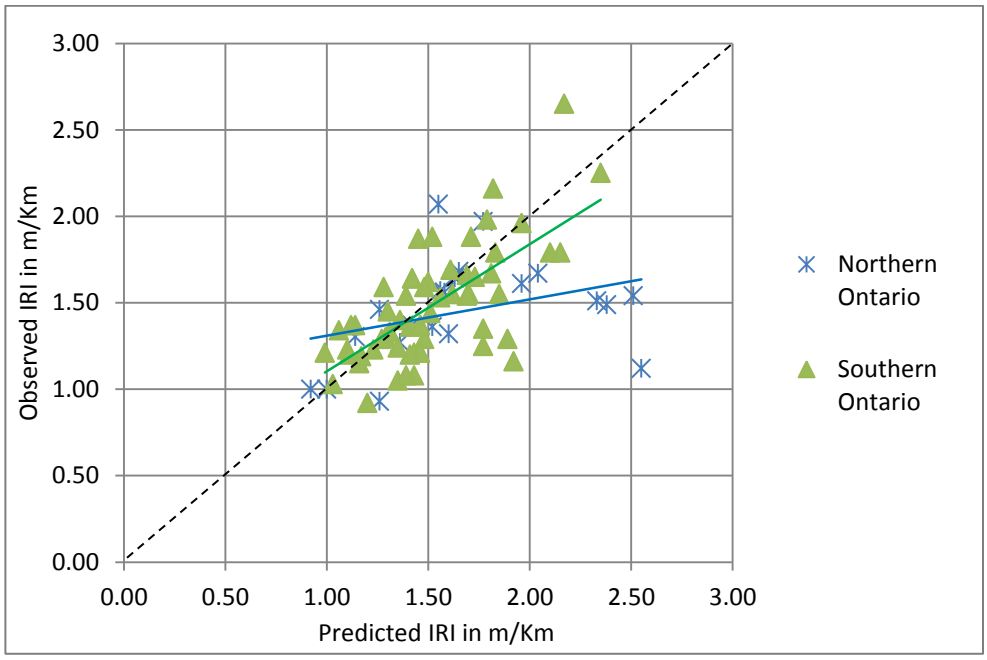

Figure 4.8: IRI Clustering by Zone

From Figure 4.8, it is found that based on the zone of Ontario (Northern and southern Ontario, where, IRI clustering improves the goodness of fit for southern Ontario only but it does not improve for northern Ontario.

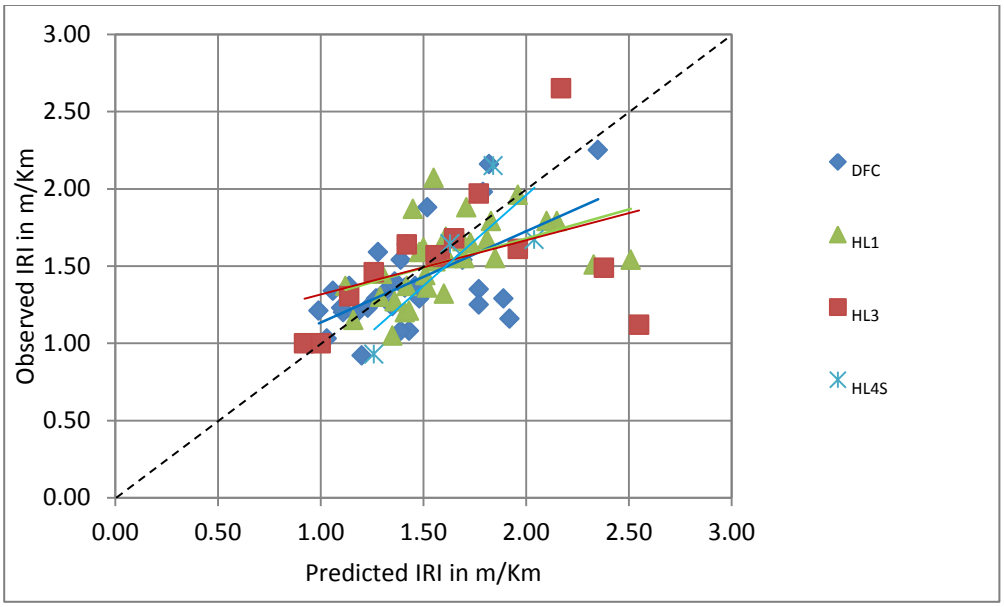

Figure 4.9: IRI Clustering by Top Layer Material

From Figure 4.9, it is found that IRI clustering by top layer material improves the goodness of fit for HL1 and DFC. It is also found that with same top material properties, the IRI predicted values follows the same pattern (This refers to material HL1 and HL3 which properties are same and trend line is also similar here).

Since some group have observations of 2 samples, the R^2 value is not considered to be the only indicator for comparing goodness of fit. Moreover, under the same cluster group, some models improve the goodness of fit while other models show opposite trend. For these reasons, to select the optimized model, composite mean square values for each group are compared with the generalized calibrated model. These values are summarized in Table 4.3.

Table 4.3: Comparison of Calibrated Predicted Models for each Clustering of IRI

Cluster Group		IRI Calibration						
		Predicted Value	No of Observations	SSD/RSS		Mean Square	Standard Error	R^2 value
Before Clustering		y = 0.4858x + 0.7252	79	5.875		0.076	0.276	0.293
Group	Name	Calibration with Clustered Group						
		Predicted Value	No of Observations	SSD/RSS	Composite Mean Square	Mean Square	Standard Error	R^2 value
Road Section	H 6	y = 0.0833x + 1.5192	2	0.000	**0.057**	65535.000	0.000	1.000
	H 7	y = 1.4062x - 0.7828	2	0.000		65535.000	0.000	1.000
	H 8	y = -0.5x + 2.235	2	0.000		65535.000	0.000	1.000
	H 11	y = 0.2165x + 1.1506	29	1.724		0.064	0.253	0.123
	H 17	y = 2.0815x - 1.7078	3	0.003		0.003	0.052	0.996
	H85	y = 0.1698x + 1.8509	2	0.000		65535.000	0.000	1.000
	H 400	y = -0.0161x + 1.6429	5	0.434		0.145	0.380	0.000
	H 401	y = 1.0222x - 5E-05	18	0.717		0.045	0.212	0.465
	H 402	y = 0.3077x + 1.05	2	0.000		65535.000	0.000	1.000
	H 403	y = 0.4539x + 0.6993	8	0.172		0.029	0.169	0.177
	H410	y = 0.5135x + 0.7016	2	0.000		65535.000	0.000	1.000
	H417	y = 1.2436x - 0.0658	3	0.006		0.006	0.076	0.994
	Total		**78**	**3.054**				
Highway Functional Class	Freeway	y = 0.5149x + 0.676	66	5.355	**0.077**	0.084	0.289	0.288
	Arterial	y = 0.2827x + 1.1046	13	0.444		0.040	0.201	0.213
	Total		**79**	**5.798**				
Zone	Southern Ontario	y = 0.7342x + 0.3705	57	3.211	**0.064**	0.058	0.242	0.475
	Northern Ontario	y = 0.2101x + 1.0996	21	1.530		0.081	0.284	0.115
	Total		**78**	**4.741**				
Top Layer Materials	HL1	y = 0.3765x + 0.9257	31	1.408	**0.078**	0.049	0.220	0.238
	HL3	y = 0.35x + 0.9674	13	1.891		0.172	0.415	0.170
	HL4S	y = 1.1765x - 0.3933	4	0.295		0.148	0.384	0.610
	DFC	y = 0.5916x + 0.5431	30	1.885		0.067	0.259	0.351
	Total		**78**	**5.480**				

Form Table 4.3, after comparing with the general calibrated model, it is found that the clustered model based on the road section is giving the optimized value as this group is showing lowest composite mean square value. The clustered group based on Ontario zone giving 2nd lowest means square value. Since the clustered group based on the road section includes some samples with observation of 2, both clustering group are considered for validation in the next stage.

Similar to the IRI clustering approach, the rutting are clustered based on Road Section, Highway Functional Class, Ontario Zone, and Top Layer Material. In addition, the Subgrade Modulus Strength is used as a potential clustering parameter. Figure 4.10 presents the rutting clustering by road section, Figure 4.11 by highway functional class, Figure 4.12 by zone, Figure 4.13 by top layer material and Figure 4.14 by subgrade modulus strength.

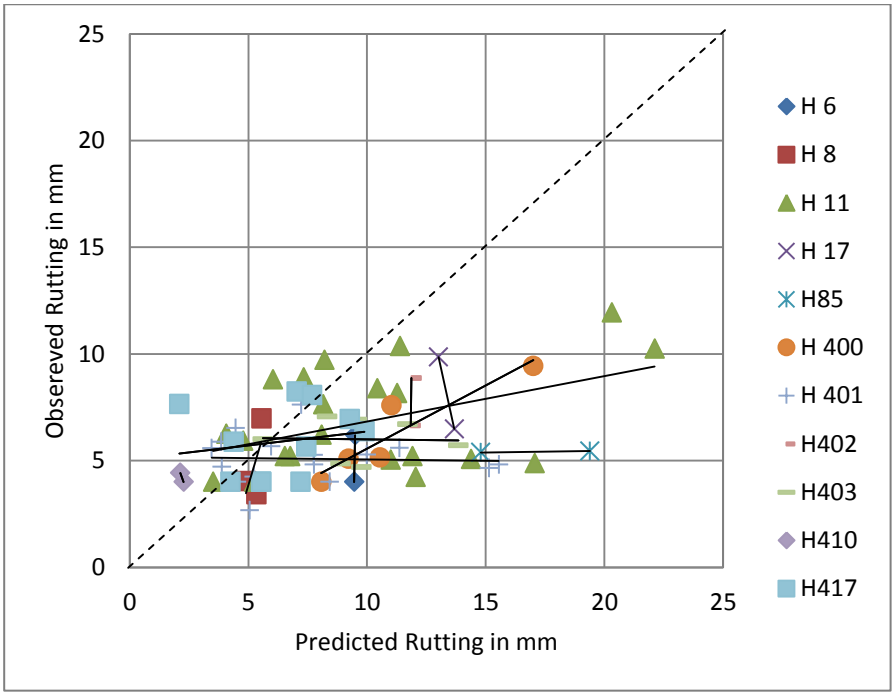

Figure 4.10: Rutting Clustering by Road Section

From Figure 4.10, it is found that based on the road section, rutting clustered model for highway 400, 401 and 403 improves the goodness of fit. For other road sections, the values cannot be compared since those subgroups have only two observations.

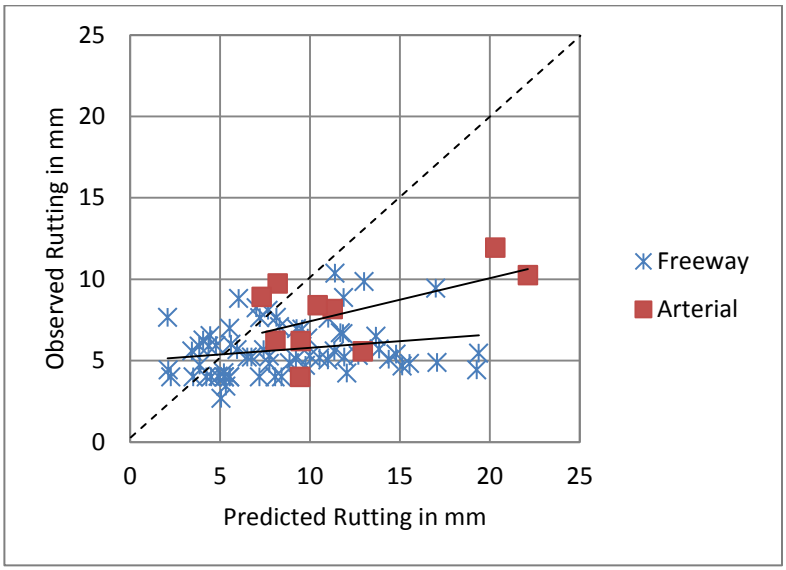

Figure 4.11 Rutting Clustering by Road Functional Class

From Figure 4.11, it is found that based on the road functional class, rutting clustering improves the goodness of fit for freeway road only.

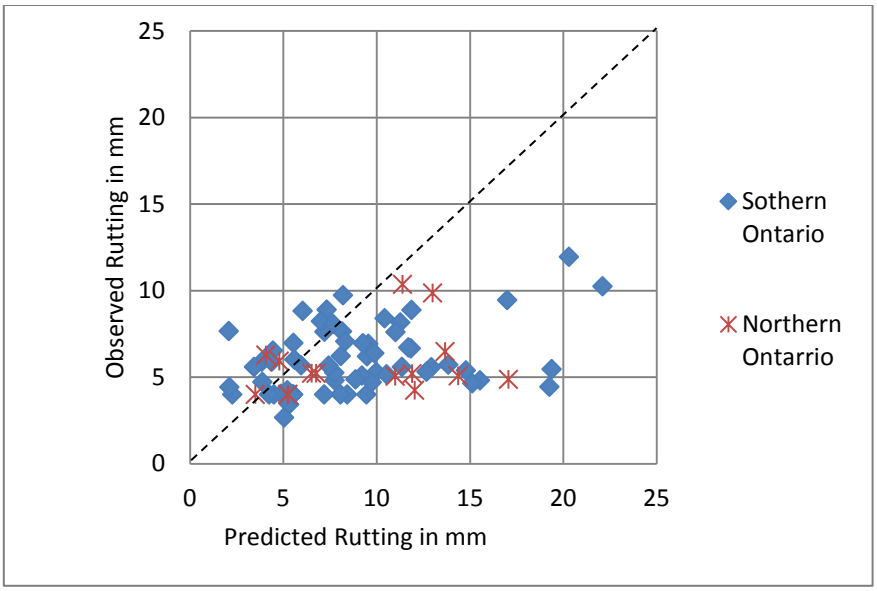

Figure 4.12 Rutting Clustering by Zone

From Figure 4.12, it is found that based on the zone of Ontario (Northern and southern Ontario,), rutting clustering does not improve the goodness of fit for both zone.

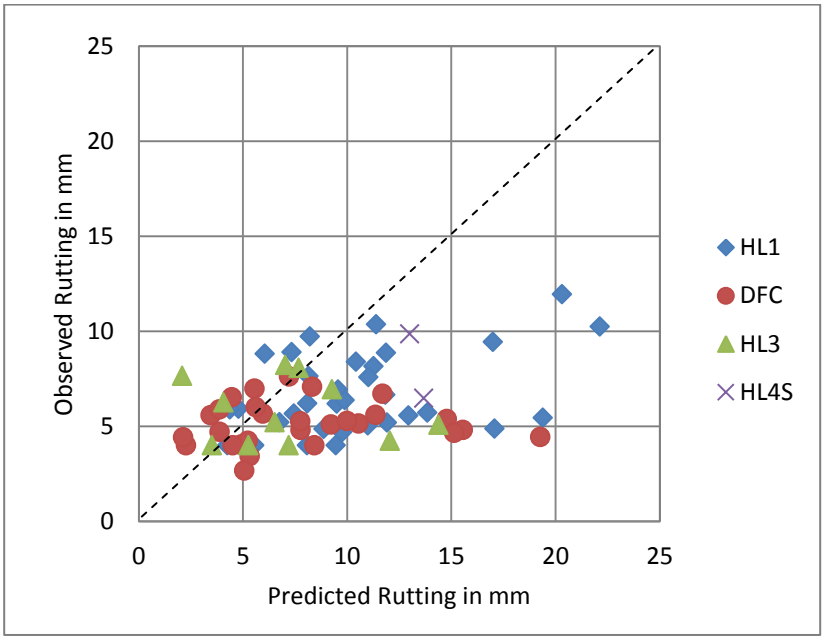

Figure 4.13 Rutting Clustering by Top Layer Materials

From Figure 4.13, it is found that based on the top layer properties, rutting clustering improves the goodness of fit for only DFC and HL3.

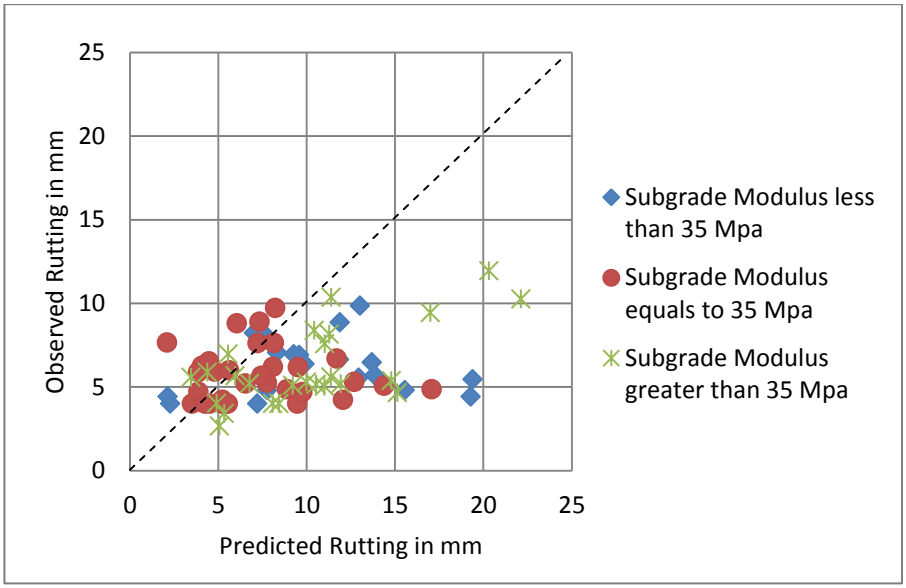

Figure 4.14 Rutting Clustering by Subgrade Modulus Strength

From Figure 4.14, it is found that based on the subgrade modulus, rutting clustering improves the goodness of fit for subgroup of modulus less than 35 MPa and equal to 35 MPa.

Similar to the criterion used for clustering the IRI, the composite mean square values for each group are compared with the general calibration model to select the best clustering parameter. These values are summarized in Table 4.4.

Form Table 4.4, after comparing with the general calibrated model, it is found that the clustered model based on the functional class is giving the optimized value. i.e. this group is showing lowest composite mean square value. The clustered group based on top layer materials and subgrade modulus is giving 2nd lowest and 3rd lowest means square value respectively. Since the clustered group based on top layer materials includes one subgroup with observation of 2, three clustering group are considered for next stage of validation.

Table 4.4: Comparison of Calibrated Predicted Models for each Clustering of Rutting

	Rutting Calibration							
	Predicted Value		**No of Observations**	**SSD/RSS**		**Mean Square**	**Standard Error**	**R^2 value**
Rutting before Clustering	Y= 0.1483x + 4.6263		77	239.446		**3.193**	1.787	0.122
Cluster Group	**Cluster Name**	**Rutting Calibration**						
		Calibrated Predicted Value	**No of Observations**	**SSD/RSS**	**Composite Mean Square**	**Mean Square**	**Standard Error**	**R^2 value**
Highway	6	y = 54.75x - 513.94	2	0.000	**3.033**	65535.000	0.000	1.000
	8	y = 3.7049x - 14.681	3	4.205		4.205	2.051	0.416
	11	y = 0.2128x + 4.7015	22	97.594		4.880	2.209	0.200
	17	y = -5.0299x + 75.288	2	0.000		65535.000	0.000	*1.000*
	85	y = 0.0152x + 5.1549	2	0.000		65535.000	0.000	1.000
	400	y = 0.5924x - 0.3626	5	2.810		0.937	0.968	0.857
	401	y = -0.012x + 5.1707	16	19.407		1.386	1.177	0.002
	402	y = 74x - 869.51	2	0.000		65535.000	0.000	1.000
	403	y = -0.0129x + 6.1194	7	5.588		1.118	1.057	0.001
	410	y = -3x + 10.81	2	0.000		65535.000	0.000	1.000
	417	y = 0.1319x + 5.049	11	28.101		3.122	1.767	0.032
	Total		**74**	**157.7057149**				
Functional Class	Freeway	y = 0.0815x + 4.9741	67	167.857	**2.794**	2.582	1.607	0.045
	Arterial	y = -0.0746x + 8.4301	10	36.122		4.515	2.125	0.317
	Total		**77**	**203.979**				
Zone	Northern Ontario	y = 0.1291x + 4.503	15	48.511	**3.255**	3.732	1.932	0.084
	Southern Ontario	y = 0.0728x + 5.3802	62	189.078		3.151	1.775	0.135
	Total		**77**	**237.589**				
Top Layer Materials	HL1	y = 0.22x + 4.3201	35	125.638	**2.837**	3.807	1.951	0.209
	HL3	y = -0.0762x + 6.3361	10	28.304		3.145	1.773	0.027
	HL4S	y = -5.0299x + 75.288	2	0.000		65535.000	0.000	1.000
	DFC	y = 0.0197x + 4.9873	28	36.145		1.390	1.179	0.006
	Total		**75**	**190.087**				
Subgrade Modulus	Less than 35 MPa	y = 0.0488x + 5.6244	20	55.005	**2.928**	3.056	1.748	0.018
	Equal to 35 MPa	y = -0.0137x + 5.7923	32	78.850		2.628	1.621	0.001
	Greater than 35 MPa	y = 0.3257x + 2.8707	25	73.998		3.217	1.794	0.446
	Total		**77**	**207.854**				

4.4 Validation of Analysis

A data set of 46 section cycles are further analyzed following the similar procedure and predicted distress are found using DARWin-ME software. The predicted values are further calculated using the calibrated models found from the analysis both for generalized model and also for all clustered groups. After minimizing the standard error, the values are compared with calibrated data set. Table 4.5 shows the comparison of calibrated IRI models with the validation data set and Table 4.6 shows the comparison of calibrated Rutting models with the validation data set.

From Table 4.5, after validation analysis it is found that clustered group based on Ontario zone is giving lowest composite mean square value for the validation data set which is 2nd lowest for calibration. Since the validation data set does not represent all the subgroup of clustered group based on road section, it does not have improved value. For these reasons, it can be said that IRI model can be clustered based on Ontario zone. Also the binder penetration grade, axle load spectra are classified as per zone for Ontario highway systems.

Table 4.5: Comparison of Calibrated IRI Models with Validation Data Set

Group		IRI			
		Predicted Value	No of Observations	SSD/RSS	Mean Square
Calibration Data Set		y = 0.4858x + 0.7252	79	5.875	0.076
Validation Data Set		y = 0.4858x + 0.7253	38	2.721	0.072

Cluster Group	Cluster Name	Calibration				Validation			
		Predicted Value	No of Observations	SSD/RSS	Composite Mean Square	No of Observations	SSD/RSS	Mean Square	Composite Mean Square
Road Section	H 6	y = 0.0833x + 1.5192	2	0.000	**0.057**				**0.103**
	H 7	y = 1.4062x - 0.7828	2	0.000		2	1.179	0.589	
	H 8	y = -0.5x + 2.235	2	0.000					
	H 11	y = 0.2165x + 1.1506	29	1.724		12	0.873	0.073	
	H 17	y = 2.0815x - 1.7078	3	0.003					
	H85	y = 0.1698x + 1.8509	2	0.000					
	H 400	y = -0.0161x + 1.6429	5	0.434		4	0.325	0.081	
	H 401	y = 1.0222x - 5E-05	18	0.717		7	0.243	0.035	
	H 402	y = 0.3077x + 1.05	2	0.000					
	H 403	y = 0.4539x + 0.6993	8	0.172		6	0.585	0.097	
	H410	y = 0.5135x + 0.7016	2	0.000					
	H417	y = 1.2436x - 0.0658	3	0.006					
	Total		**78**	**3.054**		**31**	**3.204**		
Functional Class	Freeway	y = 0.5149x + 0.676	66	5.355	**0.077**	35	2.604	0.074	**0.071**
	Arterial	y = 0.2827x + 1.1046	13	0.444		3	0.103	0.034	
	Total		**79**	**5.798**		**38**	**2.706**		
Zone	Southern Ontario	y = 0.7342x + 0.3705	57	3.211	**0.064**	28	1.808	0.065	**0.066**
	Northern Ontario	y = 0.2101x + 1.0996	21	1.530		10	0.712	0.071	
	Total		**78**	**4.741**		**38**	**2.521**		
Top Layer Materials	HL1	y = 0.3765x + 0.9257	31	1.408	**0.078**	8	0.481	0.060	**0.094**
	HL3	y = 0.35x + 0.9674	13	1.891		9	0.788	0.088	
	HL4S	y = 1.1765x - 0.3933	4	0.295		2	0.945	0.472	
	DFC	y = 0.5916x + 0.5431	30	1.885		18	1.247	1.247	
	Total		**78**	**5.480**		**37**	**3.461**		

Table 4.6: Comparison of Calibrated Rutting Models with Validation Data Set

Distress		Local Calibration								
		Predicted Value	No of Observations	SSD/RSS			Mean Square			
Calibration Data		y = 0.1483x + 4.6263	77	239.4458			3.1926			
Validation Data		y = 0.1483x + 4.6263	34	61.6035			1.8119			
		Calibration					Validation			
Cluster Group	Cluster Name	Calibrated Predicted Value	R^2 value	No of Observations	SSD/ RSS	Composite Mean Square	No of Observations	SSD/RSS	Mean Square	Composite Mean Square
Road Section	6	y = 54.75x - 513.94	1.000	2	0.000	**3.033**				2.689
	8	y = 3.7049x - 14.681	0.416	3	4.205					
	11	y = 0.2128x + 4.7015	0.200	22	97.594		8	34.932	4.367	
	17	y = -5.0299x + 75.288	1.000	2	0.000					
	85	y = 0.0152x + 5.1549	1.000	2	0.000					
	400	y = 0.5924x - 0.3626	0.857	5	2.810		4	15.731	3.933	
	401	y = -0.012x + 5.1707	0.002	16	19.407		7	11.342	1.620	
	402	y = 74x - 869.51	1.000	2	0.000					
	403	y = -0.0129x + 6.1194	0.001	7	5.588		5	2.536	0.507	
	410	y = -3x + 10.81	1.000	2	0.000					
	417	y = 0.1319x + 5.049	0.032	11	28.101					
	Total			**74**	**157.70**		**24**	**64.541**		
Highway Functional Class	Freeway	y = 0.0815x + 4.9741	0.045	67	167.857	**2.794**	32	45.960	1.436	**1.559**
	Arterial	y = -0.0746x + 8.4301	0.317	10	36.122		2	**7.035**	3.517	
	Total			**77**	**203.97**		**34**	**52.995**		
Zone	Northern Ontario	y = 0.1291x + 4.503	0.085	15	48.511	**3.255**	6	11.851	1.975	1.854
	Southern Ontario	y = 0.0728x + 5.3802	0.135	62	189.078		28	51.200	1.829	
	Total			**77**	**237.589**		**34**	**63.051**		
Top Layer Materials	HL1	y = 0.22x + 4.3201	0.209	35	125.638	**2.837**	5	3.584	0.717	1.216
	HL3	y = -0.0762x + 6.3361	0.027	10	28.304		7	7.701	1.100	
	HL4S	y = -5.0299x + 75.288	1.000	2	0.000					
	DFC	y = 0.0197x + 4.9873	0.006	28	36.145		19	26.404	1.390	
	Total			**75**	**190.087**		**31**	**37.689**		
Subgrade Modulus	<35 MPa	y = 0.0488x + 5.6244	0.018	**20**	**55.005**	**2.928**	8	4.221	0.528	1.693
	35 MPa	y = -0.0137x + 5.7923	0.001	32	78.850		12	14.483	1.207	

Distress		Local Calibration								
		Predicted Value	No of Observations	SSD/RSS			Mean Square			
Calibration Data		y = 0.1483x + 4.6263	77	239.4458			3.1926			
Validation Data		y = 0.1483x + 4.6263	34	61.6035			1.8119			
Cluster Group	Cluster Name	Calibration					Validation			
		Calibrated Predicted Value	R^2 value	No of Observations	SSD/ RSS	Composite Mean Square	No of Observations	SSD/RSS	Mean Square	Composite Mean Square
	> 35 MPa	y = 0.3257x + 2.8707	0.446	25	73.998		**14**	**38.873**	2.777	
	Total			**77**	**207.854**		**34**	**57.576**		

From Table 4.6, after validation analysis it is found that for clustered group based on top layer properties is giving lowest composite mean square value for the validation data set which is 2nd lowest for calibration data set. Since the validation data set does not represent all the subgroup (top layer materials HL4S) of clustered group based on top layer materials, it is not considered to select optimized method. The validation data set is giving 2nd lowest optimized value for clustered group based on highway functional class, which is also 2nd lowest for calibration data set. Therefore, it can be said that rutting model can be clustered based on highway functional class. Traffic pattern, speed, truck vehicle classification also vary depending on the highway functional class for Ontario highway systems.

After plotting the scatter between observed and calibrated predicted values for both IRI and rutting, the improved values are observed. Figure 4.15 shows the graphical comparison between observed IRI and calibrated predicted IRI. Figure 4.16 shows the graphical comparison between observed IRI and calibrated predicted IRI for optimized model based on Ontario Zone.

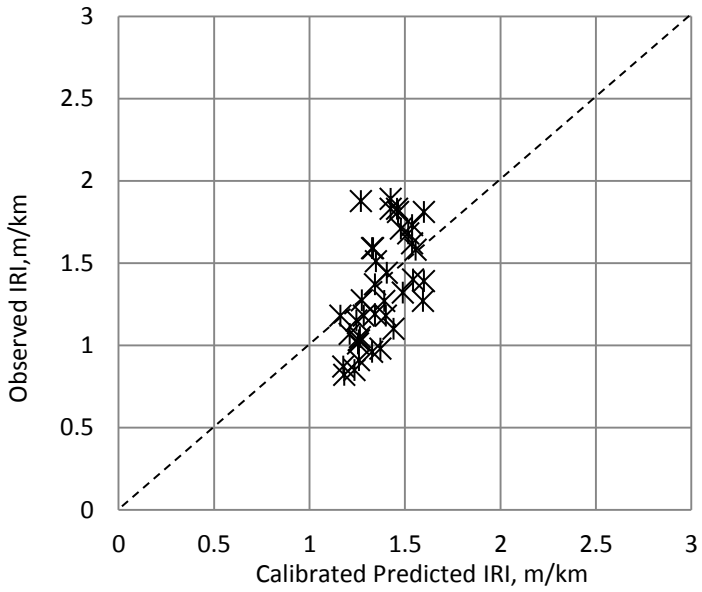

Figure 4.15: IRI Comparison for Validation Dataset

From Figure 4.15, it is found that the section cycle points are almost equally distributed between the two sides of the 45 degree broken line. From Figure 4.16, it is also found that the section cycle points for both Southern and Northern Ontario are almost equally distributed between the two sides of the 45 degree broken line.

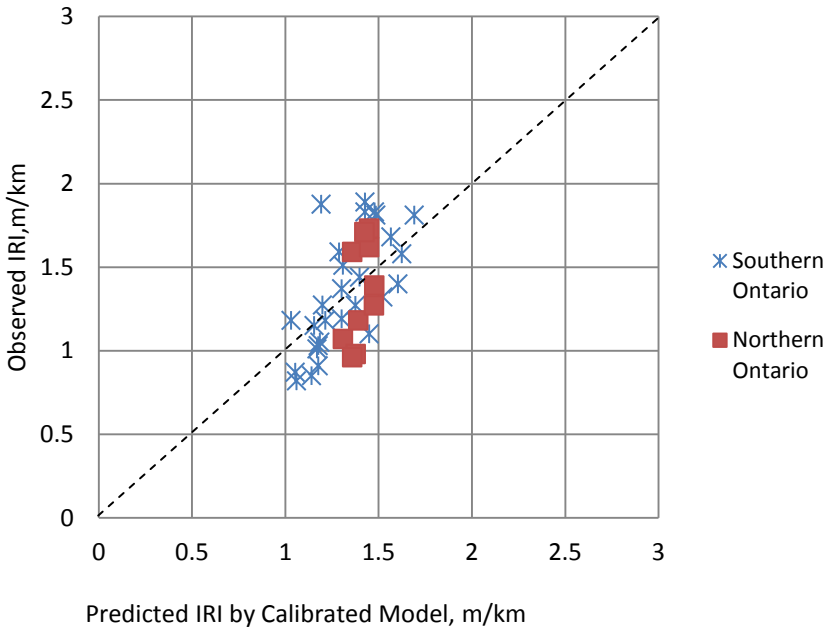

Figure 4.16: IRI Comparison for Optimized Model for Validation Dataset

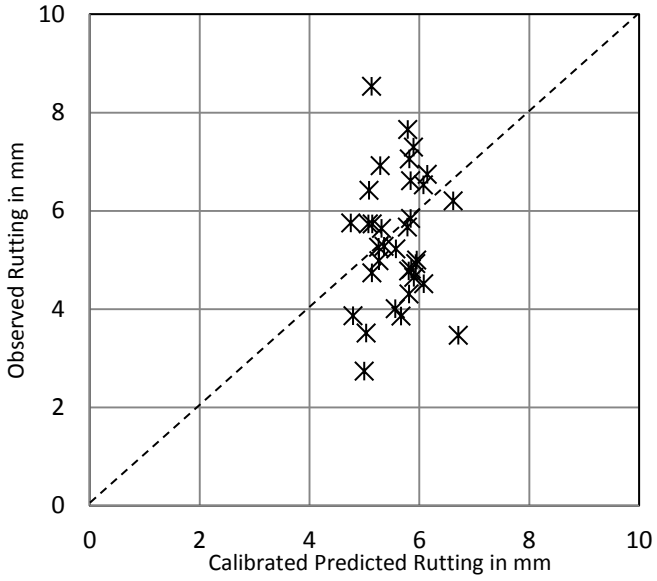

Figure 4.17: Rutting Comparison for Validation Dataset

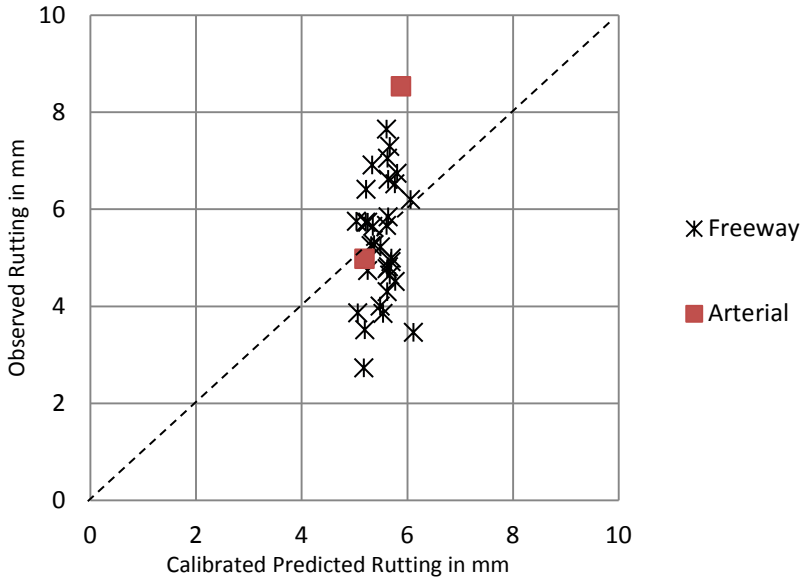

Figure 4.18: Rutting Comparison for Optimized Model for Validation Dataset

From Figure 4.17, it is found that the section cycle points are almost equally distributed between the two sides of the 45 degree broken line. From Figure 4.18, it is also found that the section cycle points for both Freeways are almost equally distributed between the two sides of the 45 degree broken line. For Arterial, only 2 observations are found, they are also distributed between the two sides.

4.5 t-test for Validation Data Set

Ideally, the mean of the deviates (equal the difference between observed distresses and the predicted distresses based on the local calibration model) should be zero. Due to randomness in sampling, the actual mean of the deviates might be nonzero. The t-test is used to test potential bias in the validation data set. For this test, the mean of residual is compared to value "0", based on the following hypothesis:

- Null Hypothesis: mean = 0

- Alternate Hypothesis: mean ≠ 0

Table 4.7 shows the summary result of t-test.

Table 4.7: Summary of t-test of Validation Data Set

Model	Observation	t Value	t-critical (99% Confidence level)	Mean	Standard Deviation	Pr > |t|	Status of Null Hypothesis
IRI	38	-0.6	2.71	-0.0264	0.2699	0.549	Accepted
Rutting	34	-0.8	2.734	-0.1854	1.3533	0.430	Accepted

It is found from Table 4.7 that for both IRI and rutting, null hypothesis is accepted, which represents 'non bias' validation data set.

4.6 F-Test for Calibration and Validation Data Set

F-test is carried out to test the validity of the validation data set. The standard deviations of residuals are compared based on the null hypothesis (H_0: $\sigma_1^2 = \sigma_2^2$) against an appropriate alternate hypothesis.Table 4.8 shows the summary of the F-test of validation and calibration data set.

Table 4.8: Summary of F-test of Calibration and Validation Data Set

Model	Observation of Calibration Data Set	Observation of Validation Data Set	P (F>=f)	F value	Status of Null Hypothesis
IRI	79	38	0.9992	0.428	Accepted
Rutting	77	34	0.0462	1.72	Rejected

From Table 4.8, null hypothesis that the validation set has the same variance as the calibration data set is accepted for IRI but rejected for rutting, i.e. rutting data sets are not from same population.

4.7 Summary

After calibration and validation analysis, it is found that IRI model based on Ontario zone is optimized model to predict the value. For rutting, calibrated model based on highway functional class is the optimized model. But a precise validation data set comprising all the subgroup with sufficient observations is required before recommending these clustered models.

Chapter 5

SUMMARY, CONCLUSIONS, AND RECOMMENDATIONS

5.1 Summary

The main objective of this study is to develop a database and a framework for sample calibration of the MEPDG distress models for the local conditions considering local traffic, climate and materials. Based on the Ontario highway PMS-2 database, the analyses are conducted for developing a framework for local calibration of the distress models for Ontario.

Using PMS-2 database as well as other required traffic data, section specific material properties and also climatic data, a calibration database is developed for the selected 101 section cycles in Microsoft Access.

The calibrated distress models are of (i) IRI and (ii) the total rutting. AC bottom up cracking is not considered for further calibration since most of the predicted values are zero. For other predicted values of distresses (Total Cracking, AC top-down fatigue cracking, and Permanent deformation - AC only) found from the software are not taken for further comparison as observed values for these distresses are not available in the PMS-2 database.

5.2 Major Findings of the Study

Analyses of this study are mainly focused on the development a framework for calibrating the

MEPDG distress models (specifically IRI and Rutting) for local conditions by comparing the observed value and predicted value (found from the software). It is clear from the analysis that, the predicted values for most of the road sections are higher than the field observed values. It reveals that the MEPDG globally calibrated distress models (for IRI and rutting) are more conservative than the existing condition of Ontario highway system.

Investigations in this study suggest that IRI clustered group based on Ontario zones is the optimized model compared to the other clustered group based on road section, functional class, and top layer materials. It is also observed that IRI predicted values for similar material properties are varying in the same pattern, as IRI predicted values for equivalent material properties of HL1 and HL3 follow the same trend. Although the IRI predictions are heavily dependent on the other distresses calculated by the MEPDG.

For rutting it is clear that the clustered groups based on highway functional class is the optimized model.

Therefore, based on this input framework and investigation result, future higher level local calibration can be carried out for other remaining Ontario highway sections.

5.3 Recommendations

Based on the local calibration database and findings from the sample local calibration, several recommendations are made below:

(1) Materials input: Materials input are very important data for pavement analysis and design. The Local Calibration Guide requires the accuracy of these data be Level 1. For a more solid local calibration, the MTO should strive to make every effort to improve the materials input accuracy.

(2) Maintenance history: The MTO is in the process of improving the data reliability of the maintenance records. The current local calibration database records a full life cycle of rehabilitated sections. However, for many sections there may be more than one life cycles before the cycle in use. Although the historical performance data are not very important, the pavement structures have been altered. This will also complicate the materials input.

(3) Traffic and Climate Data: Further accuracy in input of traffic data (site specific vehicle classification, site specific axle load spectra rather than using regional data), climate data (site specific water depth, more available climate station to avoid creating virtual station) will obviously bring more accurate calibration for local conditions. Efforts should be made to improve the accuracy in the traffic and climate data.

(4) DARWin-ME Input/Output: DARWin-ME allows maximum 4 asphalt layers (2 layers as existing and 2 layers as new rehabilitated layers) which complicates the analysis the pavement with more than 4 layers. The actual number of existing layers in the pavement structure is to be reflected in the analysis for better prediction. The minimum thickness of layer is allowed to be 25.4 mm. But the layer maintenance with less than 25.4 mm was not incorporated in the analysis or considered to be 25.4 mm. These shortcomings are to be addressed for realistic analysis. Moreover, the available penetration grade for asphalt binder was found different than the standard grade used in Ontario. This may have impact on the accurate prediction. Although the current version of DARWin-ME

allows final users to modify the parameters of the transfer functions, it is not convenient for local calibration when those exponent parameters need to be changed to reduce standard deviations. If the detailed structural responses are made available to final users, a more efficient local calibration and optimization procedure could be developed.

In addition to the above recommendations that can be taken for actions by the MTO, there are several topics that are wroth further investigating:

(1) High-level Local Calibration: The current local calibration focuses only on the bias parameters. To reduce the biases and standard deviations, there are in general two approaches. One approach is suggested by the AASHTO Local Calibration Guide to adjust the exponent parameters of the transfer models. This requires one to acquire the detailed structural responses (stress, strain and deformation) under different axle loading, season and climate conditions. The other approach is taken in this study. That is done by segmenting and clustering the pavement attributes. The pros and cons of the two approaches need to be investigated.

(2) Longitudinal Calibration and Life Prediction: A strong feature of the local calibration database developed in this study is the long historical performance records for each candidate pavement sections. Previous global and local calibration studies have not yet investigate the goodness-of-fit of the predicted damage along the time axis. A longitudinal study of the performance prediction and lifetime prediction will provide further insights on the validity of the distress and IRI models in the MEPDG.

-APPENDICES

Appendix A-

Truck Traffic Classification for Road Sections

Ontario's Truck Traffic Classification

Master ID	2008 ID	Hwy	Dir	Beg mile	End mile	Region	Function Class	TTC Class	Source of Trauck Classification
1	136	6	N	120.043	123.743	W	Arterial	7	Estimate
2	139	6	S	120.043	123.743	W	Arterial	7	Estimate
3	202	7	W	553.172	556.072	W	Arterial	3	Estimate
4	217	8	E	74.876	77.376	W	Freeway	3	Estimate
5	219	8	W	74.876	77.376	W	Freeway	3	Estimate
6	347	11	N	99.3	106.89	C	Arterial	11	C-LTPP
7	348	11	N	106.89	122.9	C	Arterial	11	C-LTPP
8	349	11	N	122.9	130.613	C	Freeway	11	C-LTPP
9	350	11	N	130.613	133.272	C	Arterial	11	C-LTPP
10	353	11	N	144.967	148.082	C	Arterial	11	C-LTPP
11	354	11	N	148.082	155.882	NE	Freeway	11	C-LTPP
12	355	11	N	155.882	163.982	NE	Freeway	11	C-LTPP
13	356	11	N	163.982	169.999	NE	Freeway	11	C-LTPP
14	357	11	N	169.999	175.886	NE	Freeway	11	C-LTPP
15	358	11	N	175.886	186.518	NE	Freeway	11	C-LTPP
16	361	11	N	208.218	213.318	NE	Freeway	11	C-LTPP
17	371	11	N	322.011	333.055	NE	Freeway	11	C-LTPP
18	376	11	N	1433.026	1437.126	NW	Arterial	11	C-LTPP
19	377	11	S	99.3	106.89	C	Arterial	11	C-LTPP
20	378	11	S	106.89	122.9	C	Arterial	11	C-LTPP
21	379	11	S	122.9	130.613	C	Arterial	11	C-LTPP
22	384	11	S	148.082	155.882	NE	Freeway	11	C-LTPP
23	385	11	S	155.882	163.982	NE	Freeway	11	C-LTPP
24	386	11	S	163.982	169.999	NE	Freeway	11	C-LTPP
25	560	17	W	694.8	708.38	NE	Freeway	11	Estimate
26	803	85	N	1.8	4.2	W	Freeway	7	Estimate
27	811	85	S	0	1.8	W	Freeway	7	Estimate
28	951	400	N	16.476	24.882	C	Freeway	7	LCCA
29	973	400	S	16.476	24.882	C	Freeway	7	LCCA
30	980	400	S	92.5	102.3	C	Freeway	7	LCCA
31	981	400	S	102.3	117.6	C	Freeway	7	LCCA
32	1017	401	E	302.57	314.83	E	Freeway	3	LCCA
33	1053	401	E	539.837	543.797	W	Freeway	3	LCCA
34	1054	401	E	543.797	548.357	W	Freeway	3	LCCA
35	1062	401	E	608.357	618.357	W	Freeway	3	LCCA
36	1092	401	W	166.84	182.86	E	Freeway	3	LCCA
37	1102	401	W	302.57	314.83	E	Freeway	3	LCCA
38	1130	401	W	485.772	494.7	c	Freeway	3	LCCA
39	1131	401	W	494.7	497.095	c	Freeway	3	LCCA
40	1132	401	W	497.095	507.326	c	Freeway	3	LCCA
41	1138	401	W	539.837	543.797	W	Freeway	3	LCCA
42	1139	401	W	543.797	548.357	W	Freeway	3	LCCA
43	1146	401	W	597.307	608.357	W	Freeway	3	LCCA
44	1156	401	W	694.187	711.397	W	Freeway	3	LCCA
45	1189	402	E	31.3	38.1	W	Freeway	5	LTPP
46	1200	402	W	23.6	28.7	W	Freeway	5	LTPP
47	1225	403	W	14.691	20.883	C	Freeway	7	LCCA
48	1229	403	W	59.134	65.628	C	Freeway	7	LCCA
49	1233	403	W	92.137	98.537	C	Freeway	7	LCCA
50	1233	403	W	92.137	98.537	C	Freeway	7	LCCA

Ontario's Truck Traffic Classification

Master ID	2008 ID	Hwy	Dir	Beg mile	End mile	Region	Function Class	TTC Class	Source of Trauck Classification
51	1234	403	W	98.537	110.637	C	Freeway	7	LCCA
52	1235	403	W	110.637	125.237	C	Freeway	7	LCCA
53	1250	404	S	20.195	24.342	C	Freeway	7	LCCA
54	1252	404	S	28.515	34.656	C	Freeway	7	LCCA
55	1273	410	N	0	9.995	C	Freeway	7	LCCA
56	1274	410	N	9.995	13.068	C	Freeway	7	LCCA
57	1276	410	S	0	9.995	C	Freeway	7	LCCA
58	1277	410	S	9.995	13.068	C	Freeway	7	LCCA
59	1287	416	N	73.436	76.32	E	Freeway	3	Estimate
60	1297	417	E	0	9.49	E	Freeway	7	LCCA
61	1302	417	E	78.85	98.41	E	Freeway	7	LCCA
62	1311	417	E	145.536	155.636	E	Freeway	10	LCCA
63	1314	417	W	0	9.49	E	Freeway	10	LCCA
64	1317	417	W	55.92	64.76	E	Freeway	10	LCCA
65	1319	417	W	78.85	98.41	E	Freeway	10	LCCA
66	1319	417	W	78.85	98.41	E	Freeway	10	LCCA
67	1320	417	W	98.41	105.52	E	Freeway	10	LCCA
68	1341	427	S	14.241	16.067	c	Freeway	7	LCCA
69	1	1	E	0.23	5.658	c	Freeway	3	LCCA
70	2	1	E	5.658	13.227	c	Freeway	3	LCCA
71	9	1	E	56.669	72.946	c	Freeway	3	LCCA
73	21	1	N	13.227	22.091	c	Freeway	3	LCCA
74	35	1	W	0.23	5.658	c	Freeway	3	LCCA
75	36	1	W	5.658	13.227	c	Freeway	3	LCCA
76	43	1	W	56.669	72.946	c	Freeway	3	LCCA
77	191	7	E	526.272	531.872	W	Freeway	3	Estimate
78	193	7	E	553.172	556.072	W	Freeway	3	Estimate
79	380	11	S	130.613	133.513	c	Arterial	11	C-LTPP
80	387	11	S	169.999	175.886	NE	Freeway	11	C-LTPP
81	388	11	S	175.886	186.518	NE	Freeway	11	C-LTPP
82	389	11	S	186.518	198.818	NE	Freeway	11	C-LTPP
83	390	11	S	198.818	208.218	NE	Freeway	11	C-LTPP
84	391	11	S	208.218	213.318	NE	Freeway	11	C-LTPP
85	401	11	S	322.011	333.055	NE	Freeway	11	C-LTPP
86	406	11	S	1433.026	1437.126	NW	Arterial	11	C-LTPP
87	807	85	S	1.8	4.2	W	Freeway	7	Estimate
89	958	400	N	92.5	102.3	c	Freeway	7	LCCA
90	959	400	N	102.3	117.6	c	Freeway	7	LCCA
91	970	400	S	8.108	10.22	c	Freeway	7	LCCA
92	974	400	S	24.882	37.296	c	Freeway	7	LCCA
95	1045	401	E	485.772	494.7	c	Freeway	3	LCCA
96	1046	401	E	494.7	497.095	c	Freeway	3	LCCA
97	1047	401	E	497.095	507.326	c	Freeway	3	LCCA
98	1049	401	E	515.491	518.984	c	Freeway	3	LCCA
99	1052	401	E	529.457	539.837	w	Freeway	3	LCCA
100	1054	401	E	543.797	548.357	w	Freeway	3	LCCA
101	1061	401	E	597.307	608.357	w	Freeway	3	LCCA
104	1188	402	E	23.6	31.3	W	Freeway	5	LTPP
105	1210	403	E	14.691	20.883	c	Freeway	7	LCCA
106	1214	403	E	59.134	65.628	c	Freeway	7	LCCA
107	1218	403	E	92.137	98.537	c	Freeway	7	LCCA
108	1219	403	E	98.537	110.637	c	Freeway	7	LCCA
109	1220	403	E	110.637	125.237	c	Freeway	7	LCCA
110	1243	404	N	24.342	28.515	c	Freeway	7	LCCA
111	1251	404	S	24.342	28.515	c	Freeway	7	LCCA
113	1302	417	E	78.85	98.41	E	Freeway	7	LCCA
114	1303	417	E	98.41	105.52	E	Freeway	7	LCCA

Appendix B-

Ontario’s Available Weather Station

Ontario's Available Weather Station

Station	Station Name	Location	Lattitude	Longitude	Elevation	From	To
15801	ARMSTRONG| ON	ARMSTRONG AIRPORT	50.294	-88.905	322	19530101	19680630
94932	ATIKOKAN| ON	ATIKOKAN	48.75	-91.617	395	19661001	19860930
15806	BIG TROUT LAKE| ON	BIG TROUT LAKE	53.833	-89.867	224	19700101	19891231
94862	CHAPLEAU| ON	CHAPLEAU	47.833	-83.433	428	19651101	19760331
94797	EARLTON| ON	EARLTON AIRPORT	47.7	-79.85	243	19591001	19790930
94864	GERALDTON| ON	GERALDTON	49.7	-86.95	331	19671101	19770331
94888	GERALDTON| ON	GERALDTON AIRPORT	49.783	-86.931	349	19870701	20070630
94803	GORE BAY| ON	GORE BAY AIRPORT	45.883	-82.567	194	19711001	19910930
14998	GRAHAM| ON	GRAHAM AIRPORT	49.267	-90.583	503	19530101	19661231
4797	HAMILTON| ON	HAMILTON AIRPORT	43.172	-79.934	238	19590101	20060531
14899	KAPUSKASING| ON	KAPUSKASING AIRPORT	49.414	-82.468	226	19870701	20070630
14999	KENORA| ON	KENORA AIRPORT	49.79	-94.365	410	19870701	20070630
94799	KILLALOE| ON	KILLALOE	45.567	-77.417	174	19530101	19720731
94805	LONDON| ON	LONDON AIRPORT	43.033	-81.151	278	19740201	19940131
94857	MOUNT FOREST| ON	MOUNT FOREST	43.983	-80.75	415	19620101	19760731
15804	NAKINA| ON	NAKINA AIRPORT	50.183	-86.7	325	19530101	19671031
4705	NORTH BAY| ON	NORTH BAY AIRPORT	46.364	-79.423	370	19390101	19940131
4772	OTTAWA| ON	MACDONALD-CARTIER INTERNATIONAL AIRPORT	45.323	-75.669	114	19380101	20070630
4706	OTTAWA| ON	OTTAWA ROCKCLIFFE AIRPORT	45.45	-75.633	54	19420101	19640331
54706	PETAWAWA| ON	PETAWAWA AIRPORT	45.95	-77.317	130	19730701	19930630
94842	SAULT STE MARIE| ON	SAULT STE MARIE AIRPORT	46.483	-84.509	192	19870701	20070630
94858	SIMCOE| ON	SIMCOE	42.85	-80.267	240	19620101	19770731
15909	SIOUX LOOKOUT| ON	SIOUX LOOKOUT AIRPORT	50.117	-91.9	383	19870701	20070630
4713	STIRLING| ON	STIRLING	44.317	-77.633	139	19400101	19681130
94828	SUDBURY| ON	SUDBURY AIRPORT	46.625	-80.799	347	19870701	20070630
94804	THUNDER BAY| ON	THUNDER BAY AIRPORT	48.369	-89.327	199	19740101	19931231
94831	TIMMINS| ON	VICTOR POWER AIRPORT	48.57	-81.377	295	19740701	19940630
54753	TORONTO| ON	BUTTONVILLE AIRPORT	43.862	-79.37	198	19870701	20070630
94791	TORONTO| ON	LESTER B. PEARSON INTERNATIONAL AIRPORT	43.677	-79.631	173	19870701	20070630
4715	TRENTON| ON	TRENTON AIRPORT	44.117	-77.533	86	19350101	19940531
94808	WHITE RIVER| ON	WHITE RIVER	48.6	-85.283	379	19560101	19751231
94809	WIARTON| ON	WIARTON AIRPORT	44.746	-81.107	222	19750701	19950630
94810	WINDSOR| ON	WINDSOR AIRPORT	42.276	-82.956	190	19750701	19950630
15807	WINISK| ON	WINISK AIRPORT	55.233	-85.117	13	19590201	19650630

Appendix C-

Material Layer information of Road Section

Material Layer Information

			Layers															
2008 ID	Hwy	Dir	Lay 1 Mat.	Lay 1 (mm)	Lay 2 Mat.	Lay 2 (mm)	Lay 3 Mat.	Lay 3 (mm)	Lay 4 Mat.	Lay 4 (mm)	Lay 5 Mat.	Lay 5 (mm)	Lay 6 Mat.	Lay 6 (mm)	Lay 7 Mat.	Lay 7 (mm)	Subgrade	Subgrade Strength
136	6	N	HL1	40	HL4B	50	HL1	40	HL 4B	75	HL 2	25	GrA	150	GrB1	425	Sandy si	35
139	6	S	HL1	40	HL4B	50	HL1	40	HL 4B	75	HL 2	25	GrA	150	GrB1	425	Sandy si	35
202	7	W	HL1	40	RHL	105	GrA	150	GrB1	550							Sandy si	25
217	8	E	DFC	40	HDB	100	HL1	35	HL4B	100	GrA	150	GrB1	450			Sandy si	40
219	8	W	DFC	40	HDB	100	HL1	35	HL4B	100	GrA	150	GrB1	450			Sandy si	40
347	11	N	HL1	40	HL8	50	HL8	20	HL1	40	HL8	60	GrA	250	GrB1	400	Sandy si	40
348	11	N	HL1	40	HL8	50	**HL2**	**20**	HL4S	40	HL8	20	GrA	250	GrB1	400	Sandy si	35
349	11	N	HL1	40	HL8	50	HL8	20	HL1	40	**HL8**	**60**	GrA	250	GrB1	400	Sandy si	35
350	11	N	HL1	40	HL8	50	HL8	20	HL1	40	**HL8**	**60**	GrA	250	GrB1	400	Sandy si	35
353	11	N	HL1	40	HL8	50	HL2	30	**HL1**	40	HL8	60	GrA	250	GrB1	400	Sandy si	40
354	11	N	HL1	40	RHL	40	HL8	60	GrA	250	GrB1	400					Sandy si	40
355	11	N	HL3M	40	RHL	40	GrA	150	GrB1	450							Sandy si	35
356	11	N	HL3M	50	CIR	90	HL2	19	GrA	150	GrB1	450					Sandy si	35
357	11	N	HL 3	50	HL1	32	HL 4B	38	**HL1**	**40**	HL 4B	100	GrA	150	GrB1	450	Sandy si	35
358	11	N	HL1	40	HL 4B	76	HL2	25	GrA	150	GrB1	450					Sandy si	50
361	11	N	HL1	40	HL 4B	76	HL2	25	GrA	150	GrB1	450					Sandy si	50
371	11	N	HL 4S	40	RHL	90	GrA	150	GrB1	450							Sandy si	35
376	11	N	HL1	40	HL8	90	GrA	270	GrB1	600							Sandy si	27.6
377	11	S	HL1	40	MDB	20	HL 4S	40	HL8	20	GrA	250	GrB1	400			Sandy si	40
378	11	S	HL 1	40	MDB	20	HL 4S	40	HL8	20	GrA	250	GrB1	400			Sandy si	40
379	11	S	HL 1	40	MDB	80	HL8	20	HL1	40	**HL8**	**60**	GrA	250	GrB1	400	Sandy si	35
384	11	S	HL1	40	RHL	40	GrA	150	GrB1	450							Sandy si	35
385	11	S	HL3M	40	RHL	40	GrA	150	GrB1	450							Sandy si	50
386	11	S	HL3M	25	RHL	40	HL4B	81	HL2	19	GrA	150	GrB1	450			Sandy si	35
560	17	W	HL4S	50	RHL	80	GrA	190	GrB1	430							Lacus.	34.5
803	85	N	DFC	40	HDB	50	HL 1	40	HL 4B	80	BTB	20	**GrA**	**150**	GrB1	450	Sandy si	25
811	85	S	DFC	40	HDB	50	HL 4B	95	BTB	20	**GrA**	**150**					Sandy si	40
951	400	N	DFC	40	HDB	40	HL5	190.5	GrA	152.4	GrB3	609.6						41
973	400	S	DFC	40	HDB	40	HL5	190	GrA	153	GrB3	610					Sandy si	41
980	400	S	HL1	40	HL4B	35	HL1	40	**HL4B**	**50**	HL2	30	GrA	150	GrB1	300	Sandy si	40
981	400	S	HL1	40	MDB	50	HL2	10	GrA	150	GrB1	400					Sandy si	40
1017	401	E	DFC	40	HDB	40	HDB	50	HL 3	40	HL 8	188	GrA	375	GrB3	375	Sandy si	41
1053	401	E	DFC	40	HL4S	200	GrA	150	GrB1	500							Sandy si	15
1054	401	E	DFC	40	HL4B	50	HL1	190	GrA	150	GrB1	500					Sandy si	40
1062	401	E	DFC	40	HDB	80	HL1	175	GrA	150	GrB1	450					Sandy si	25
1092	401	W	DFC	40	HDB	50	HDB	40	GrA	80							Sandy si	35
1102	401	W	DFC	40	HDB	40	HDB	50	HL 3	40	HL 8	188	GrA	375	GrB3	375	Sandy si	41.4
1130	401	W	DFC	40	HDB	40	HDB	50	HL 3	40	HL 8	188	GrA	375	GrB3	375	Sandy si	35

Material Layer Information

			Layers															
2008 ID	Hwy	Dir	Lay 1 Mat.	Lay 1 (mm)	Lay 2 Mat.	Lay 2 (mm)	Lay 3 Mat.	Lay 3 (mm)	Lay 4 Mat.	Lay 4 (mm)	Lay 5 Mat.	Lay 5 (mm)	Lay 6 Mat.	Lay 6 (mm)	Lay 7 Mat.	Lay 7 (mm)	Subgrade	Subgrade Strength
1131	401	W	DFC	40	HDB	50	HDB	50	HL 3	40	HL 8	188	GrA	375	GrB3	375	Sandy si	35
1132	401	W	DFC	40	HDB	50	HL8	38	HL 3	40	HL 8	188	GrA	375	GrB3	375	Sandy si	35
1138	401	W	DFC	40	HDB	50	HL1	38	HL8	38	HL1	200	GrA	500			Sandy si	40
1139	401	W	DFC	40	HL4B	50	HL1	38	HL8	38	HL1	190	GrA	150	GrB1	500	Sandy si	40
1146	401	W	DFC	40	HDB	80	HL4B	140	GrA	150	GrB1	700					Sandy si	35
1156	401	W	DFC	40	HDB	50	HL1	40	HL4S	30	HL4M	50	GrA	150	GrB1	450	Sandy si	40
1189	402	E	HL1	40	MDB	80	HL4B	100	GrA	150	GrB1	450					Sandy si	25
1200	402	W	HL1	40	MDB	80	HL4B	100	GrA	150	GrB1	450					Lacus.	25
1225	403	W	DFC	40	HDB	50	HL8	160	GrA	300							Sandy si	35
1229	403	W	DFC	40	HDB	80	HL8	100	GrA	300							Sandy si	31
1233	403	W	HL1	40	HL4B	90	GrA	250	GrB1	400							sandy si	35
1233	403	W	DFC	40	HDB	50	HL4B	90	GrA	250	GrB1	400					sandy si	35
1234	403	W	HL1	40	HL4B	90	GrA	250	GrB1	400							sandy si	35
1235	403	W	HL1	40	HL 4M	90	GrA	250	GrB1	400							sandy si	30
1250	404	S	DFC	40	HL6	102	BTB	114	GrA	76	GrB3	305					Sandy si	31
1252	404	S	DFC	40	HDB	50	HL8	50	GrA	225	GrB2	550					Sandy si	31
1273	410	N	DFC	41	HDB	51	HDBC	100	GrA	150	GrB2	500					Sandy si	35
1274	410	N	DFC	42	HDB	52	HDB	90	HL8	75	GrA	150	GrB2	450				31
1276	410	S	DFC	43	HDB	53	HL 8	100	GrA	150	GrB2	500					Sandy si	35
1277	410	S	DFC	44	HDB	54	HL 8	125	HL 8	210	GrA	280						31
1287	416	N	DFC	40	HDB	80	HL 8	105	GrO	225	GrB2	400					Sandy si	35
1297	417	E	HL1	40	HL 3	40	HL 4B	60	HL 8	135	GrA	150	SSM	300			Sandy si	35
1302	417	E	HL3	40	HL 4M	50	HL 4M	60	HL 4S	40	HL 8	190	GrA	150			Sandy si	25
1311	417	E	HL 1	40	HDB	40	HDB	60	GrO	150	GrB1	450					Varved	17.2
1314	417	W	HL1	40	HL 4B	45	HL 4S	40	HL 8	135	GrA	150	SSM	300			Sandy si	35
1317	417	W	HL 3	40	HDB	50	HL 4M	70	HL 4S	40	HL 8	135	CTB	150			Lacus.	35
1319	417	W	HL1	40	HDB	50	HL 4M	60	HL 4S	40	HL 8	190	GrA	150			Sandy si	25
1319	417	W	HL 3M	40	HL 4M	60	HL 4S	40	HL 8	190	GrA	150					Sandy si	25
1320	417	W	HL 3	40	HL 4B	50	HL 4S	40	HL 8	120	GrA	150					Sandy si	31
1341	427	S	SP12.5	40	HL 8	190	GrA	330									Sandy si	35

Appendix D –

A sample Output of DARWin-ME Software

Sec 136

File Name: C:\Documents and Settings\OPS_Guest\My Documents\My DarwinME\Projects\Project Ryerson 2011\Sec 136.dgpx

Design Inputs

Design Life: 12 years
Design Type: AC over AC

Existing construction: August, 1975
Pavement construction: September, 1998
Traffic opening: January, 1999

Climate Data Sources (Lat/Lon): 43.983, -80.75; 43.677, -79.631; 43.172, -79.934; 43.862, -79.37

Design Structure

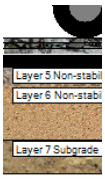

Layer type	Material Type	Thickness(mm):
Flexible	HL1	40.0
Flexible	HL-4B	50.0
Flexible	HL1	40.0
Flexible	HL-4B	100.0
NonStabilized	Granular A	150.0
NonStabilized	Granular B1	425.0
Subgrade	ML	Semi-infinite

Volumetric at Construction:

Effective binder content (%)	12.4
Air voids (%)	4.0

Traffic

Age (year)	Heavy Trucks (cumulative)
1999 (initial)	2,310
2005 (6 years)	2,500,730
2011 (12 years)	5,614,180

Design Outputs

Distress Prediction Summary

Distress Type	Distress @ Specified Reliability		Reliability (%)		Criterion Satisfied?
	Target	Predicted	Target	Achieved	
Terminal IRI (m/km)	2.30	1.69	50.00	89.79	Pass
Permanent deformation - total pavement (mm)	19.00	9.50	50.00	100.00	Pass
Total Cracking (Reflective + Alligator) (percent)	100.00	34.27	-	-	-
AC thermal fracture (m/km)	189.40	3.70	50.00	100.00	Pass
AC bottom-up fatigue cracking (percent)	25.00	0.00	50.00	100.00	Pass
AC top-down fatigue cracking (m/km)	378.80	0.04	50.00	100.00	Pass
Permanent deformation - AC only (mm)	6.00	3.63	50.00	96.46	Pass

Distress Charts

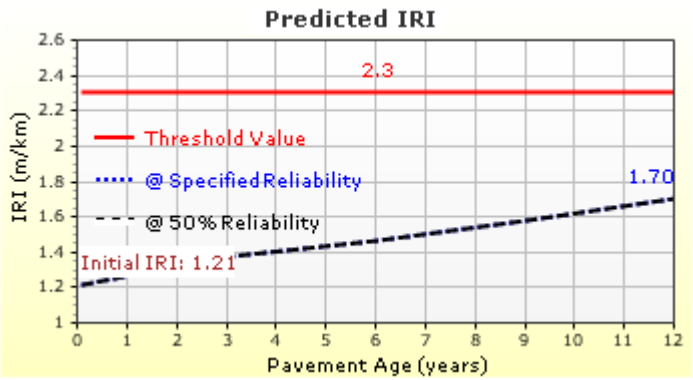

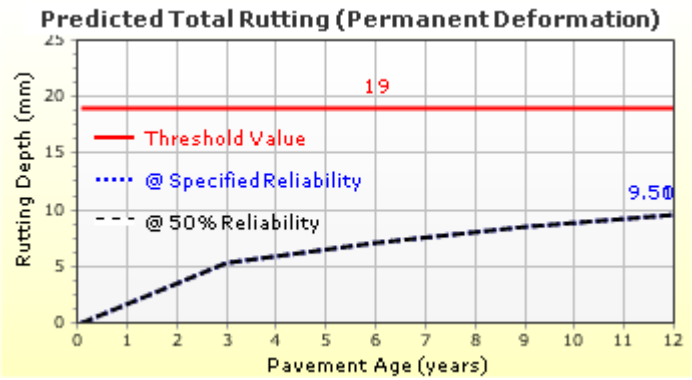

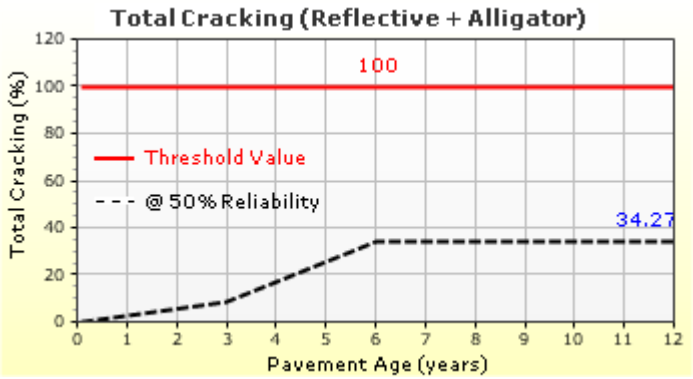

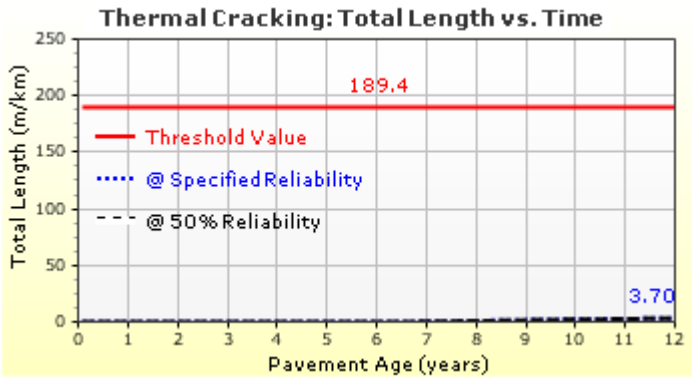

Traffic Inputs

Graphical Representation of Traffic Inputs

Initial two-way AADTT:	2,310	Percent of trucks in design direction (%):	50.0
Number of lanes in design direction:	2	Percent of trucks in design lane (%):	90.0
		Operational speed (kph)	80.0

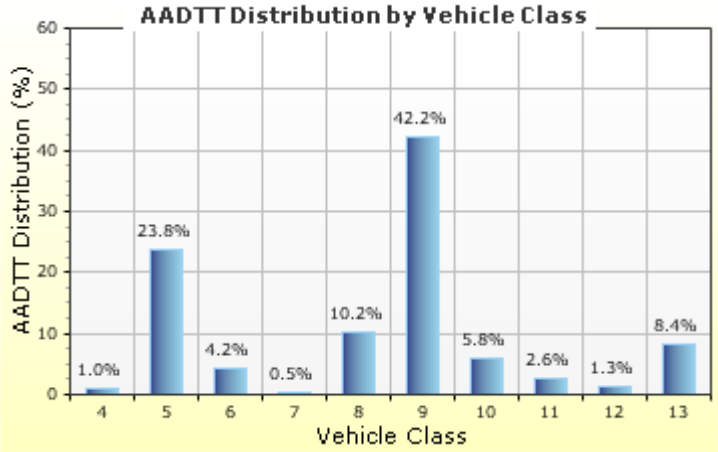

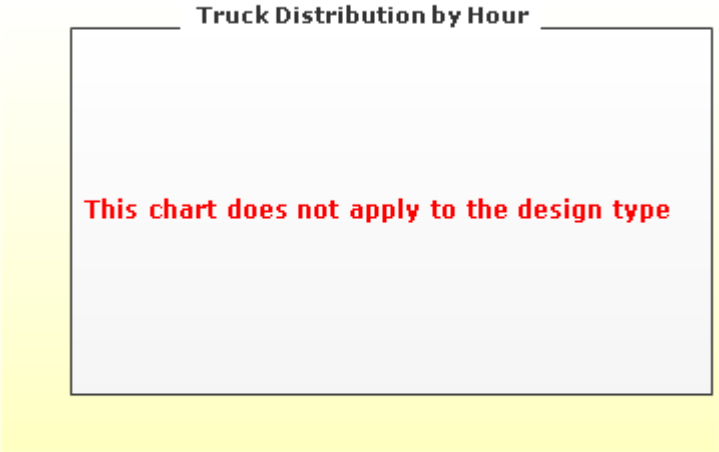

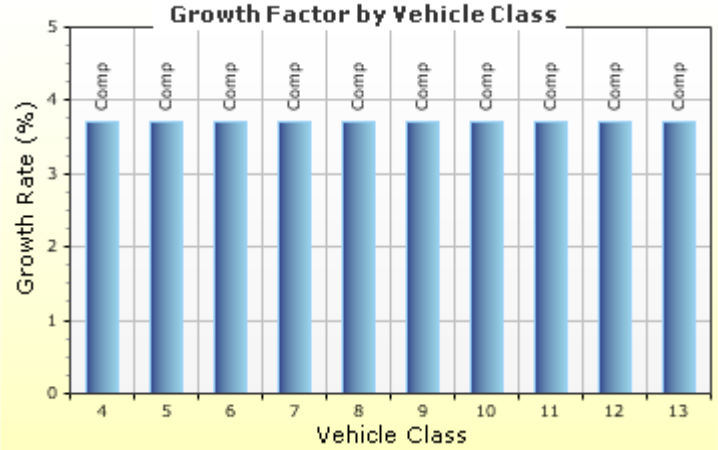

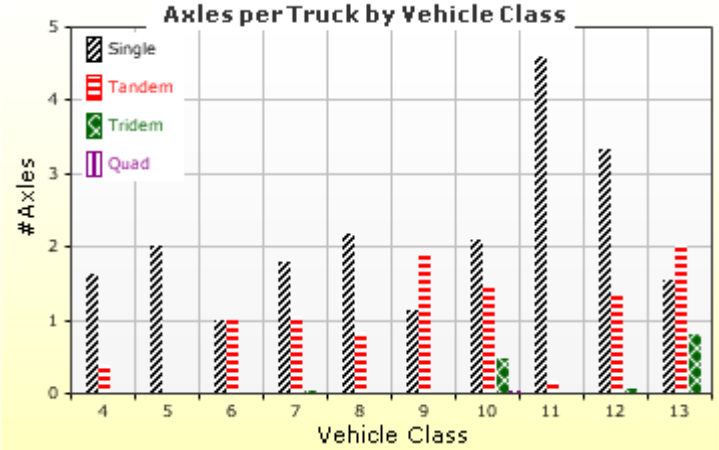

Traffic Volume Monthly Adjustment Factors

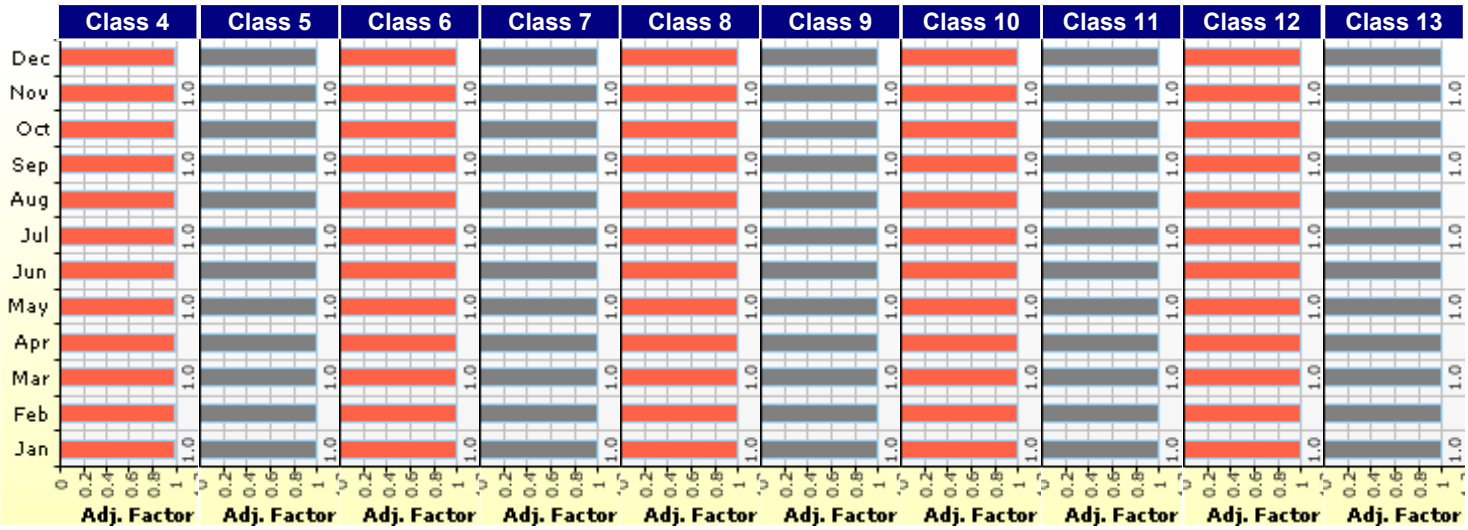

Tabular Representation of Traffic Inputs

Volume Monthly Adjustment Factors

Level 3: Default MAF

Month	Vehicle Class									
	4	5	6	7	8	9	10	11	12	13
January	1.0	1.0	1.0	1.0	1.0	1.0	1.0	1.0	1.0	1.0
February	1.0	1.0	1.0	1.0	1.0	1.0	1.0	1.0	1.0	1.0
March	1.0	1.0	1.0	1.0	1.0	1.0	1.0	1.0	1.0	1.0
April	1.0	1.0	1.0	1.0	1.0	1.0	1.0	1.0	1.0	1.0
May	1.0	1.0	1.0	1.0	1.0	1.0	1.0	1.0	1.0	1.0
June	1.0	1.0	1.0	1.0	1.0	1.0	1.0	1.0	1.0	1.0
July	1.0	1.0	1.0	1.0	1.0	1.0	1.0	1.0	1.0	1.0
August	1.0	1.0	1.0	1.0	1.0	1.0	1.0	1.0	1.0	1.0
September	1.0	1.0	1.0	1.0	1.0	1.0	1.0	1.0	1.0	1.0
October	1.0	1.0	1.0	1.0	1.0	1.0	1.0	1.0	1.0	1.0
November	1.0	1.0	1.0	1.0	1.0	1.0	1.0	1.0	1.0	1.0
December	1.0	1.0	1.0	1.0	1.0	1.0	1.0	1.0	1.0	1.0

Distributions by Vehicle Class

Vehicle Class	AADTT Distribution (%) (Level 3)	Growth Factor	
		Rate (%)	Function
Class 4	1%	3.72%	Compond
Class 5	23.8%	3.72%	Compond
Class 6	4.2%	3.72%	Compond
Class 7	0.5%	3.72%	Compond
Class 8	10.2%	3.72%	Compond
Class 9	42.2%	3.72%	Compond
Class 10	5.8%	3.72%	Compond
Class 11	2.6%	3.72%	Compond
Class 12	1.3%	3.72%	Compond
Class 13	8.4%	3.72%	Compond

Truck Distribution by Hour

Hour	Distribution (%)	Hour	Distribution (%)
12 AM	2.3%	12 PM	5.9%
1 AM	2.3%	1 PM	5.9%
2 AM	2.3%	2 PM	5.9%
3 AM	2.3%	3 PM	5.9%
4 AM	2.3%	4 PM	4.6%
5 AM	2.3%	5 PM	4.6%
6 AM	5%	6 PM	4.6%
7 AM	5%	7 PM	4.6%
8 AM	5%	8 PM	3.1%
9 AM	5%	9 PM	3.1%
10 AM	5.9%	10 PM	3.1%
11 AM	5.9%	11 PM	3.1%
		Total	100%

Axle Configuration

Traffic Wander	
Mean wheel location (mm)	460
Traffic wander standard deviation (mm)	254
Design lane width (m)	3.75

Axle Configuration	
Average axle width (m)	2.6
Dual tire spacing (mm)	300
Tire pressure (kPa)	827.4

Average Axle Spacing	
Tandem axle spacing (m)	1.45
Tridem axle spacing (m)	1.68
Quad axle spacing (m)	1.32

Wheelbase does not apply

Number of Axles per Truck

Vehicle Class	Single Axle	Tandem Axle	Tridem Axle	Quad Axle
Class 4	1.62	0.39	0	0
Class 5	2	0	0	0
Class 6	1.001	1	0	0
Class 7	1.783	1.056	0.036	0
Class 8	2.171	0.842	0	0
Class 9	1.128	1.932	0.003	0
Class 10	2.087	1.459	0.475	0.032
Class 11	4.589	0.185	0	0
Class 12	3.336	1.332	0.06	0
Class 13	1.536	2.038	0.797	0.004

AADTT (Average Annual Daily Truck Traffic) Growth

*** Traffic cap is not enforced**

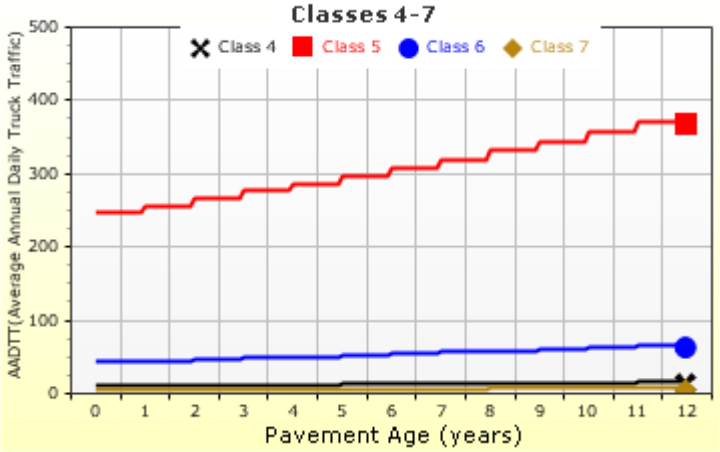

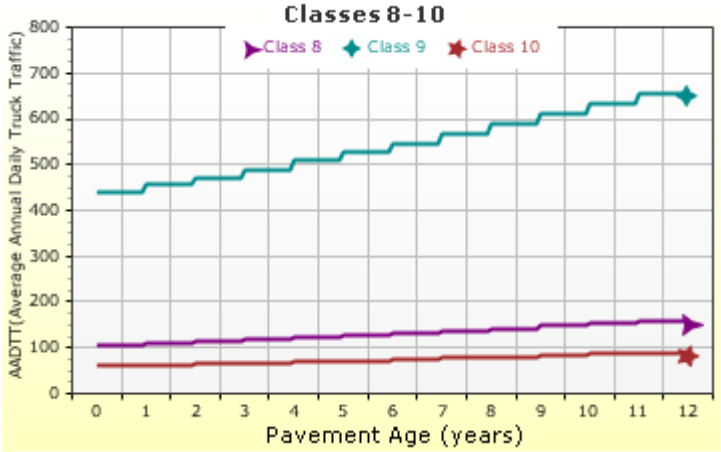

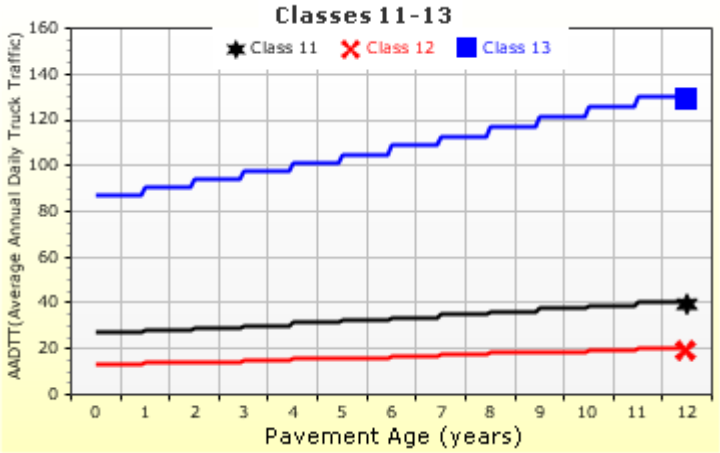

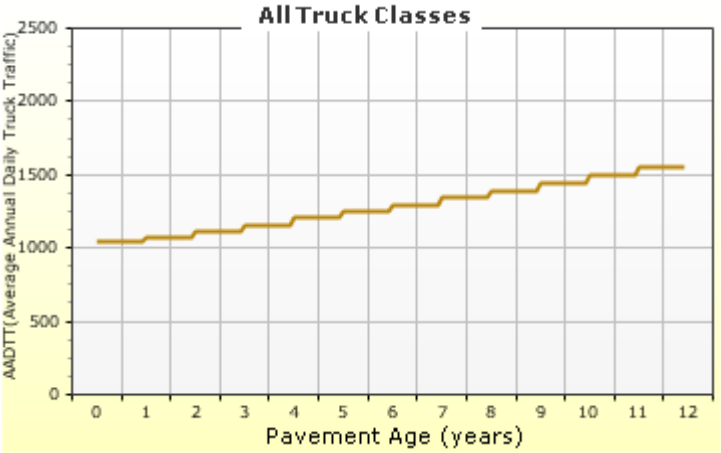

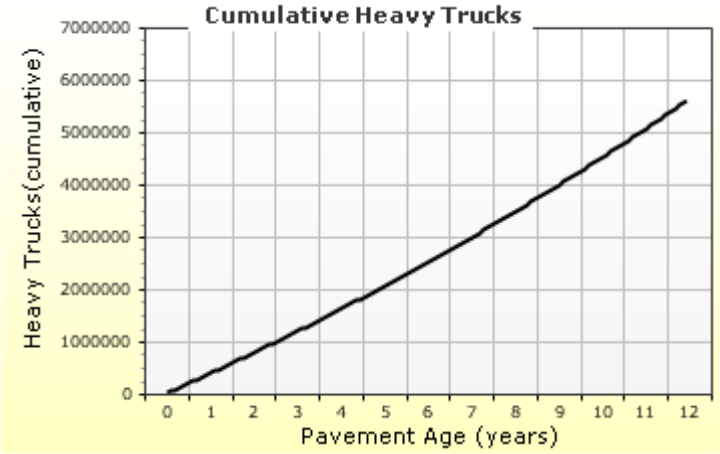

Climate Inputs

Climate Data Sources:

Climate Station Cities:	Location (lat lon elevation(m))
MOUNT FOREST, ON	43.98300 -80.75000 415
TORONTO, ON	43.67700 -79.63100 173
HAMILTON, ON	43.17200 -79.93400 238

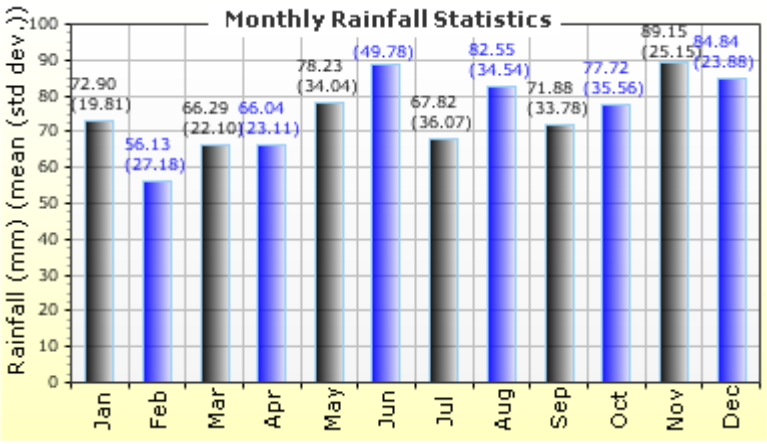

Annual Statistics:

Mean annual air temperature (ºC)	5.40
Mean annual precipitation (mm)	904.24
Freezing index (ºC - days)	873.25
Average annual number of freeze/thaw cycles:	57.14

Monthly Climate Summary:

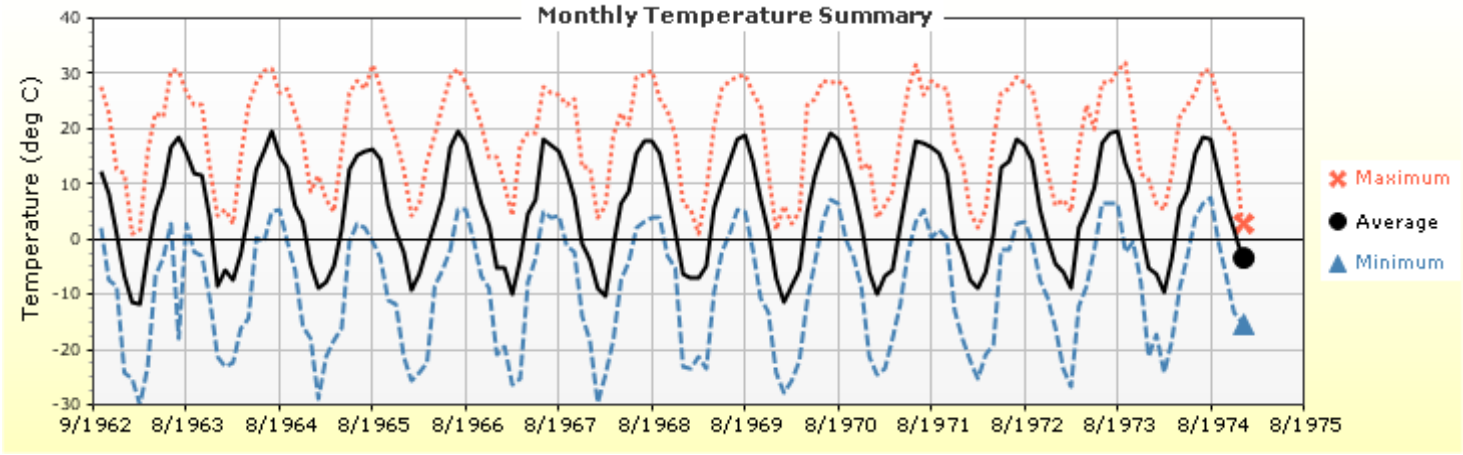

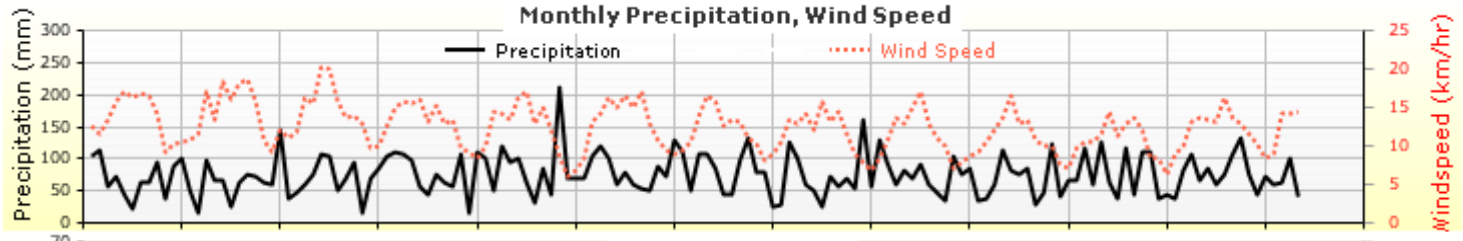

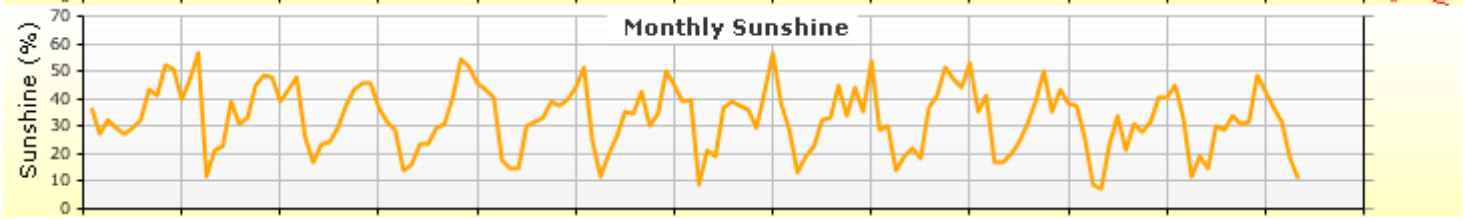

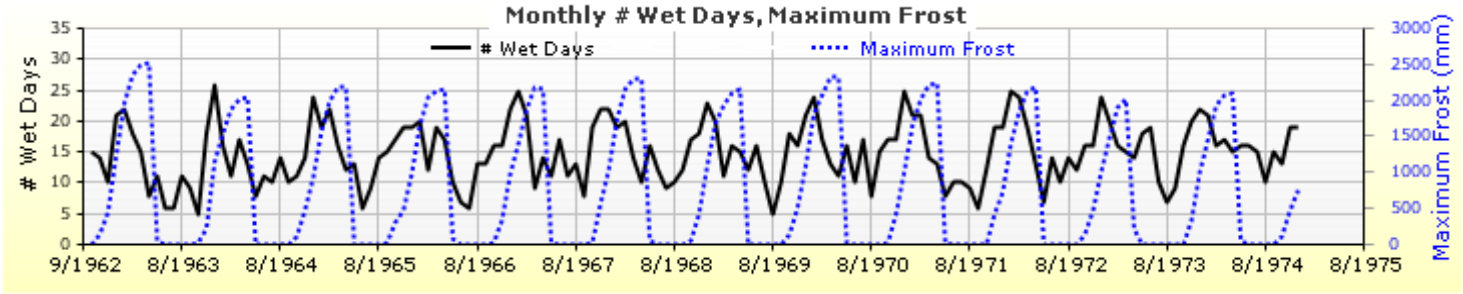

Hourly Air Temperature Distribution by Month:

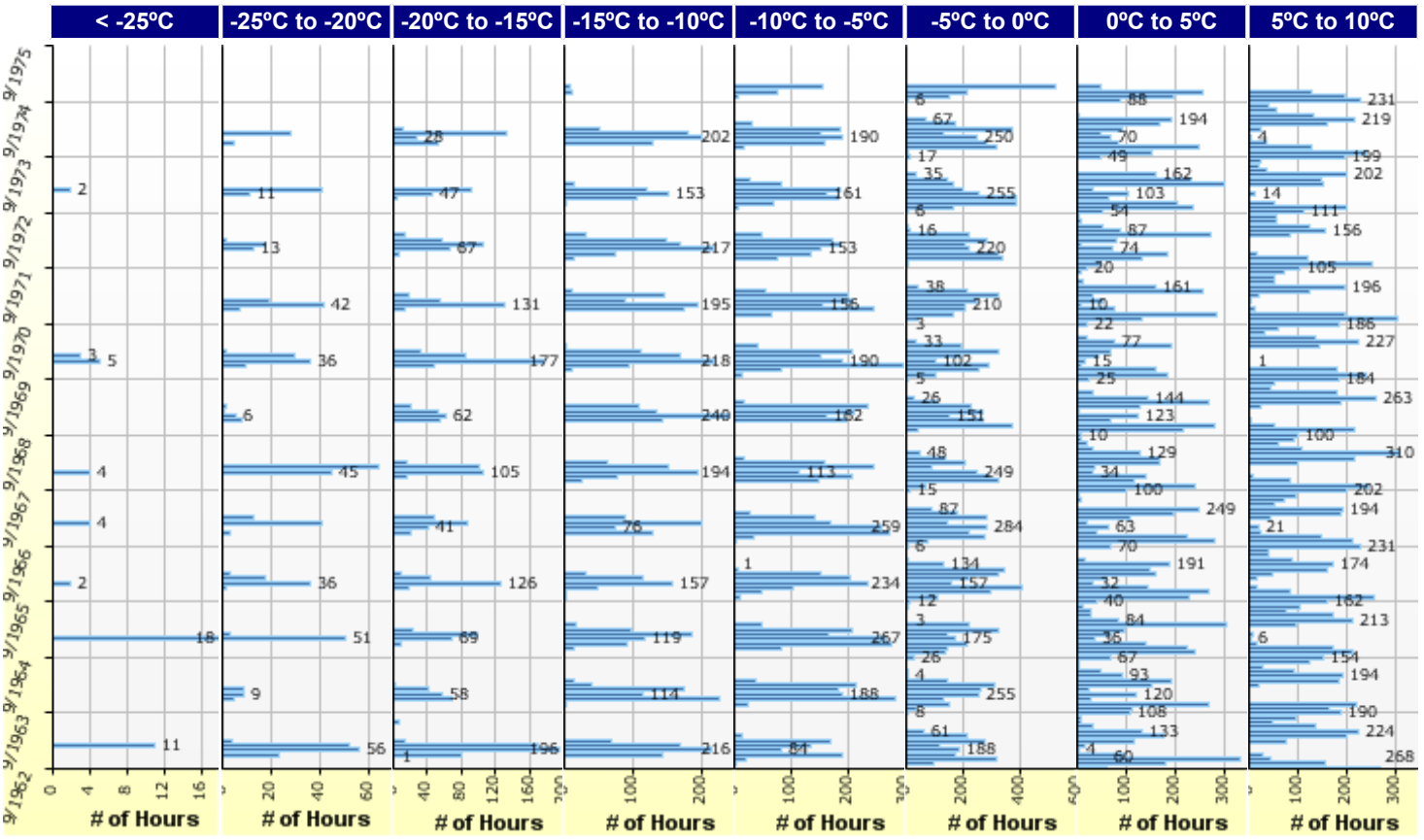

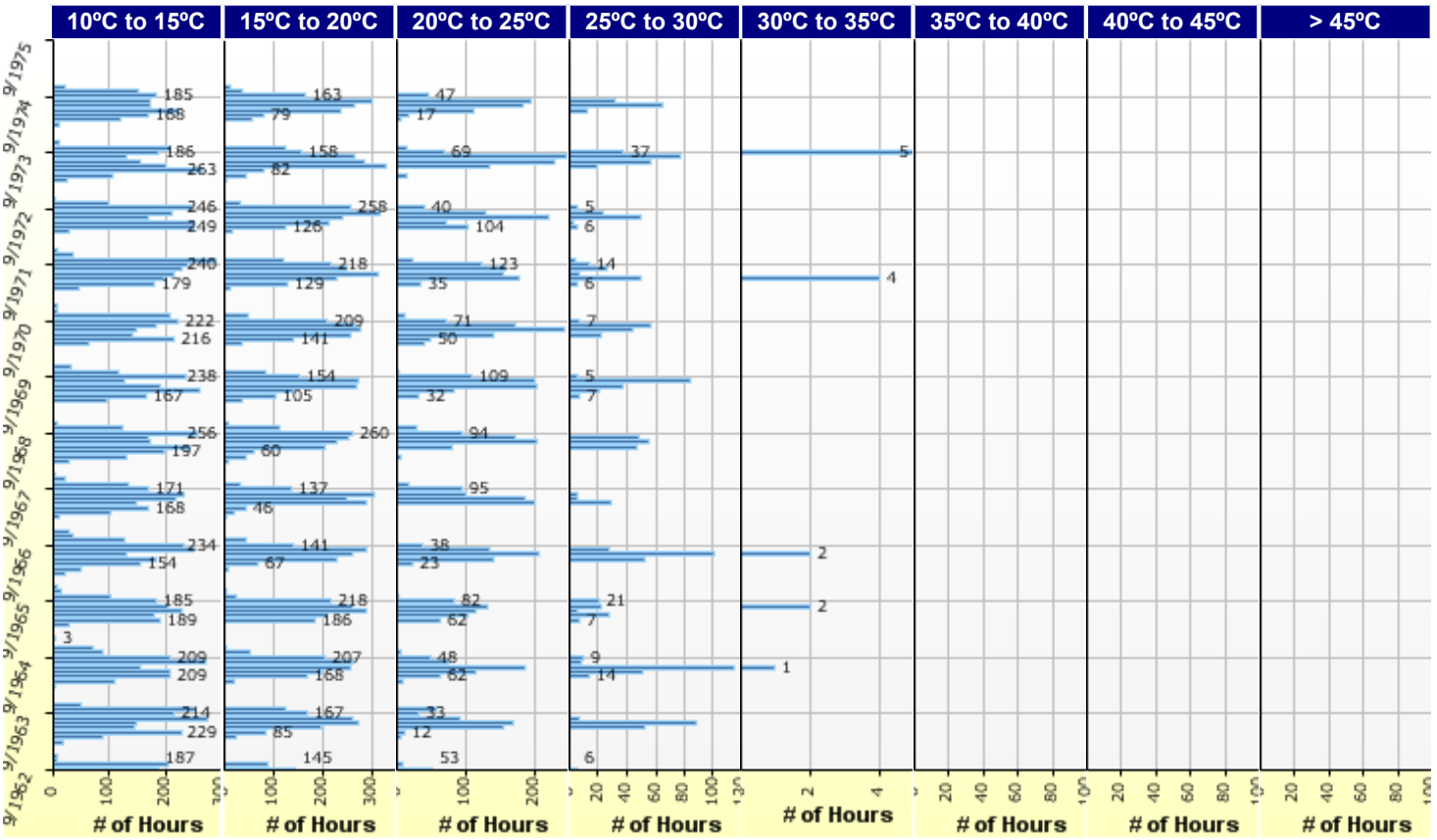

Design Properties

HMA Design Properties

Using G* based model (not nationally calibrated)	False
Is NCHRP 1-37A HMA Rutting Model Coefficients	True
Endurance Limit	-
Use Reflective Cracking	True

Structure - ICM Properties	
AC surface shortwave absorptivity	0.85

Layer Name	Layer Type	Interface Friction
Layer 1 Flexible : HL1	Flexible (1)	1.00
Layer 2 Flexible : HL-4B	Flexible (1)	1.00
Layer 3 Flexible : HL1	Flexible (1)	1.00
Layer 4 Flexible : HL-4B	Flexible (1)	1.00
Layer 5 Non-stabilized Base : Granular A	Non-stabilized Base (4)	1.00
Layer 6 Non-stabilized Base : Granular B1	Non-stabilized Base (4)	1.00
Layer 7 Subgrade : ML	Subgrade (5)	-

HMA Rehabilitation (Input Level: 3)

Milled thickness (mm)	-
Fatigue cracking	-
Pavement rating	Fair
Total rut depth (mm)	4.00

Thermal Cracking (Input Level: 3)

Indirect tensile strength at -10 ºC (MPa)	2.49

Thermal Contraction	
Is thermal contraction calculated?	True
Mix coefficient of thermal contraction (mm/mm/ºC)	-
Aggregate coefficient of thermal contraction (mm/mm/ºC)	9.0e-006
Voids in Mineral Aggregate (%)	16.4

	Creep Compliance (1/GPa)		
Loading time (sec)	-20 ºC	-10 ºC	0 ºC
1	4.57e-002	6.08e-002	7.57e-002
2	4.93e-002	6.99e-002	9.48e-002
5	5.46e-002	8.41e-002	1.28e-001
10	5.90e-002	9.67e-002	1.60e-001
20	6.38e-002	1.11e-001	2.00e-001
50	7.07e-002	1.34e-001	2.70e-001
100	7.64e-002	1.54e-001	3.38e-001

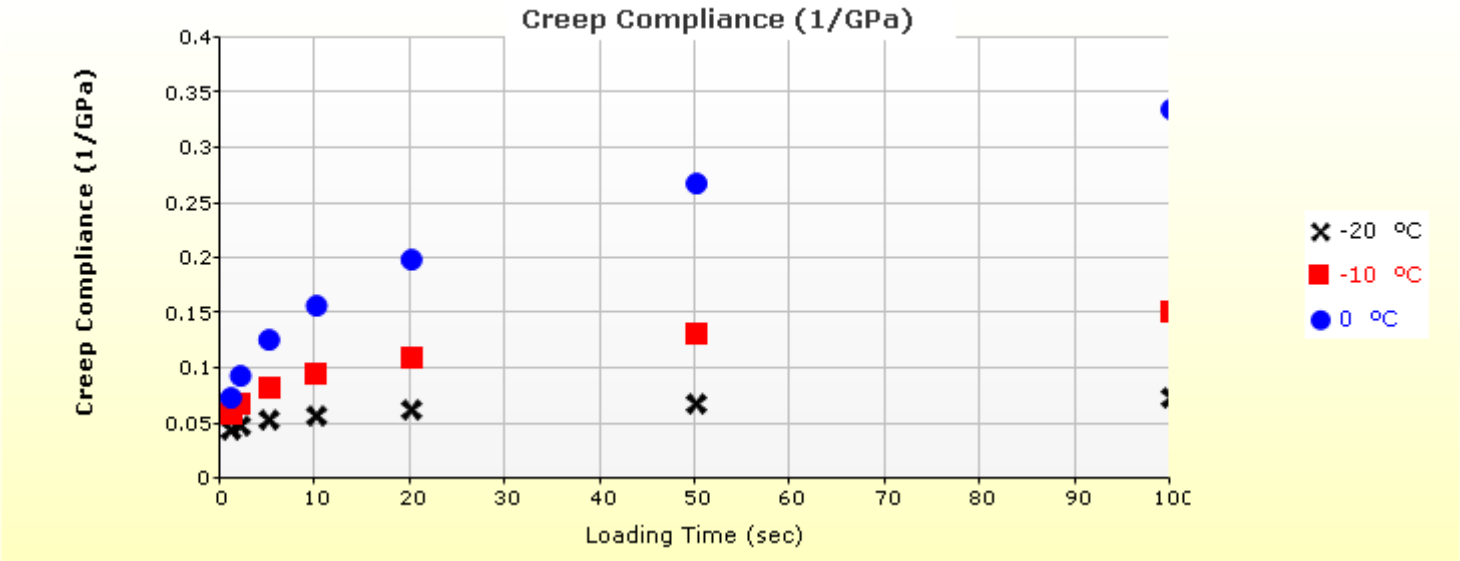

HMA Layer 1: Layer 1 Flexible : HL1

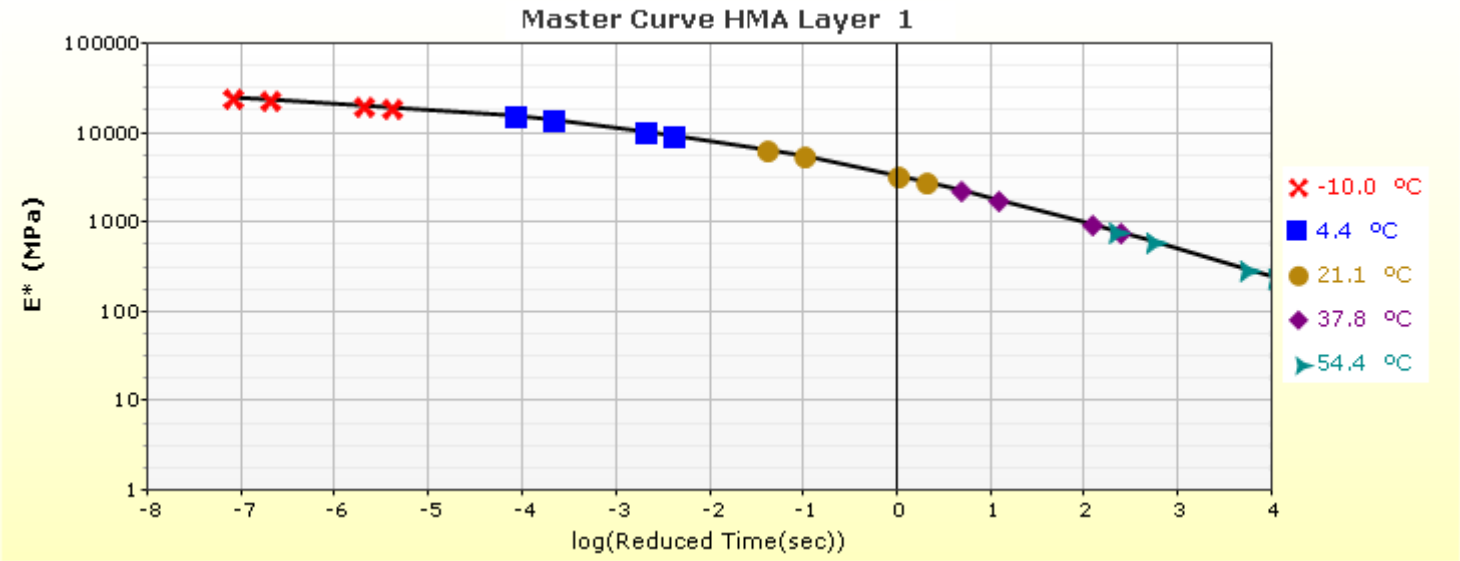

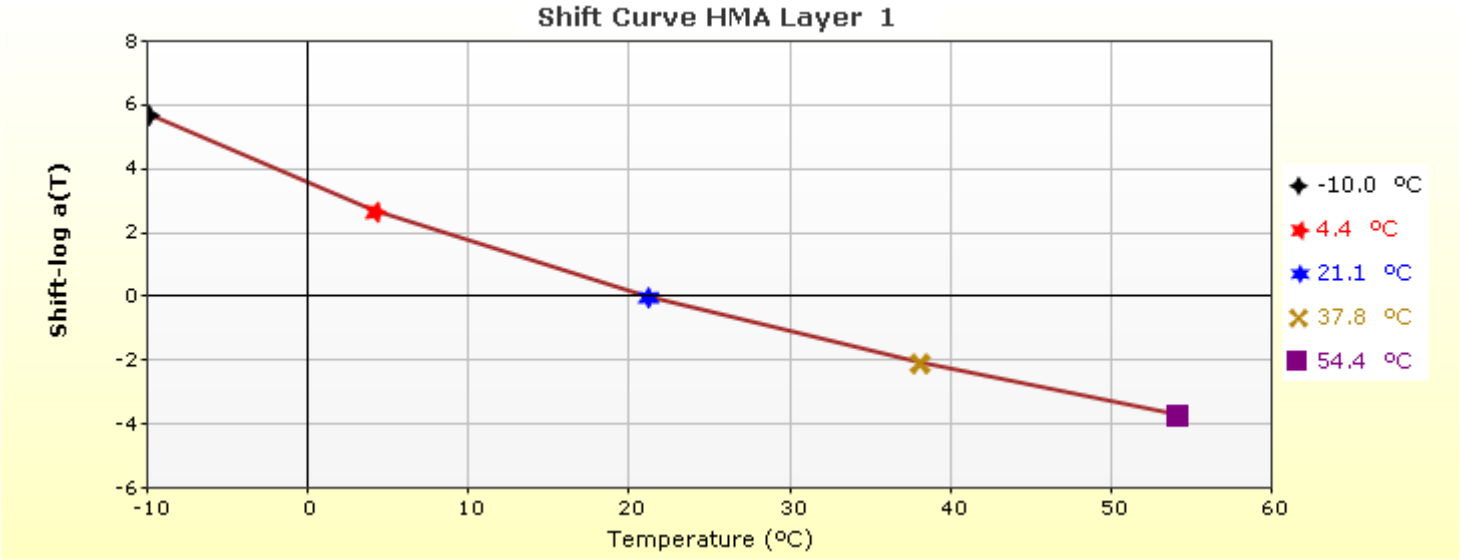

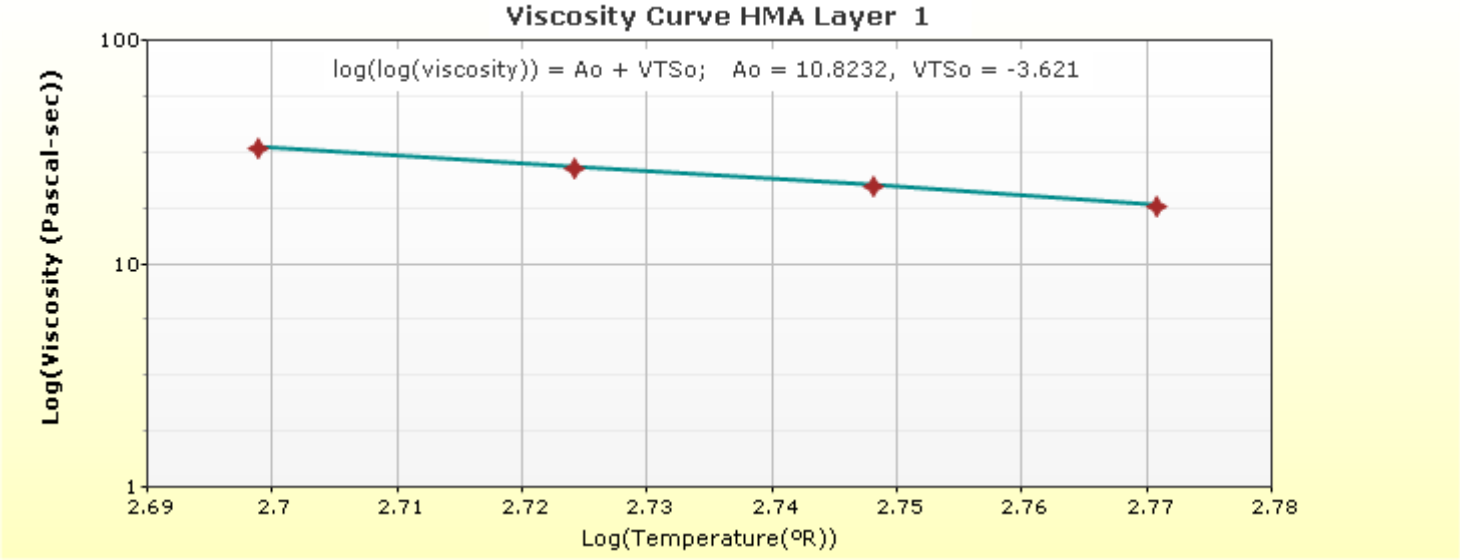

HMA Layer 2: Layer 2 Flexible : HL-4B

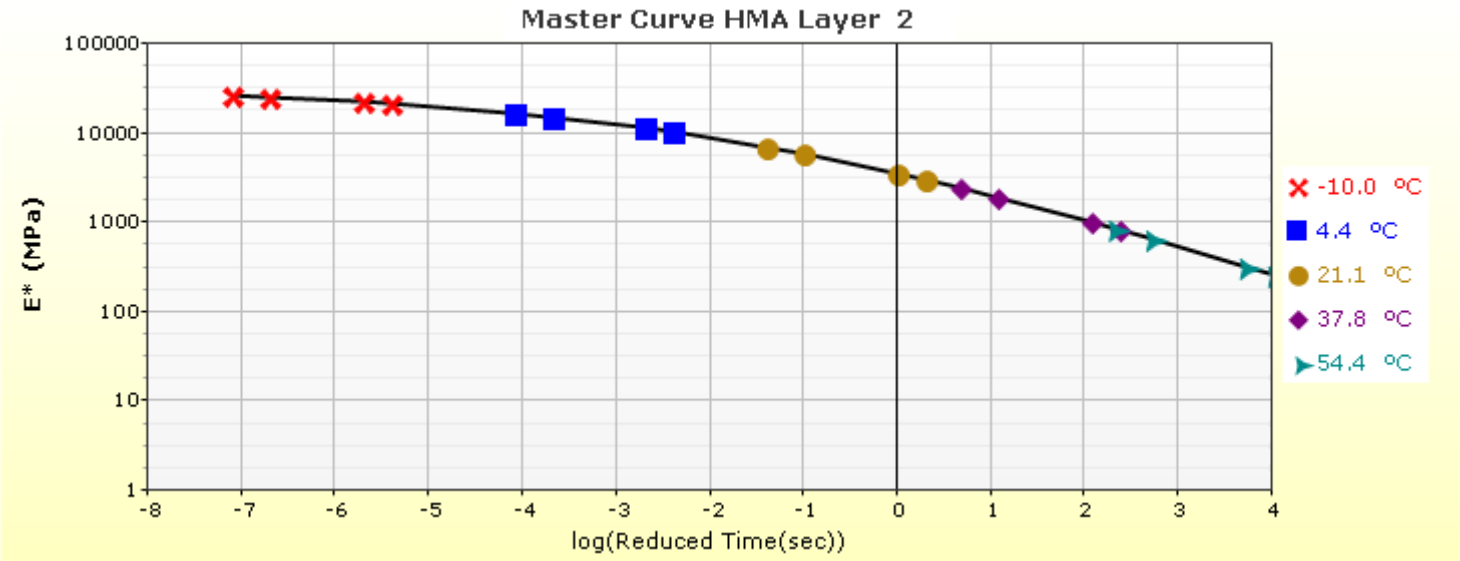

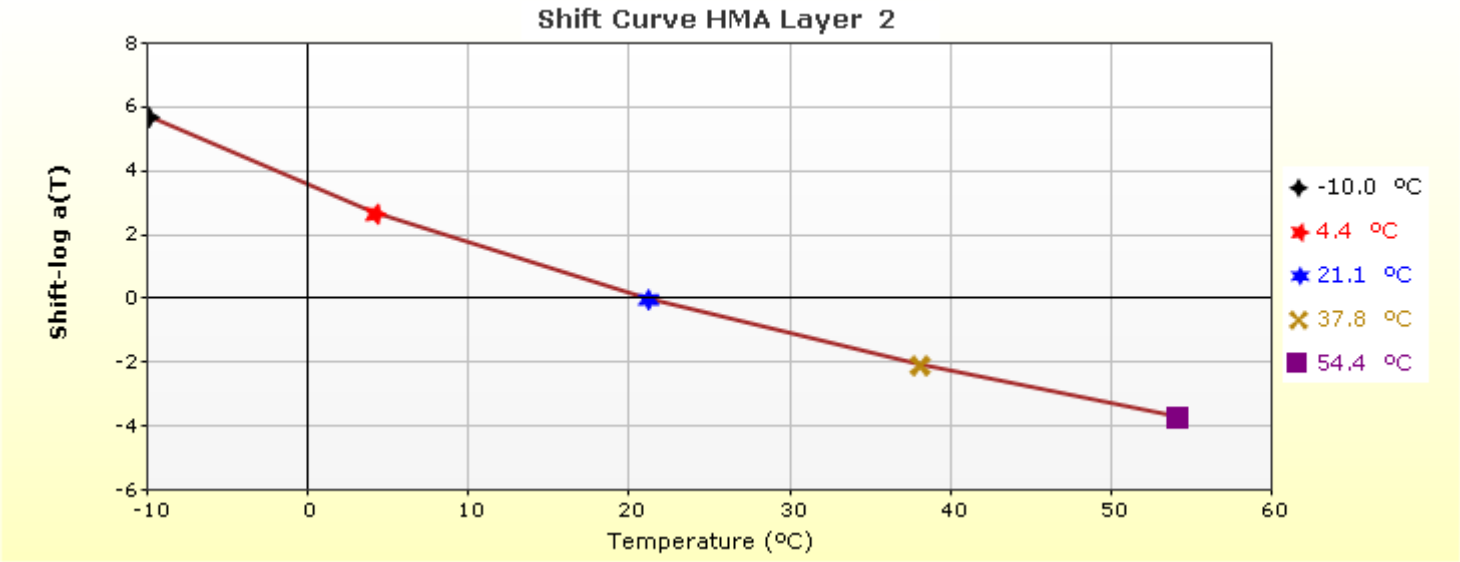

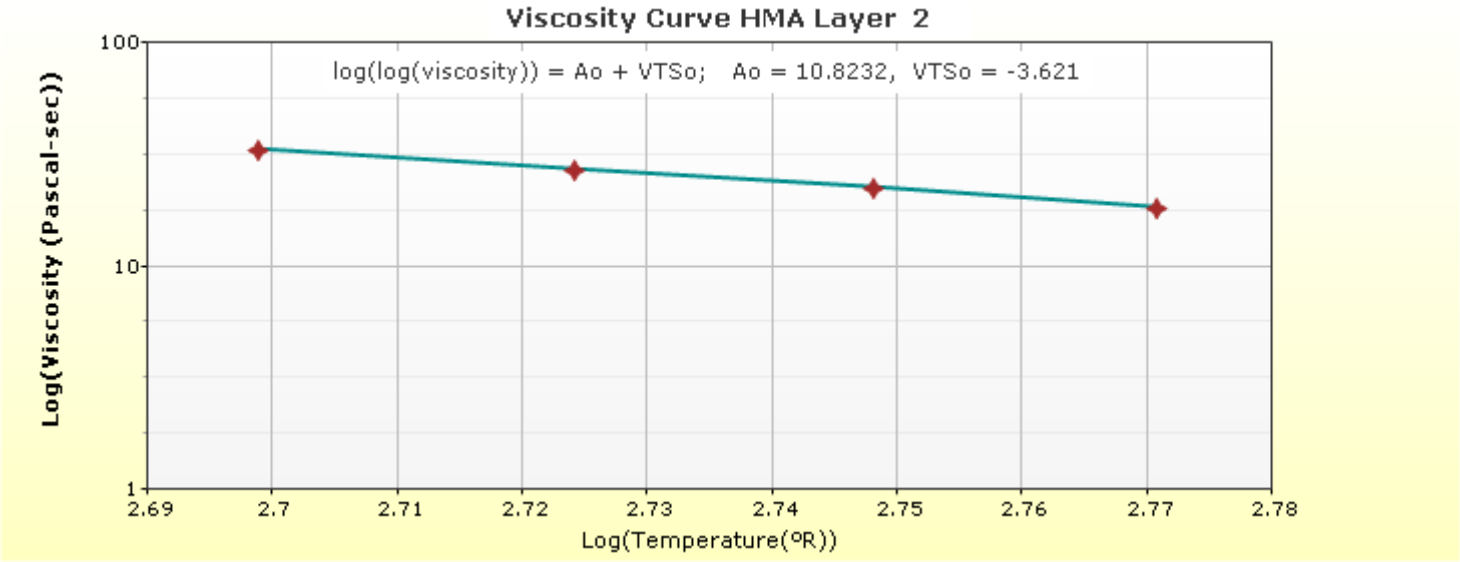

HMA Layer 3: Layer 3 Flexible : HL1

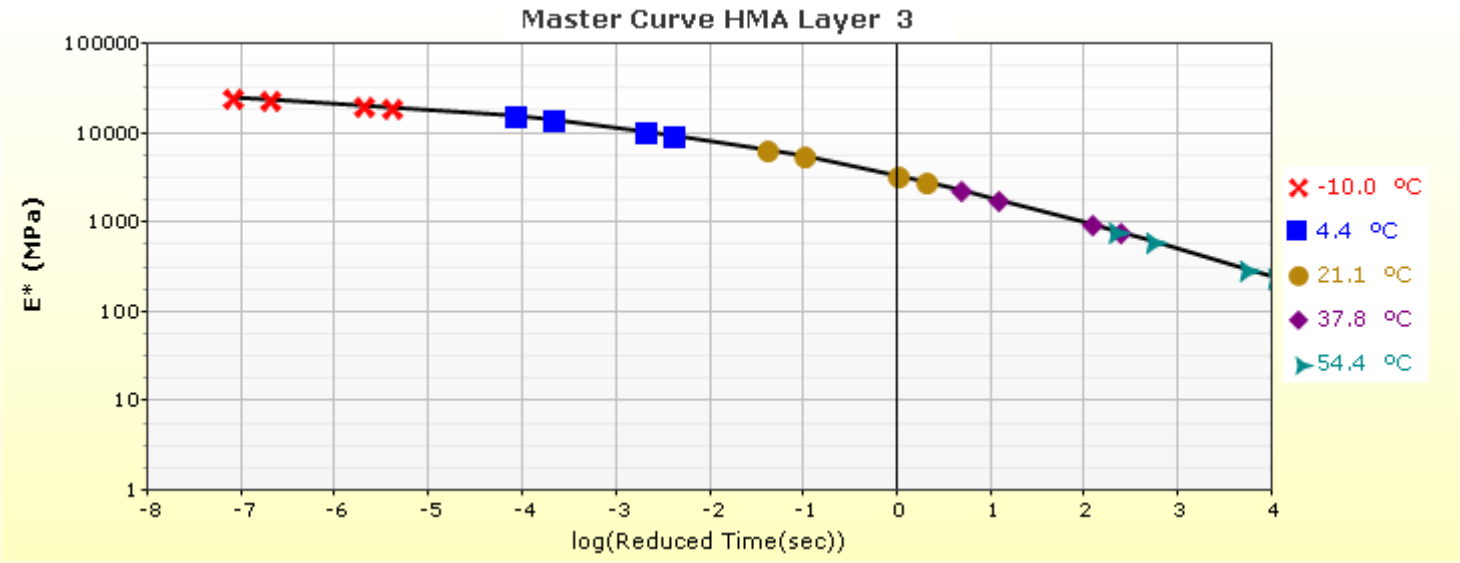

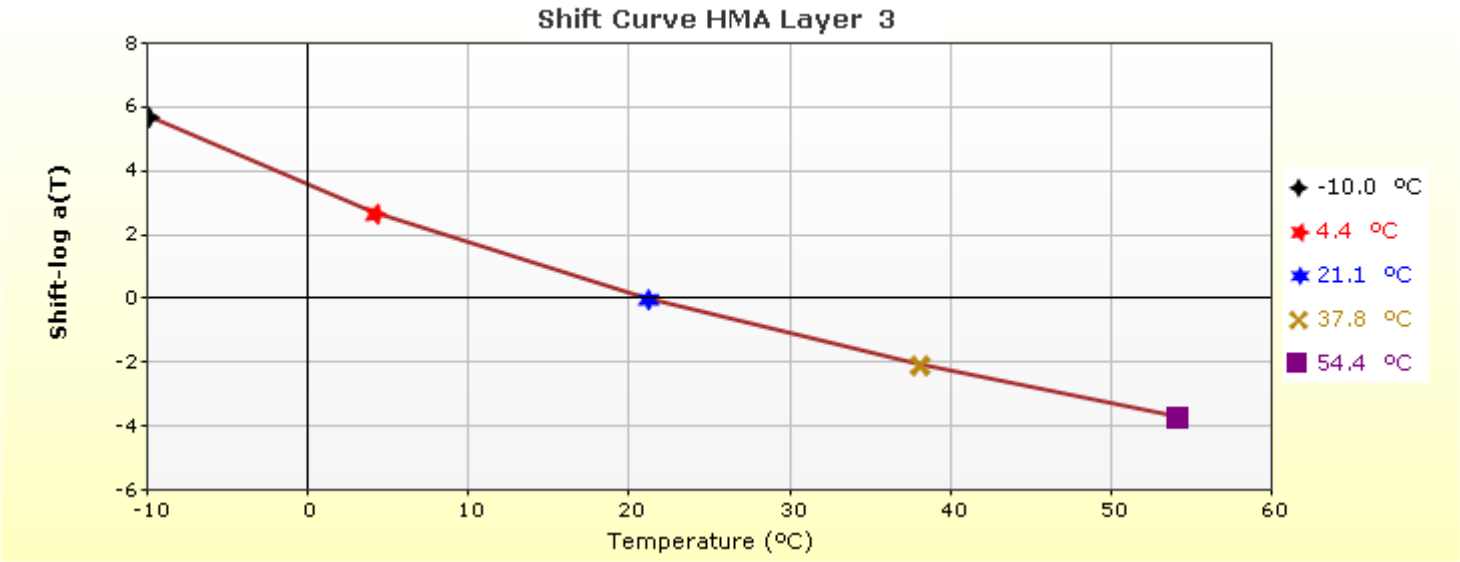

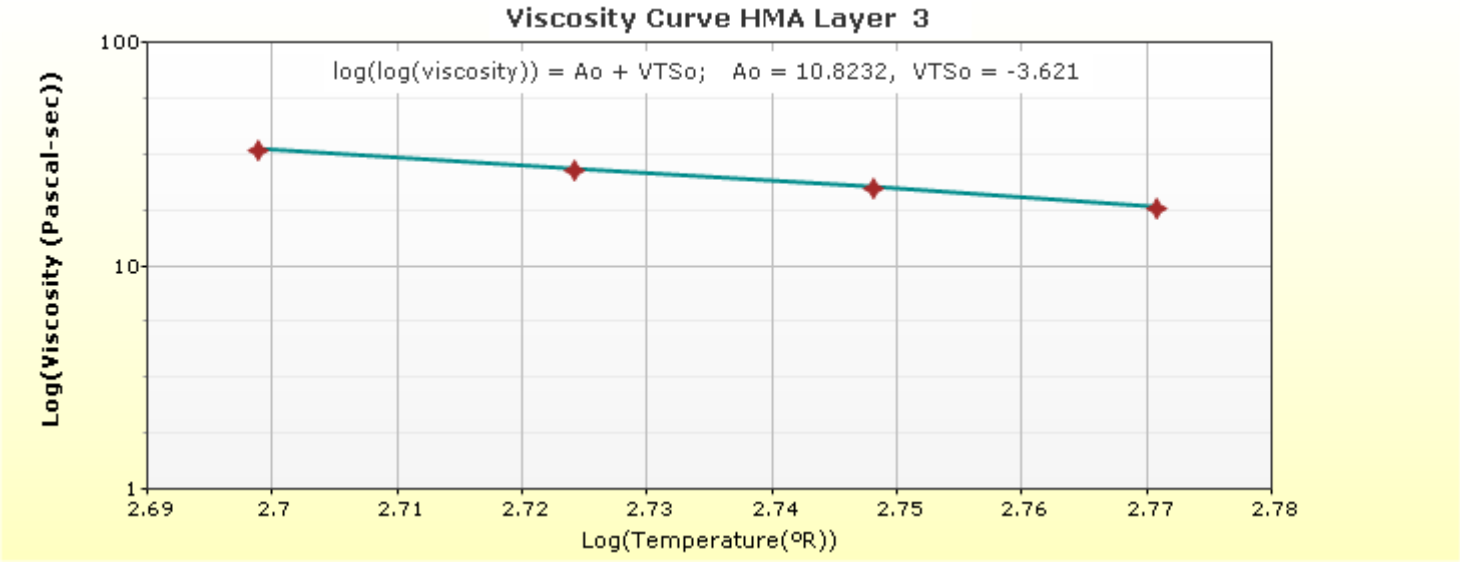

HMA Layer 4: Layer 4 Flexible : HL-4B

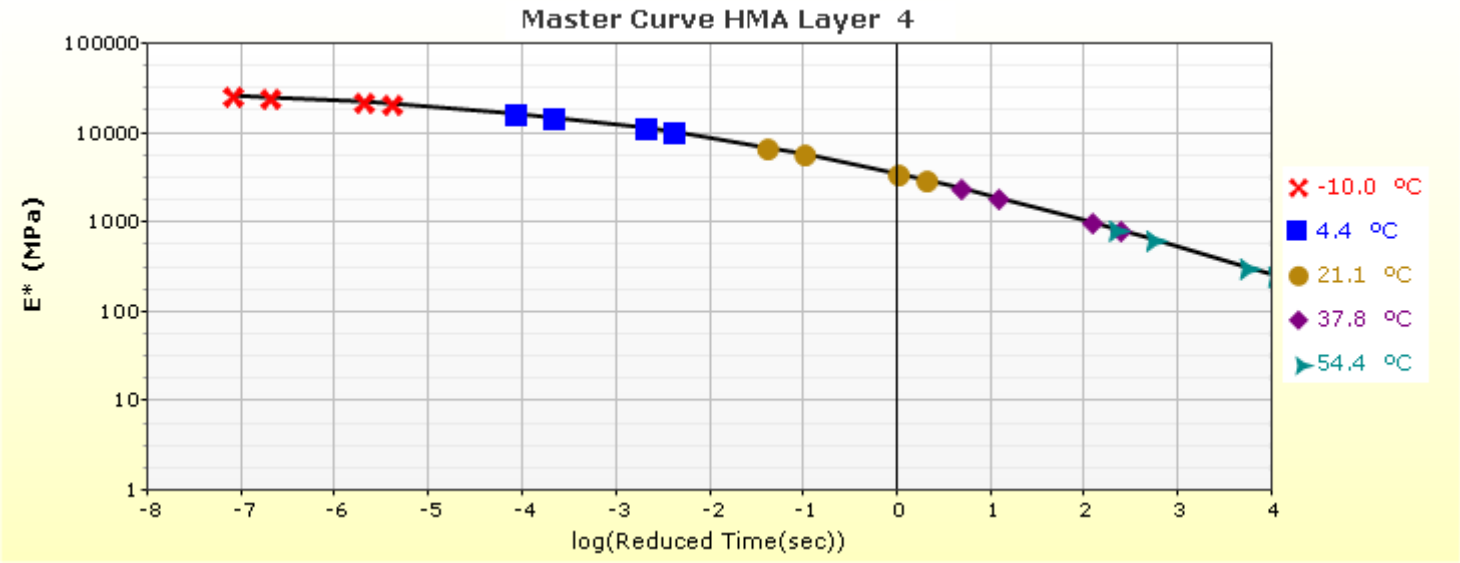

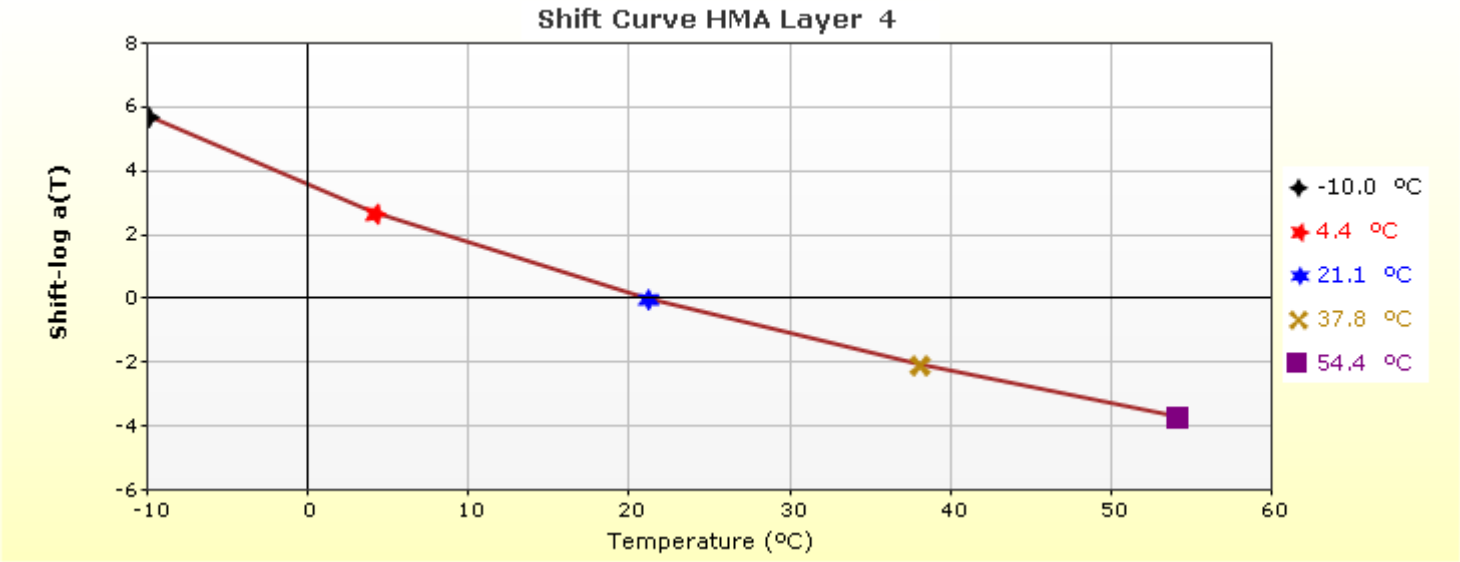

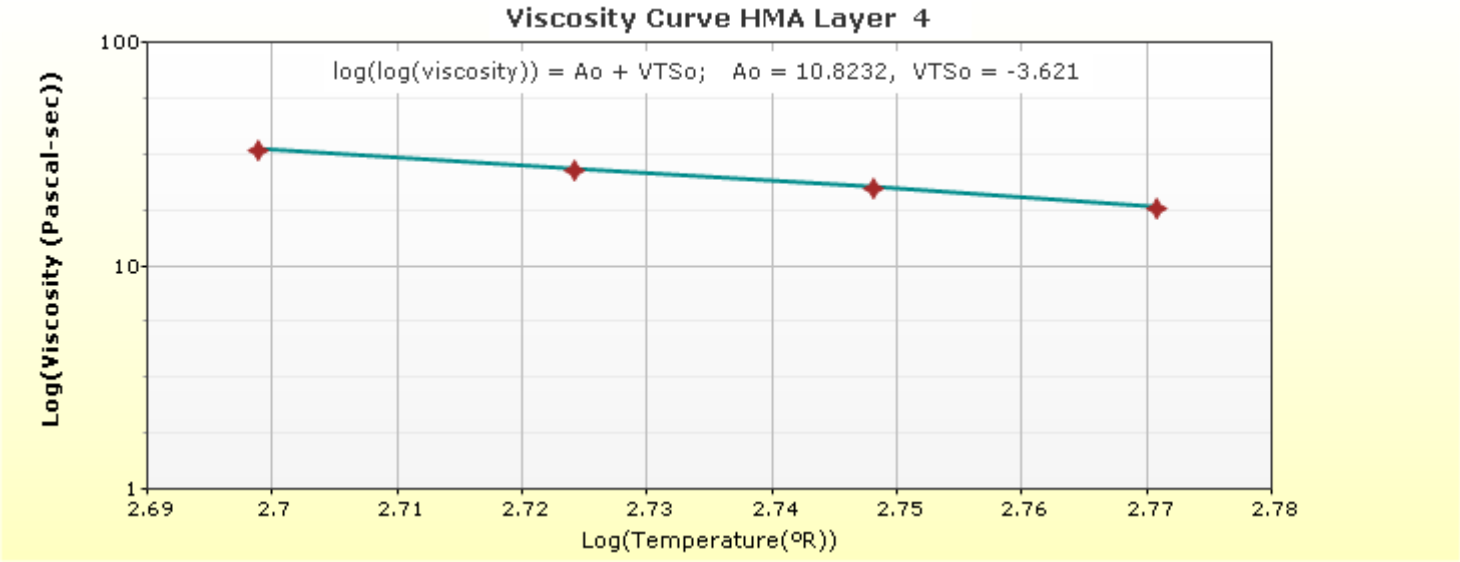

Analysis Output Charts

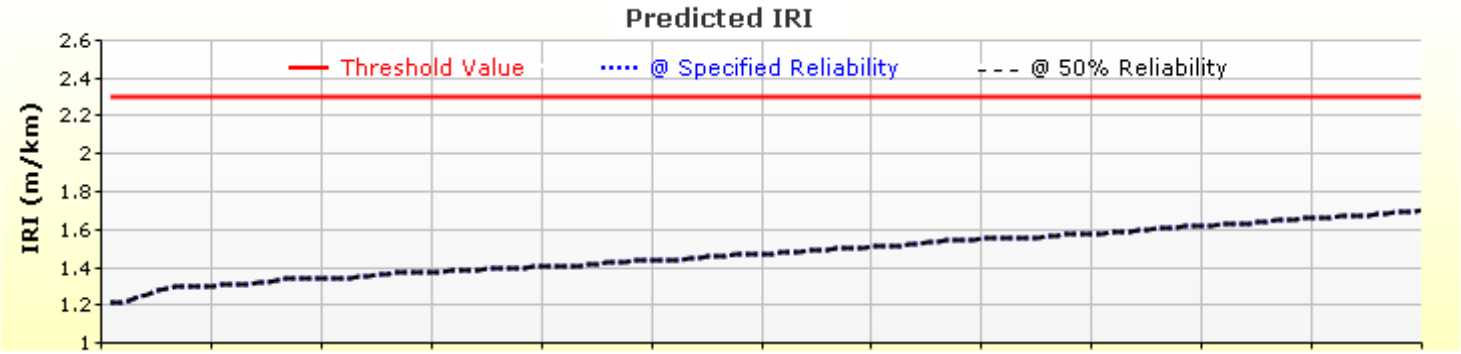

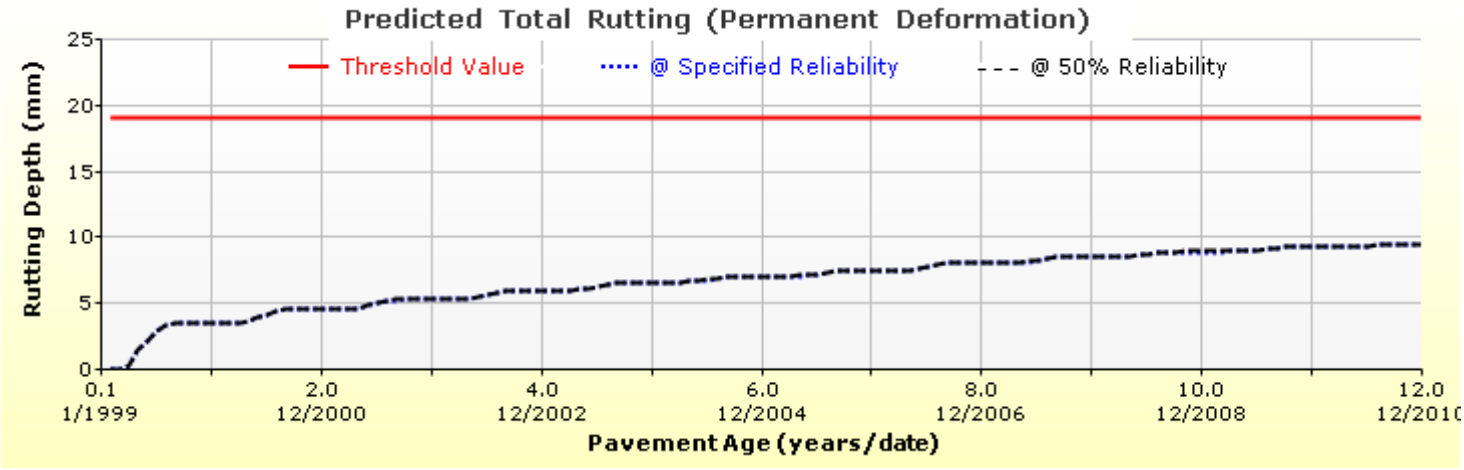

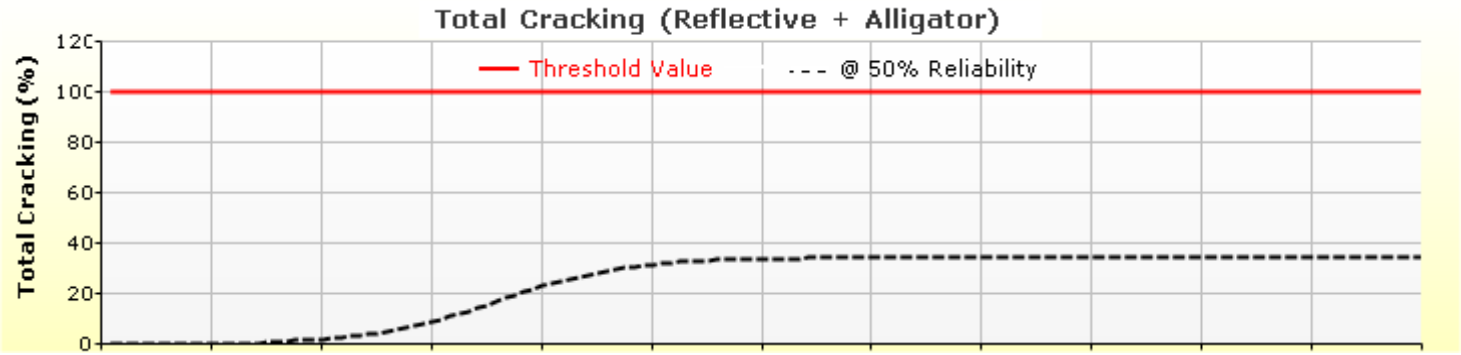

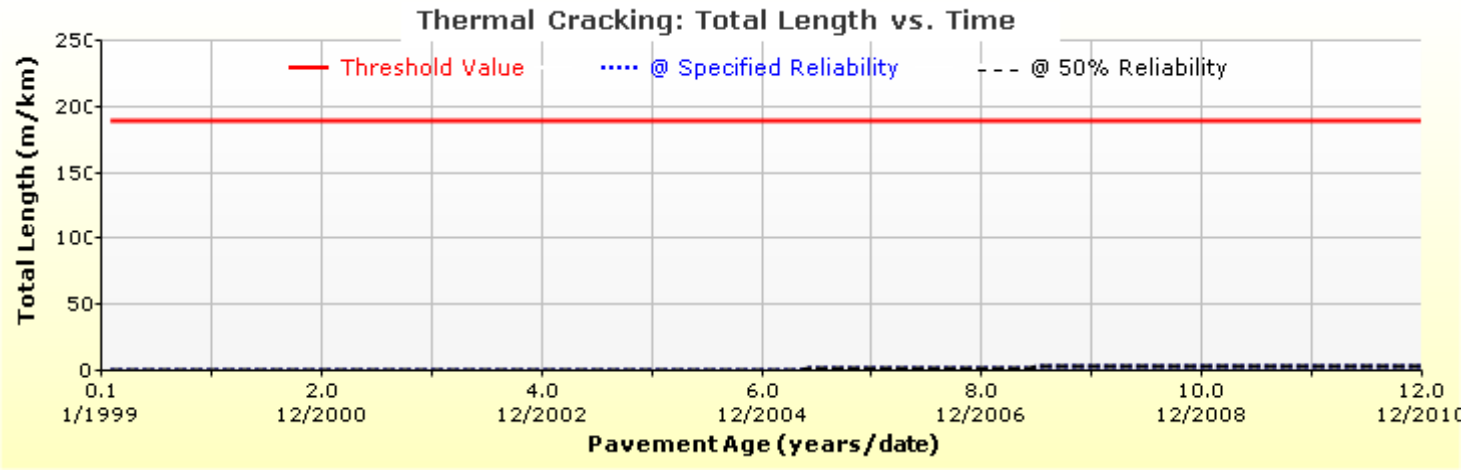

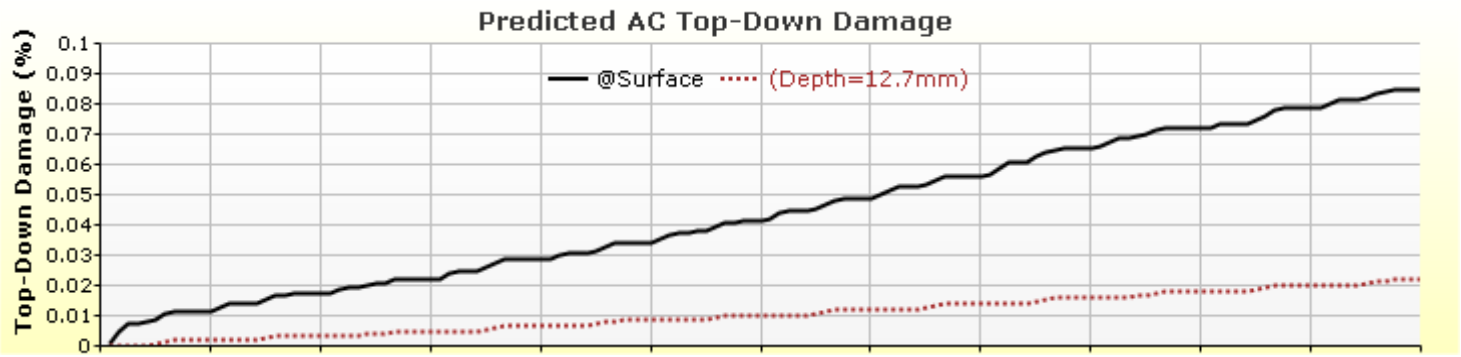
Predicted AC Top-Down Damage
Top-Down Damage (%)
0.1
0.09
0.08
0.07
0.06
0.05
0.04
0.03
0.02
0.01
0
@Surface
(Depth=12.7mm)

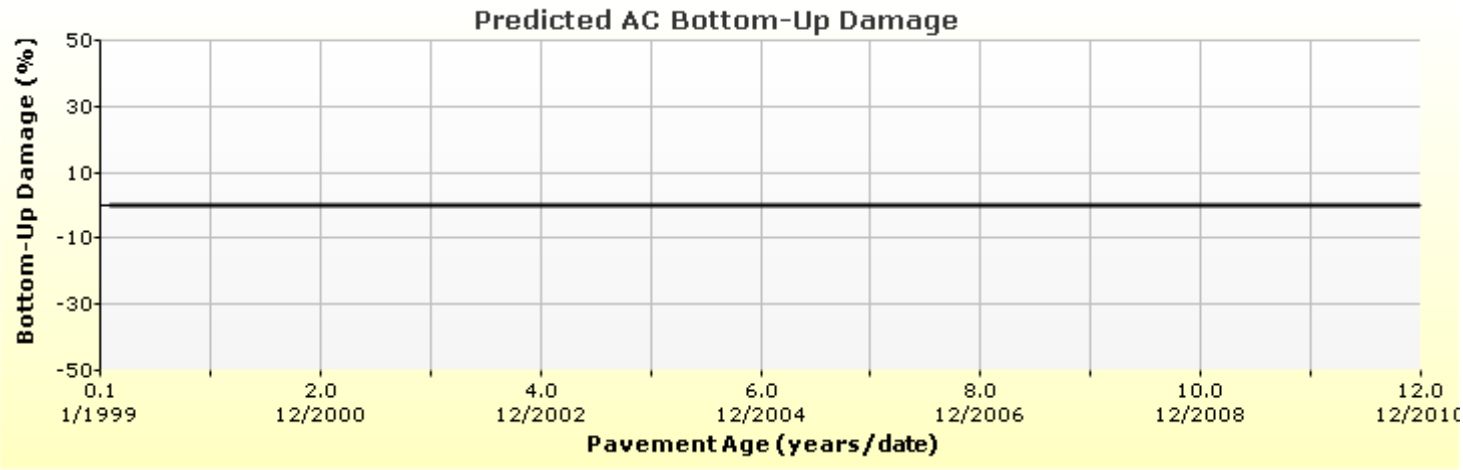
Predicted AC Bottom-Up Damage
Bottom-Up Damage (%)
50
30
10
-10
-30
-50
0.1
1/1999
2.0
12/2000
4.0
12/2002
6.0
12/2004
8.0
12/2006
10.0
12/2008
12.0
12/2010
Pavement Age (years/date)

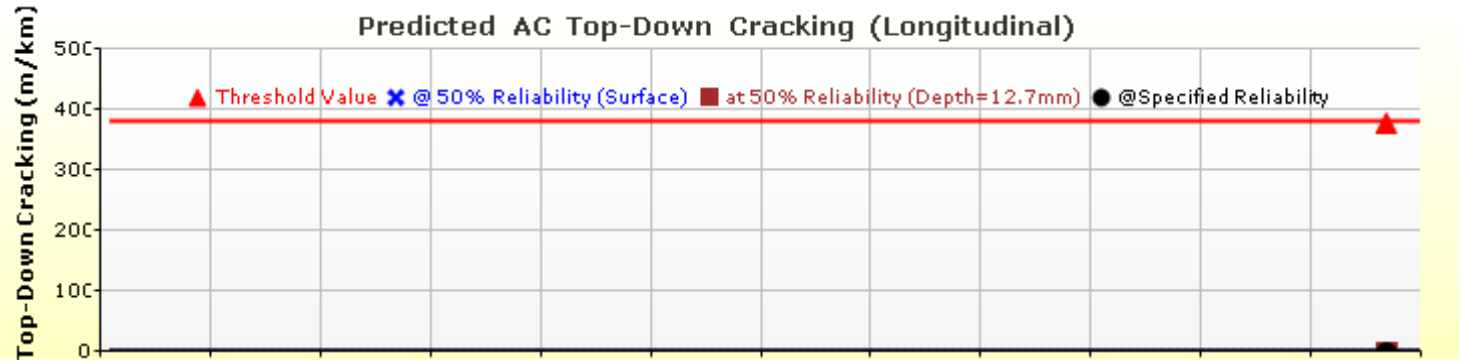
Predicted AC Top-Down Cracking (Longitudinal)
Top-Down Cracking (m/km)
500
400
300
200
100
0
Threshold Value
@ 50% Reliability (Surface)
at 50% Reliability (Depth=12.7mm)
@Specified Reliability

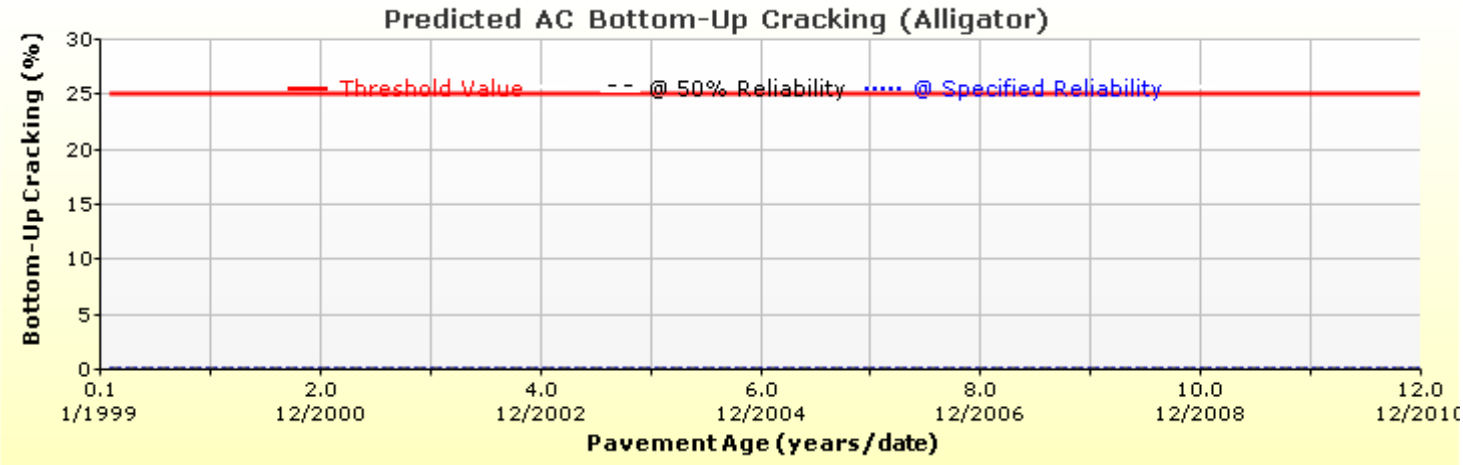
Predicted AC Bottom-Up Cracking (Alligator)
Bottom-Up Cracking (%)
30
25
20
15
10
5
0
Threshold Value
@ 50% Reliability
@ Specified Reliability
0.1
1/1999
2.0
12/2000
4.0
12/2002
6.0
12/2004
8.0
12/2006
10.0
12/2008
12.0
12/2010
Pavement Age (years/date)

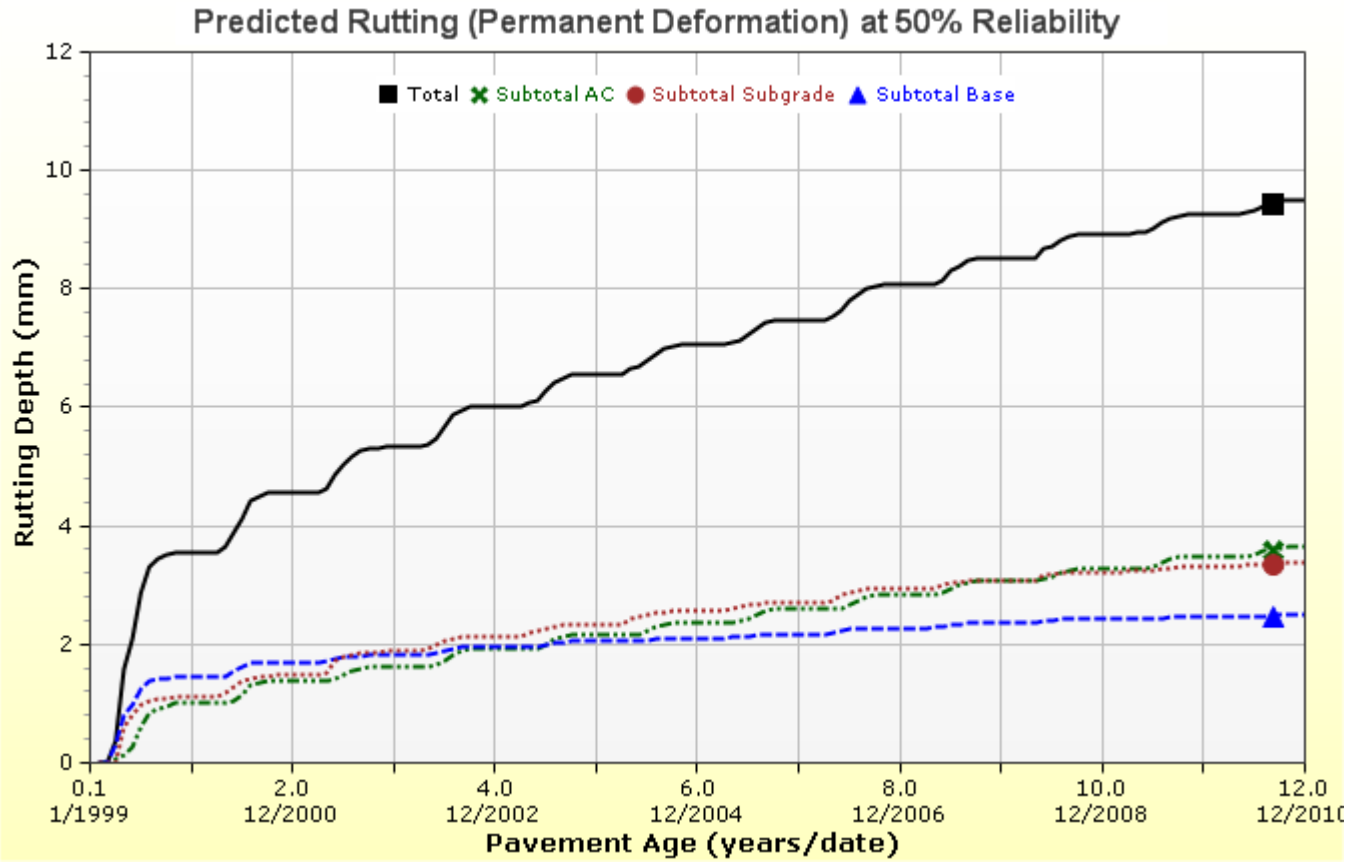
Predicted Rutting (Permanent Deformation) at 50% Reliability
Total
Subtotal AC
Subtotal Subgrade
Subtotal Base
Rutting Depth (mm)
0
2
4
6
8
10
12
0.1
1/1999
2.0
12/2000
4.0
12/2002
6.0
12/2004
8.0
12/2006
10.0
12/2008
12.0
12/2010
Pavement Age (years/date)

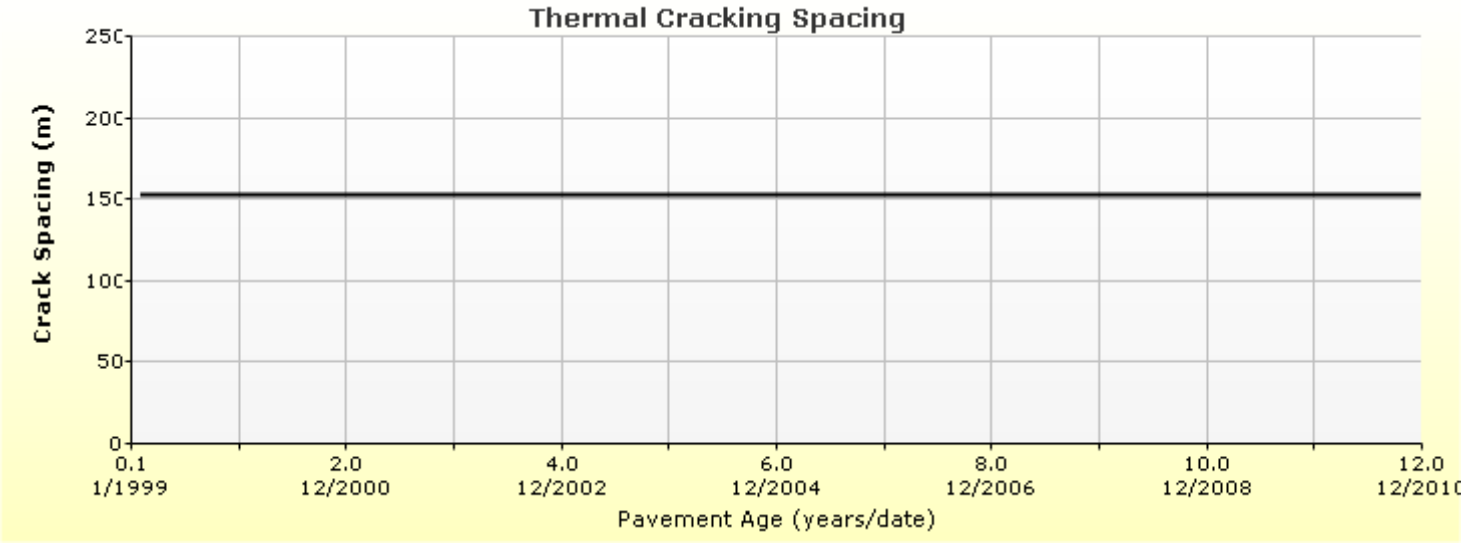
Thermal Cracking Spacing
Crack Spacing (m)
250
200
150
100
50
0
0.1
1/1999
2.0
12/2000
4.0
12/2002
6.0
12/2004
8.0
12/2006
10.0
12/2008
12.0
12/2010
Pavement Age (years/date)

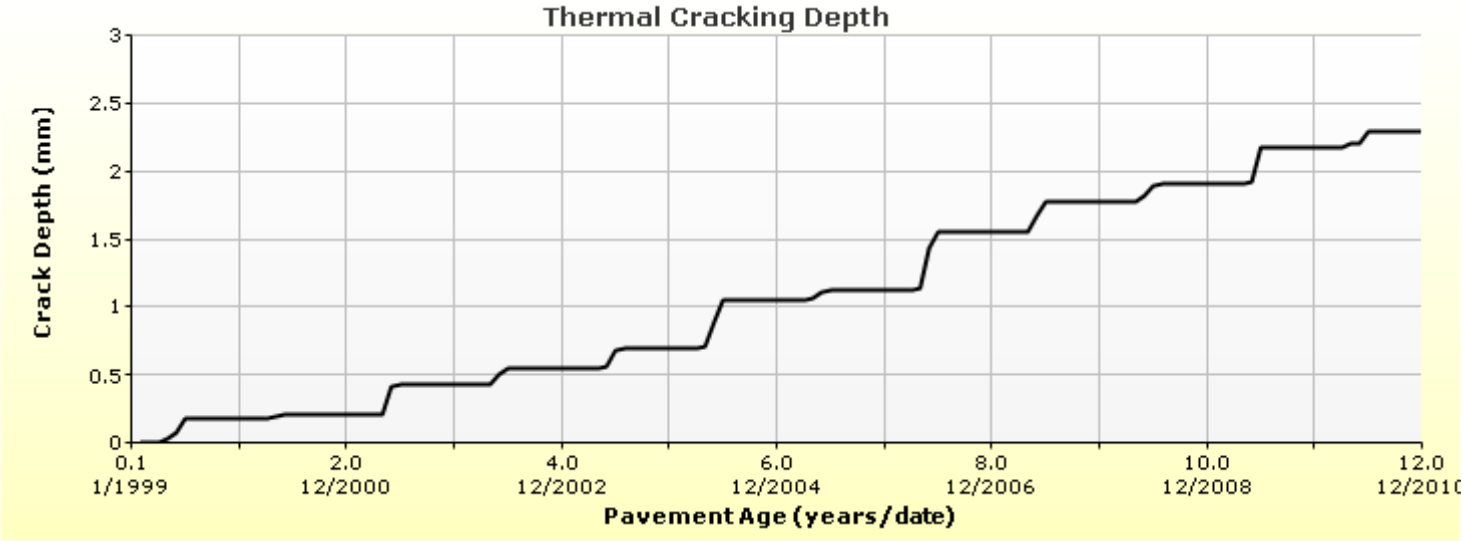
Thermal Cracking Depth
Crack Depth (mm)
3
2.5
2
1.5
1
0.5
0
0.1
1/1999
2.0
12/2000
4.0
12/2002
6.0
12/2004
8.0
12/2006
10.0
12/2008
12.0
12/2010
Pavement Age (years/date)

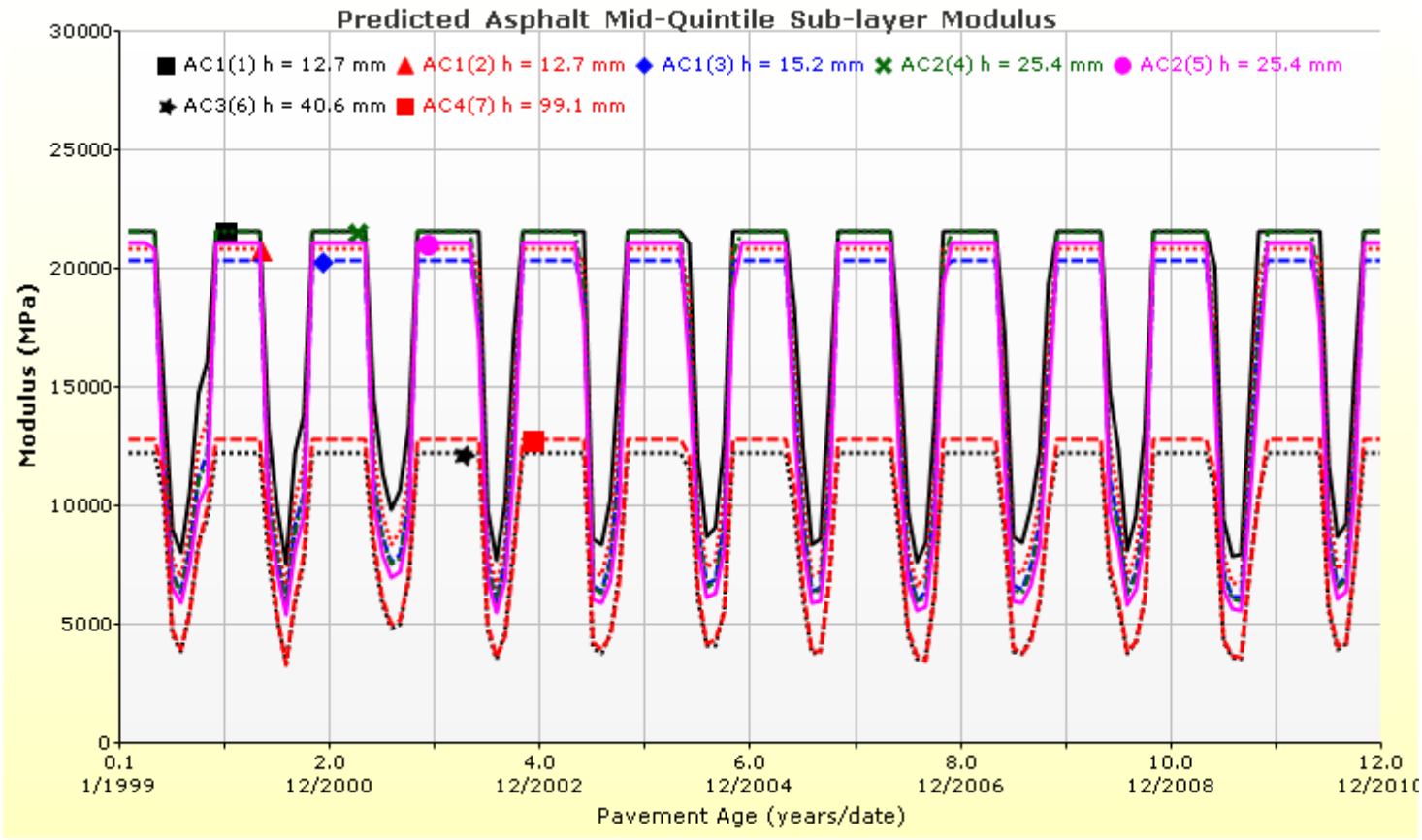
Predicted Asphalt Mid-Quintile Sub-layer Modulus
AC1(1) h = 12.7 mm
AC1(2) h = 12.7 mm
AC1(3) h = 15.2 mm
AC2(4) h = 25.4 mm
AC2(5) h = 25.4 mm
AC3(6) h = 40.6 mm
AC4(7) h = 99.1 mm
Modulus (MPa)
30000
25000
20000
15000
10000
5000
0
0.1
1/1999
2.0
12/2000
4.0
12/2002
6.0
12/2004
8.0
12/2006
10.0
12/2008
12.0
12/2010
Pavement Age (years/date)

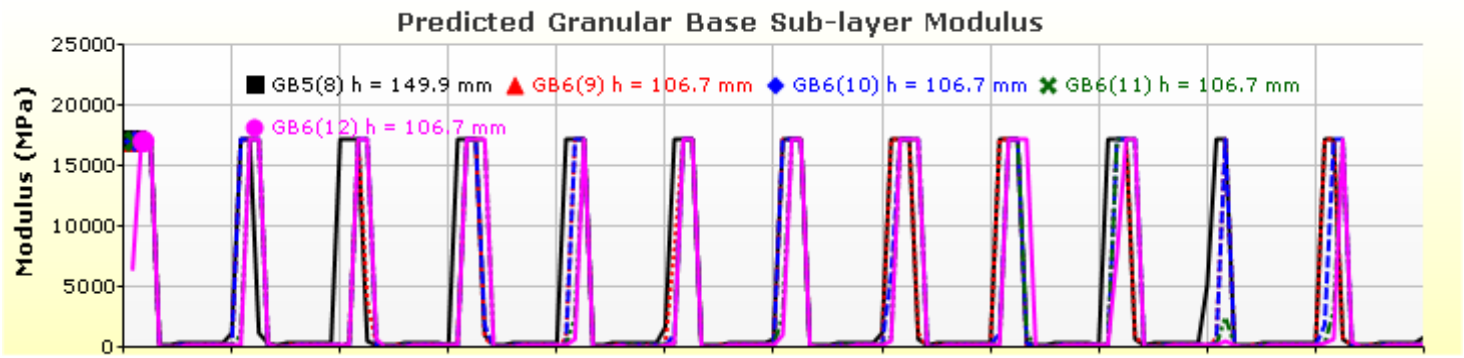
Predicted Granular Base Sub-layer Modulus
GB5(8) h = 149.9 mm
GB6(9) h = 106.7 mm
GB6(10) h = 106.7 mm
GB6(11) h = 106.7 mm
GB6(12) h = 106.7 mm
Modulus (MPa)
25000
20000
15000
10000
5000
0

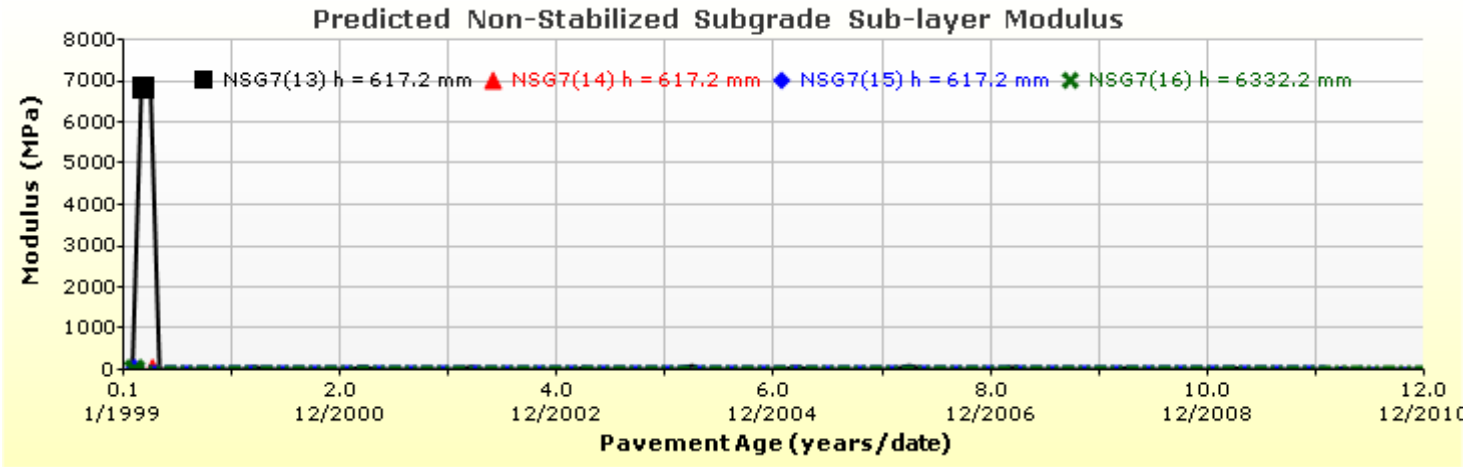
Predicted Non-Stabilized Subgrade Sub-layer Modulus
NSG7(13) h = 617.2 mm
NSG7(14) h = 617.2 mm
NSG7(15) h = 617.2 mm
NSG7(16) h = 6332.2 mm
Modulus (MPa)
8000
7000
6000
5000
4000
3000
2000
1000
0
0.1
1/1999
2.0
12/2000
4.0
12/2002
6.0
12/2004
8.0
12/2006
10.0
12/2008
12.0
12/2010
Pavement Age (years/date)

Layer Information

Layer 1 Flexible : HL1

Asphalt		
Thickness (mm)	40.0	
Unit weight (kg/m^3)	2520.0	
Poisson's ratio	Is Calculated?	False
	Ratio	0.35
	Parameter A	-
	Parameter B	-

Asphalt Dynamic Modulus (Input Level: 3)

Gradation	Percent Passing
19 mm-inch sieve	100
9.5 mm sieve	82.5
4.75 mm sieve	55
0.075mm sieve	2.5

Asphalt Binder

Parameter	Value
Grade	Penetration Grade
Binder Type	Pen 85-100
A	10.8232
VTS	-3.621

General Info

Name	Value
Reference temperature (ºC)	21.1
Effective binder content (%)	12.4
Air voids (%)	4
Thermal conductivity (watt/meter-kelvin)	1.16
Heat capacity (joule/kg-kelvin)	963

Identifiers

Field	Value
Display name/identifier	HL1
Description of object	
Author	
Date Created	09/16/2010 1:00:00 AM
Approver	
Date approved	09/16/2010 1:00:00 AM
State	
District	
County	
Highway	
Direction of Travel	
From station (km)	
To station (km)	
Province	
User defined field 2	
User defined field 3	
Revision Number	0

Layer 2 Flexible : HL-4B

Asphalt		
Thickness (mm)	50.0	
Unit weight (kg/m^3)	2480.0	
Poisson's ratio	Is Calculated?	False
	Ratio	0.35
	Parameter A	-
	Parameter B	-

Asphalt Dynamic Modulus (Input Level: 3)

Gradation	Percent Passing
19 mm-inch sieve	100
9.5 mm sieve	72
4.75 mm sieve	53.5
0.075mm sieve	3

Asphalt Binder

Parameter	Value
Grade	Penetration Grade
Binder Type	Pen 85-100
A	10.8232
VTS	-3.621

General Info

Name	Value
Reference temperature (ºC)	21.1
Effective binder content (%)	12.2
Air voids (%)	4
Thermal conductivity (watt/meter-kelvin)	1.16
Heat capacity (joule/kg-kelvin)	963

Identifiers

Field	Value
Display name/identifier	HL-4B
Description of object	
Author	
Date Created	09/16/2010 1:00:00 AM
Approver	
Date approved	09/16/2010 1:00:00 AM
State	
District	
County	
Highway	
Direction of Travel	
From station (km)	
To station (km)	
Province	
User defined field 2	
User defined field 3	
Revision Number	0

Layer 3 Flexible : HL1

Asphalt		
Thickness (mm)	40.0	
Unit weight (kg/m^3)	2520.0	
Poisson's ratio	Is Calculated?	False
	Ratio	0.35
	Parameter A	-
	Parameter B	-

Asphalt Dynamic Modulus (Input Level: 3)

Gradation	Percent Passing
19 mm-inch sieve	100
9.5 mm sieve	82.5
4.75 mm sieve	55
0.075mm sieve	2.5

Asphalt Binder

Parameter	Value
Grade	Penetration Grade
Binder Type	Pen 85-100
A	10.8232
VTS	-3.621

General Info

Name	Value
Reference temperature (ºC)	21.1
Effective binder content (%)	12.4
Air voids (%)	4
Thermal conductivity (watt/meter-kelvin)	1.16
Heat capacity (joule/kg-kelvin)	963

Identifiers

Field	Value
Display name/identifier	HL1
Description of object	
Author	
Date Created	09/16/2010 1:00:00 AM
Approver	
Date approved	09/16/2010 1:00:00 AM
State	
District	
County	
Highway	
Direction of Travel	
From station (km)	
To station (km)	
Province	
User defined field 2	
User defined field 3	
Revision Number	0

Layer 4 Flexible : HL-4B

Asphalt		
Thickness (mm)	100.0	
Unit weight (kg/m^3)	2480.0	
Poisson's ratio	Is Calculated?	False
	Ratio	0.35
	Parameter A	-
	Parameter B	-

Asphalt Dynamic Modulus (Input Level: 3)

Gradation	Percent Passing
19 mm-inch sieve	100
9.5 mm sieve	72
4.75 mm sieve	53.5
0.075mm sieve	3

Asphalt Binder

Parameter	Value
Grade	Penetration Grade
Binder Type	Pen 85-100
A	10.8232
VTS	-3.621

General Info

Name	Value
Reference temperature (ºC)	21.1
Effective binder content (%)	12.2
Air voids (%)	4
Thermal conductivity (watt/meter-kelvin)	1.16
Heat capacity (joule/kg-kelvin)	963

Identifiers

Field	Value
Display name/identifier	HL-4B
Description of object	
Author	
Date Created	09/16/2010 1:00:00 AM
Approver	
Date approved	09/16/2010 1:00:00 AM
State	
District	
County	
Highway	
Direction of Travel	
From station (km)	
To station (km)	
Province	
User defined field 2	
User defined field 3	
Revision Number	0

Layer 5 Non-stabilized Base : Granular A

Unbound	
Layer thickness (mm)	150.0
Poisson's ratio	0.35
Coefficient of lateral earth pressure (k0)	0.5

Modulus (Input Level: 3)

Analysis Type:	Modify input values by temperature/moisture
Method:	Resilient Modulus (MPa)

Resilient Modulus (MPa)
250.0

Use Correction factor for NDT modulus?	-
NDT Correction Factor:	-

Identifiers

Field	Value
Display name/identifier	Granular A
Description of object	
Author	MTO
Date Created	01/01/2011 12:00:00 AM
Approver	
Date approved	01/01/2011 12:00:00 AM
State	
District	
County	
Highway	
Direction of Travel	
From station (km)	
To station (km)	
Province	
User defined field 2	
User defined field 3	
Revision Number	0

Sieve

Liquid Limit	6.0
Plasticity Index	0.0
Is layer compacted?	True

	Is User Defined?	Value
Maximum dry unit weight (kg/m^3)	False	2170
Saturated hydraulic conductivity (m/hr)	False	2.376e-02
Specific gravity of solids	False	2.7
Optimum gravimetric water content (%)	False	5.7

User-defined Soil Water Characteristic Curve (SWCC)	
Is User Defined?	False
af	3.0201
bf	2.5984
cf	0.7539
hr	100.0000

Sieve Size	% Passing
0.001mm	
0.002mm	
0.020mm	
0.075mm	5.0
0.150mm	
0.180mm	
0.250mm	
0.300mm	13.5
0.425mm	
0.600mm	
0.850mm	
1.18mm	27.5
2.0mm	
2.36mm	
4.75mm	45.0
9.5mm	61.5
12.5mm	77.5
19.0mm	92.5
25.0mm	100.0
37.5mm	
50.0mm	
63.0mm	
75.0mm	
90.0mm	

Layer 6 Non-stabilized Base : Granular B1

Unbound	
Layer thickness (mm)	425.0
Poisson's ratio	0.35
Coefficient of lateral earth pressure (k0)	0.5

Modulus (Input Level: 3)

Analysis Type:	Modify input values by temperature/moisture
Method:	Resilient Modulus (MPa)

Resilient Modulus (MPa)
150.0

Use Correction factor for NDT modulus?	-
NDT Correction Factor:	-

Identifiers

Field	Value
Display name/identifier	Granular B1
Description of object	
Author	MTO
Date Created	01/01/2011 12:00:00 AM
Approver	
Date approved	01/01/2011 12:00:00 AM
State	
District	
County	
Highway	
Direction of Travel	
From station (km)	
To station (km)	
Province	
User defined field 2	
User defined field 3	
Revision Number	0

Sieve

Liquid Limit	11.0
Plasticity Index	0.0
Is layer compacted?	True

	Is User Defined?	Value
Maximum dry unit weight (kg/m^3)	False	1885
Saturated hydraulic conductivity (m/hr)	False	3.48e-03
Specific gravity of solids	False	2.7
Optimum gravimetric water content (%)	False	10.3

User-defined Soil Water Characteristic Curve (SWCC)	
Is User Defined?	False
af	5.2796
bf	2.1903
cf	0.8803
hr	100.0000

Sieve Size	% Passing
0.001mm	
0.002mm	
0.020mm	
0.075mm	4.0
0.150mm	
0.180mm	
0.250mm	
0.300mm	33.5
0.425mm	
0.600mm	
0.850mm	
1.18mm	55.0
2.0mm	
2.36mm	
4.75mm	55.0
9.5mm	
12.5mm	
19.0mm	
25.0mm	75.0
37.5mm	
50.0mm	
63.0mm	
75.0mm	
90.0mm	

Layer 7 Subgrade : ML

Unbound	
Layer thickness (mm)	Semi-infinite
Poisson's ratio	0.35
Coefficient of lateral earth pressure (k0)	0.5

Modulus (Input Level: 3)

Analysis Type:	Modify input values by temperature/moisture
Method:	Resilient Modulus (MPa)

Resilient Modulus (MPa)
35.0

Use Correction factor for NDT modulus?	-
NDT Correction Factor:	-

Identifiers

Field	Value
Display name/identifier	ML
Description of object	USCS
Author	MTO
Date Created	01/01/2011 12:00:00 AM
Approver	
Date approved	01/01/2011 12:00:00 AM
State	
District	
County	
Highway	
Direction of Travel	
From station (km)	
To station (km)	
Province	
User defined field 2	
User defined field 3	
Revision Number	0

Sieve

Liquid Limit	25.0
Plasticity Index	5.0
Is layer compacted?	True

	Is User Defined?	Value
Maximum dry unit weight (kg/m^3)	False	1906.1
Saturated hydraulic conductivity (m/hr)	False	1.636e-06
Specific gravity of solids	False	2.7
Optimum gravimetric water content (%)	False	11.8

User-defined Soil Water Characteristic Curve (SWCC)	
Is User Defined?	False
af	68.8377
bf	0.9983
cf	0.4757
hr	500.0000

Sieve Size	% Passing
0.001mm	
0.002mm	
0.020mm	
0.075mm	60.6
0.150mm	
0.180mm	73.9
0.250mm	
0.300mm	
0.425mm	82.7
0.600mm	
0.850mm	
1.18mm	
2.0mm	89.9
2.36mm	
4.75mm	93.0
9.5mm	95.6
12.5mm	96.7
19.0mm	98.0
25.0mm	98.7
37.5mm	99.4
50.0mm	99.6
63.0mm	
75.0mm	
90.0mm	99.8

Calibration Coefficients

AC Fatigue

$$N_f = 0.00432 * C * \beta_{f1} k_1 \left(\frac{1}{\varepsilon_1}\right)^{k_2\beta_{f2}} \left(\frac{1}{E}\right)^{k_3\beta_{f3}}$$

$$C = 10^M$$

$$M = 4.84\left(\frac{V_b}{V_a + V_b} - 0.69\right)$$

k1: 0.007566	
k2: 3.9492	
k3: 1.281	
Bf1: 1	
Bf2: 1	
Bf3: 1	

AC Rutting

$$\frac{\varepsilon_p}{\varepsilon_r} = k_z \beta_{r1} 10^{k_1} T^{k_2\beta_{r2}} N^{k_3\beta_{r3}}$$

$$k_z = (C_1 + C_2 * depth) * 0.328196^{depth}$$

$$C_1 = -0.1039 * H_a^2 + 2.4868 * H_a - 17.342$$

$$C_2 = 0.0172 * H_a^2 - 1.7331 * H_a + 27.428$$

Where:

$H_{ac} = total\ AC\ thickness(in)$

$\varepsilon_p = plastic\ strain\left({}^{in}/_{in}\right)$
$\varepsilon_r = resilient\ strain\left({}^{in}/_{in}\right)$
$T = layer\ temperature\left(^{\circ}F\right)$
$N = number\ of\ load\ repetitions$

K1: -3.35412	K2: 1.5606	K3: 0.4791
Br2: 1	Br3: 1	Br1: 1

AC Rutting Standard Deviation

0.24*Pow(RUT,0.8026)+0.001

Thermal Fracture

$$C_f = 400 * N\left(\frac{\log C / h_{ac}}{\sigma}\right)$$

$$\Delta C = (k * \beta t)^{n+1} * A * \Delta K^n$$

$$A = 10^{(4.389 - 2.52 * \log(E * \sigma_m * n))}$$

$C_f = observed\ amount\ of\ thermal\ cracking(ft/500ft)$
$k = refression\ coefficient\ determined\ through\ field\ calibration$
$N(\,) = standard\ normal\ distribution\ evaluated\ at(\,)$
$\sigma = standard\ deviation\ of\ the \log\ of\ the\ depth\ of\ cracks\ in\ the\ pavments$
$C = crack\ depth(in)$
$h_{ac} = thickness\ of\ asphalt\ layer(in)$
$\Delta C = Change\ in\ the\ crack\ depth\ due\ to\ a\ cooling\ cycle$
$\Delta K = Change\ in\ the\ stress\ intensity\ factor\ due\ to\ a\ cooling\ cycle$
$A, n = Fracture\ parameters\ for\ the\ asphalt\ mixture$
$E = mixture\ stiffness$
$\sigma_M = Undamaged\ mixture\ tensile\ strength$
$\beta_t = Calibration\ parameter$

Level 1 K: 1.5	Level 1 Standard Deviation: 0.1468 * THERMAL + 65.027
Level 2 K: 0.5	Level 2 Standard Deviation: 0.2841 *THERMAL + 55.462
Level 3 K: 1.5	Level 3 Standard Deviation: 0.3972 * THERMAL + 20.422

CSM Fatigue

$$N_f = 10^{\left(\frac{k_1 \beta_{c1} \left(\frac{\sigma_s}{M_r}\right)}{k_2 \beta_{c2}}\right)}$$

$N_f = number\ of\ repetitions\ to\ fatigue\ cracking$
$\sigma_s = Tensile\ stress(psi)$
$M_r = modulus\ of\ rupture(psi)$

k1: 1	k2: 1	Bc1: 1	Bc2:1

Subgrade Rutting

$$\delta_a(N) = \beta_{s_1} k_1 \varepsilon_v h \left(\frac{\varepsilon_0}{\varepsilon_r}\right) \left| e^{-\left(\frac{\rho}{N}\right)^{\beta}} \right|$$

δ_a = permanent deformation for the layer
N = number of repetitions
ε_v = average veritcal strain(in/in)
$\varepsilon_0, \beta, \rho$ = material properties
ε_r = resilient strain(in/in)

Granular		Fine	
k1: 2.03	Bs1: 1	k1: 1.35	Bs1: 1
Standard Deviation (BASERUT) 0.1477*Pow(BASERUT,0.6711)+0.001		Standard Deviation (BASERUT) 0.1235*Pow(SUBRUT,0.5012)+0.001	

AC Cracking

AC Top Down Cracking

$$FC_{top} = \left(\frac{C_4}{1 + e^{(C_1 - C_2 * log_{10}(Damage))}}\right) * 10.56$$

c1: 7	c2: 3.5	c3: 0	c4: 1000

AC Cracking Top Standard Deviation

200 + 2300/(1+exp(1.072-2.1654*LOG10 (TOP+0.0001)))

AC Bottom Up Cracking

$$FC = \left(\frac{6000}{1 + e^{(C_1 * C_1' + C_2 * C_2' log_{10}(D * 100))}}\right) * \left(\frac{1}{60}\right)$$

$$C_2' = -2.40874 - 39.748 * (1 + h_{ac})^{-2.856}$$

$$C_1' = -2 * C_2'$$

c1: 1	c2: 1	c3: 6000

AC Cracking Bottom Standard Deviation

1.13+13/(1+exp(7.57-15.5*LOG10 (BOTTOM+0.0001)))

CSM Cracking

$$FC_{ctb} = C_1 + \frac{C_2}{1 + e^{C_3 - C_4 (Damage)}}$$

C1: 1	C2: 1	C3: 0	C4: 1000

CSM Standard Deviation

CTB*11

IRI Flexible Pavements

C1 - Rutting
C2 - Fatigue Crack
C3 - Transverse Crack
C4 - Site Factors

C1: 40	C2: 0.4	C3: 0.008	C4: 0.015

Reflective Cracking

$$RC = \frac{100}{1 + e^{c.a + d.b.t}}$$

RC = Percent of cracks reflected, %
t = Time, years
h_{ac} = Overlay thickness(in)
a = 3.5 + 0.75(Heff)
b = -0.688584 – 3.37302(Heff)$^{-0.915469}$
c = 1
d = Calibration parameter (user input)

	AC over AC	AC over Rigid, Good Load Transfer	AC over Rigid, Poor Load Transfer
Heff	h_{ac}	$h_{ac} - 1$	$h_{ac} - 3$

Heff	Recommended Calibration Parameter - d	
	Delay Cracking by 2 years	Accelerate Cracking by 2 years
< 4"	0.6	3
4 – 6"	0.7	1.7
> 6"	0.8	1.4

C: 1	D: 1

Appendix E-

Comparison between Observed Values and Predicted Values of Terminal IRI, Permanent Deformation and AC Bottom-up Fatigue Cracking

Comparison between Observed Values and Predicted Values of Terminal IRI, Permanent Deformation and AC bottom-up Fatigue Cracking

SecNum	SCCycle	Evaluation Year	RCI	PCI	Observed IRI (m/km)	Predicted IRI (m/km)	Observed Rutting (mm)	Predicted Rutting (mm)	Observed AC Bottom up (%)	Predicted AC Bottom up (%)
136	136 1	2010	6.97	69.52	1.66	1.69	6.19	9.5	5	0
139	139 1	2010	7.60	72.59	1.67	1.81	4	9.46	0	0
202	202 1	2002	6.99	73.02	1.65	1.73	3.78	26.52	0	0.49
202	202 2	2010	7.95	81.52	1.20	1.41	5.56	12.94	0	0
217	217 3	2008	7.59	90.19	1.35	1.77	6.97	5.55	35	0
219	219 2	2008	7.21	88.38	1.54	1.39	4.03	4.90	35	0
347	347 2	2009	7.18	69.01	1.55	1.85	8.16	11.27	0	0
348	348 1	2009	7.18	69.01	1.55	1.70	9.72	8.21	0	0
349	349 1	2004	7.40	74.86	1.44	1.51	7.64	8.15	0	0
349	349 2	2009	7.18	69.01	1.55	1.62	8.81	6.04	0	0
350	350 1	2002	8.07	83.94	1.15	1.16	6.21	8.09	0	0
350	350 1	2010	7.06	72.77	1.62	1.50	8.9	7.33	5	0
353	353 1	2010	6.61	71.73	1.87	1.45	8.39	10.43	0	0
354	354 1	2002	6.30	65.08	2.07	1.55	10.36	11.39	0	0
354	354 2	2010	7.55	75.30	1.37	1.42	5.21	6.76	0	0
355	355 1	2000	7.06	62.24	1.61	1.96	4	30.4	35	1.96
355	355 2	2008	7.37	76.83	1.46	1.26	5.07	14.38	0	0
356	356 1	1996	8.50	87.70	1.00	0.92	4	5.26	0	0
356	356 2	2004	7.14	72.81	1.57	1.56	5.21	6.53	0	0
356	356 3	2009	6.46	63.90	1.97	1.77	6.26	4.07	15	0
357	357 1	2001	7.70	80.39	1.30	1.14	4	5.25	0	
357	357 2	2010	7.16	72.62	1.56	1.58	5.92	4.79	0	0
358	358 1	2007	7.58	74.95	1.36	1.52	5.2	11.92	0	0
361	361 1	2008	7.66	74.76	1.32	1.60	5.04	11	0	0
371	371 1	2002	6.95	66.11	1.67	2.04	8.38	25.22	0	0.66
376	376 1	2001	7.20	75.12	1.54	2.51	4	35.04	0	1.67
377	377 2	2009	6.74	66.20	1.79	2.10	10.25	22.12	0	0
378	378 1	2009	6.74	66.20	1.79	2.15	11.94	20.31	0	0
379	379 1	2009	6.74	66.20	1.79	1.83	8.15	10.93	0	0
384	384 1	2000	7.26	65.17	1.51	2.33	4	43.87	35	6
384	384 2	2007	7.78	78.30	1.27	1.36	4.87	17.07	0	0
385	385 1	1996	7.30	75.76	1.49	2.38	4	43.03	0	12.4
385	385 2	2000	6.93	69.27	1.68	1.65	4	15.88	0	0
385	385 3	2010	8.16	72.68	1.12	2.55	6.01	27.2	15	0
386	386 1	1996	8.50	85.36	1.00	1.00	4	3.51	0	0
560	560 1	1992	7.00	65.15	1.64	1.63	4	21.17	0	0.31
560	560 2	1999	6.19	51.27	2.15	1.84	9.85	13.01	15	0
560	560 3	2009	8.74	85.39	0.93	1.26	6.48	13.68	0	0
803	803 1	2008	6.05	61.22	2.25	2.35	5.45	19.39	0	0
811	811 2	2007	6.18	63.91	2.16	1.82	5.38	14.79	0	0
951	951 1	2010	7.83	72.97	1.25	1.77	5.15	10.54	0	0
973	973 1	2010	7.75	77.85	1.29	1.89	5.09	9.22	0	0
980	980 1	1996	6.60	78.07	1.88	1.71	4	8.07	0	0
980	980 2	2008	6.47	50.63	1.96	1.96	7.59	11.02	5	0

Comparison between Observed Values and Predicted Values of Terminal IRI, Permanent Deformation and AC bottom-up Fatigue Cracking

SecNum	SCCycle	Evaluation Year	RCI	PCI	Observed IRI (m/km)	Predicted IRI (m/km)	Observed Rutting (mm)	Predicted Rutting (mm)	Observed AC Bottom up (%)	Predicted AC Bottom up (%)
981	981 1	2010	6.92	64.90	1.69	1.61	9.44	17	5	0
1017	1017 1	2002	8.75	87.31	0.92	1.20	2.67	5.06	0	0
1017	1017 2	2009	7.96	82.45	1.20	1.11	5.58	3.45	0	0
1053	1053 1	2007	7.85	74.56	1.24	1.35	4.81	15.55	5	0
1054	1054 1	1997	7.62	67.79	1.34	1.06	4	8.43	0	0
1054	1054 2	2008	7.02	62.17	1.64	1.42	5.28	9.99	5	0
1062	1062 1	2008	7.56	67.86	1.37	1.46	4.81	7.76	35	0
1092	1092 1	2007	7.64	84.06	1.33	1.31	5.26	7.75	0	0
1102	1102 1	2009	8.28	81.28	1.08	1.43	5.67	5.96	0	0
1130	1130 1	2003	7.10	70.23	1.59	1.28	4.24	5.23	5	0
1130	1130 2	2008	6.44	65.33	1.98	1.79	6.53	4.46	0	0
1131	1131 1	2008	6.59	67.22	1.88	1.52	7.62	7.22	0	0
1132	1132 1	2001	8.40	85.47	1.03	1.03	4	4.51	0	0
1132	1132 2	2007	7.87	77.50	1.23	1.10	4.71	3.88	0	0
1138	1138 1	2007	8.27	73.79	1.08	1.39	4.65	15.14	5	0
1139	1139 1	1997	7.73	70.31	1.29	1.27	4	13.88	0	0
1146	1146 2	2008	7.97	67.63	1.19	1.17	5.88	3.86	0	0
1156	1156 1	2008	7.87	70.75	1.23	1.23	5.59	11.36	0	0
1189	1189 1	2006	7.39	67.81	1.45	1.30	6.65	11.84	5	0
1200	1200 1	2009	7.22	66.37	1.53	1.56	8.87	11.87	5	0
1225	1225 1	2005	7.57	79.78	1.36	1.41	6.71	11.7	0	0
1225	1225 2	2010	7.73	77.87	1.29	1.48	6	5.61	0	0
1229	1229 1	2002	7.22	75.37	1.54	1.69	7.07	8.32	0	0
1233	1233 2	2008	7.55	64.05	1.37	1.14	4.69	9.76	5	0
1234	1234 2	2009	7.72	73.88	1.30	1.29	4.86	8.88	0	0
1235	1235 1	1998	7.10	68.16	1.59	1.48	4	14.27	5	0
1235	1235 2	2004	8.35	78.59	1.05	1.35	5.71	13.85	0	0
1235	1235 3	2009	7.94	72.40	1.21	1.43	6.92	9.57	0	0
1250	1250 1	2009	8.06	79.95	1.16	1.92	4.43	19.27	0	0
1277	1277 1	2001	7.92	86.65	1.21	0.99	4	2.27	0	0
1277	1277 2	2009	7.49	71.40	1.40	1.36	4.42	2.13	5	0
1314	1314 2	2010	7.55	78.81	1.37	1.12	5.88	4.38	0	0
1319	1319 2	2010	7.01	72.03	1.64	1.42	8.23	7.03	0	0
1320	1320 2	2010	5.56	53.93	2.65	2.17	8.07	7.68	0	0
1341	1341 2	2007	7.92	77.56	1.21	1.46	5.31	12.69	0	0

REFRENCES

AASHTO. (2008). “Mechanistic-Empirical Pavement Design Guide: A Manual of Practice”, Washington DC: AASHTO.

AASHTO (2010). “Guide for the Local Calibration of the Mechanical-Empirical Pavement Design Guide”, Joint Technical Committee on Pavements, 2008/2009

AASHTO (2011). “DARWin-ME v.1.0 Help Manual”, AASHTOWare 2011.

Ali, H.A., Tayabji, S.D., (1998). “Evaluation of Mechanistic –Empirical Performance Models for Flexible Pavements’, Transportation Research Board, Transportation Research Record-1629-19:169-180

Ali, O., (2005). “Evaluation of the Mechanistic Empirical Pavement Design Guide (NCHRP 1-37A)”, Report, National Research Council, Canada.

Chatti, K., (2009). “Effect of Michigan Multi-Axle Trucks on Pavement Distress”, Executive Summary, Project RC-1504, Pavement Research Center of Excellence, Michigan State University.

Chatti, K., Yun, K. K., Kim, H. B., Utamsingh, R. (1995) “PACCAR Full-Scale Pavement Tests,” University of California Berkeley, and the California Department of Transportation, Berkeley, CA.

Chong, G.J., Phang, W.A., Wrong, G.A., (1989). “Manual for Condition Rating of Flexible Pavements”, Distress Manifestations, Ministry of Transportation Ontario, Research and Development Branch, SP-024.

Darter, M., Khazanovich, L., Yu, T.,Mallela, J.,(2005). “Reliability Analysis of Cracking and Faulting Prediction in the New Mechanistic–Empirical Pavement Design Procedure”, Transportation Research Record: Journal of the Transportation Research Board, No. 1936:150–160.

Deshpande, V. P., Damnjanovic, I. D., Gardoni, P., (2010). “Reliability-Based Optimization Models for Scheduling Pavement Rehabilitation”, Computer-Aided Civil and Infrastructure Engineering, 25:227–237

Dzotepe, G. A., Ksaibati, K., (2010). “ Implementation of the Mechanistic-Empirical Pavement Design Guide (MEPDG)”, MPC Report No. 10-225A, University of Wyoming.

Dzotepe, G. A., Ksaibati, K., (2011). “The Effect of Environmental Factors on the Implementation of the Mechanistic Empirical Pavement Design Guide”, Report, University of Wyoming.

Flintsch, G., McGHEE, K.K., (2009). “Quality Management of Pavement Condition Data Collection- A Synthesis of Highway Practice” NCHRP Synthesis 401,TRB

Guo, R., (2007). “Predicting In-Service Fatigue Life of Flexible Pavements Based on a Accelerated Pavement Testing”, Phd Thesis, The University of Texas at Austin, December 2007

Hall, K. D., Xiao, D. X., Wang, K. C.P., (2010). “Calibration of the MEPDG for Flexible Pavement Design in Arkansas”, TRB 2011 Annual Meeting CDROM.

Hoegh, K., Khazanovich, L., Jensen, M., (2010). “Local Calibration of MEPDG Rutting Model for MnRoad Test Sections”, TRB 2010 Annual Meeting CD-ROM

Hsiang, W., K., Lee, Y.H., Wu, P.H., (2007). “ Development of Fatigue Cracking Performance Prediction Models for Flexible Pavements Using LTPP Data base”, TRB 2007 Annual Meeting CDROM.

Jackson, N. C., Mahoney, J. P, (2007) “Pavement Design and Construction Mechanistic-Empirical” July 2007.

Jiang, Y. J., Selezneva, O., Mladenovic, G. Aref, S., Darter, M. (2003). “Estimation of Pavement Layer Thickness Variability for Reliability-Based Design”, Transportation Research Board, Transportation Research Record, 1849, Paper No. 03-2886

Kang, M. Adams, T. M., (2007). “Local Calibration for Fatigue Cracking Models Used in the Mechanistic-Empirical Pavement Design Guide”, Proceedings of the 2007 Mid-Continent Transportation Research Symposium, Ames, Iowa, August 2007

Kenis, W., Wang, W., (1998). “Pavement Variability and Reliability”, U.S. Department of Transportation, Federal Highway Administration

Kim, H.B., Lee, S.H., (2002). “Reliability Based Design Model Applied to Mechanistic Empirical Pavement Design”, KSCE Journal of Civil Engineering, 6 (3):263-272

Kim, H. B., Buch, N., (2003). “Reliability Based Pavement Design Model Accounting for Inherent Variability of Design Parameters”, 82nd Transportation Research Board Annual Meeting, Washington D.C., January 12-16, 2003

Li, N., Xie, W.C., Haas, R. (1996). “Reliability Based Processing of Markov Chains for Modeling Pavement Network Deterioration”, Transportation Research Board, Transportation Research Record 1524:203-213.

Mathew, T. V., Rao, K. V. K. (2007).“IRC method of Design of Flexible Pavements”, Introduction to Transportation Engineering, NPTEL May 3, 2007

Moulthrop, J. S., Quintus, H. L. V., (2007). “Mechanistic-Empirical Pavement Design Guide Flexible Pavement Performance Prediction Models for Montana” Montana Department of Transportation, Project Summary Report 8158.

Myers, L. A., Roque, R., Birgisson, B., (2001). “Propagation Mechanisms for Surface-Initiated Longitudinal Wheel-path Cracks, Transportation Research Record 1778 _ 113. Paper No. 01-0433

NCHRP (2003). “Guide for Mechanistic-Empirical Design of New and Rehabilitated Pavement Structures”, Final Document, Appendix BB, ‘Design Reliability’, National Cooperative Highway Research Program Transportation Research Board National Research Council.

NCHRP (2004). “Guide for Mechanistic-Empirical Design of New and Rehabilitated Pavement Structures”, Final Document, Appendix II-1, ‘Calibration of Fatigue Cracking Models for

Flexible Pavement, National Cooperative Highway Research Program Transportation Research Board National Research Council, 1-37A Report.

NCP (2010). “Pavement Performance Models”, Project Report, NordFoU, Nordic Coorperation Program, Norway.

Pell, P. S., Cooper, K. E. (1975) “The Effect of Testing and Mix Variables on the Fatigue Performance of Bituminous Materials”, Journal of the Association of Asphalt Paving Technologists,, (44) :1-37.

Prozzi, J. A., Gossain, V. and Manuel, L., (2005). “Reliability of Pavement Structures using Empirical-Mechanistic Models”, Transportation Research Board.

Salem, H.M.A., (2008). “Effect of Excess Axle Weights on Pavement Life”, Emirates Journal for Engineering Research, 13 (1):21-28

Simmons, J. W., Seaman, L. (2000). “Finite Element Analysis of Fatigue Lifetime in Pavements,” Presented at the 79th Annual Meeting, Transportation Research Board, Washington, DC

Schram, S., Abdelrahman, M., (2006). “Improving Prediction Accuracy in Mechanistic-Empirical Pavement Design Guide”, Transportation Research Board, Washington, DC.

Schwartz, W.C., Carvalho, R. L., (2007). “Implementation of the NCHRP 1-37A -Design Guide: Evaluation of Mechanistic-Empirical Design Procedure”, Final Report MDSHA Project No. SP0077B41 UMD FRS No. 430572, Maryland State Highway Administration Volume: 2

Siraj,N., Mehta, Y.A., Muriel, K.M., Sauber, R.W., (2009). “Verification of mechanistic-empirical pavement design guide for the state of New Jersey”, Department of Civil and Environmental Engineering, Rowan University, Glassboro, NJ, USA; Taylor & Francis Group.

TAC (2011), “Mechanistic-Emperical Pavement Design Using DARWinME”, TAC Spring Meeting Presentation, April 2011, Ottowa.

Tanquist, B. A., (2001).“Development of a Quick Reliability Method for Mechanistic-Empirical Asphalt Pavement Design”, Minnesota Department of Transportation

Tarefder, R.A., Saha, N.; Stormont,J. C. (2010).“Evaluation of Subgrade Strength and Pavement Designs for Reliability”, Journal of Transportation Engineering ASCE , 379

Timm, D.H., Newcomb, D. E. , Galambos T. V., (2000).“ Incorporation of Reliability into Mechanistic-Empirical Pavement Design”, Transportation Research Board, Transportation Research Record 1760:73-80.

Timm, D.H., Turochy, R.E., Davis, K.P., (2010), “Guidance for ME Pavement Design Implementation” Final Report, ALDOT Project 930-685.

Velasquez,R., Hoegh, K., Yut, I., Funk, N., Cochran, G., Marasteanu, M., Khazanovich, L., (2009).“Implementation of the MEPDG for New and Rehabilitated Pavement Structures for Design of Concrete and Asphalt Pavements in Minnesota” Final Report, Minnesota Department of Transportation, Research Services Section.

Walid, M. N., (2001). “Utilization of Instrument Response of SuperPaveTM Mixes at the Virginia Smart Road to Calibrate Laboratory Developed Fatigue Equations”, Virginia Polytechnic Institute and State University, Blacksburg, VA 24061 Blacksburg, Virginia, July 2001

Wardle, L.J., (1998). “Layered Elastic Design of Heavy Duty and Industrial Pavements” Proc. AAPA Pavements Industry Conf., Surfers Paradise, Australia, 1998.

WSDOT, (2005), “Washington State Department of Transportation's Pavement Guide Interactive”, Washington State Department of Transportation.

Xiao, D. X., Wang, K. C.P., Hall, K. D., (2010).“Matching Distress Definitions in Field and in MEPDG for Local Calibration”, Pavement Evaluation Presentation, University of Arkansas.

Yang, H. H., (1993). “Pavement Analysis and Design”, Prentice Hall, Englewood Cliffs, New Jersey 1993.

Yu,T.,H., (2010). “Updates on Mechanistic Empirical Pavement Design Guide (MEPDG)”, US Department of Transportation, Federal Highway Administration, Presentation: Moving the American Economy.

LIST OF ACRONYMS

AADT	Annual Average Daily Traffic
AASHO	American Association of State Highway Officials
AASHTO	American Association of State Highway and Transportation Officials
AI	Asphalt Institute
ARE	Austin Research Engineers
ARS	Average Rectified Slope
BRRC	Belgian Road Research Center
CBR	California Bearing Ratio
DMI	Distress Manifestation Index
ESALs	Equivalent Single-Axle Loads
HMA	Hot Mix Asphalt
HRB	Highway Research Board
IRI	International Roughness Index
LRRB	Local Road Research Board
LTPP	Long Term Pavement Performance

ME	Mechanistic-Empirical
MEPDG	Mechanistic-Empirical Pavement Design Guide
MnDOT	Minnesota Department of Transportation
MnRoad	Minnesota Road
MTO	Ministry of Transportation, Ontario
NCHRP	National Cooperative Highway Research Program
PCI	Pavement Condition Index
PCR	Pavement Condition Rating
PMS	Pavement Management Systems
PR	Public Roads
RCI	Riding Comfort Index
RCR	Ride Comfort Rating
SHRP	Strategic Highway Research Program
SMA	Stone Matrix Asphalt
USCE	U.S. Corps of Engineers